A Cyclostratigraphic and Borehole-Geophysical Approach to Development of a Three-Dimensional Conceptual Hydrogeologic Model of the Karstic Biscayne Aquifer, Southeastern Florida

By Kevin J. Cunningham, Michael A. Wacker, Edward Robinson, Joann F. Dixon, and G. Lynn Wingard

Prepared in cooperation with the
South Florida Water Management District

Scientific Investigations Report 2005-5235

U.S. Department of the Interior
U.S. Geological Survey

U.S. Department of the Interior
Gale A. Norton, Secretary

U.S. Geological Survey
P. Patrick Leahy, Acting Director

U.S. Geological Survey, Reston, Virginia: 2006

For product and ordering information:
World Wide Web: http://www.usgs.gov/pubprod
Telephone: 1-888-ASK-USGS

For more information on the USGS--the Federal source for science about the Earth, its natural and living resources, natural hazards, and the environment:
World Wide Web: http://www.usgs.gov
Telephone: 1-888-ASK-USGS

Suggested citation:

Cunningham, K.J., Wacker, M.A., Robinson, Edward, Dixon, J.F., and Wingard, G.L., 2006, A Cyclostratigraphic and Borehole-Geophysical Approach to Development of a Three-Dimensional Conceptual Hydrogeologic Model of the Karstic Biscayne Aquifer, Southeastern Florida: U.S. Geological Survey Scientific Investigations Report 2005-5235, 69 p., plus CD.

Contents

Plates [on CD, back pocket]

Figures

Tables

Conversion Factors and Datums

Multiply	By	To obtain
inch (in.)	25.4	millimeter
foot (ft)	0.3048	meter
mile (mi)	1.609	kilometer
square mile (mi^2)	2.590	square kilometer
gallon per minute (gal/min)	0.06309	liter per second

Temperature in degrees Fahrenheit (˚F) is converted to degrees Celsius (˚C) as follows:

˚C = (˚F–32)/1.8

Vertical coordinate information is referenced to the National Geodetic Vertical Datum of 1929 (NGVD 1929).

Horizontal coordinate information is referenced to the North American Datum of 1983 (NAD 83). Altitude, as used in this report, refers to distance above the vertical datum.

Acronyms

BIPS	Borehole Image Processing System
ENP	Everglades National Park
FWWB	Fair weather wave base
FISC-WRS	Florida Integrated Science Center for Water and Restoration Studies
HFC	High-frequency cycle
NWWF	Northwest Well Field
PVC	polyvinyl chloride
SFWMD	South Florida Water Management District
SPT	Standard penetration test
SWB	Storm wave base
USGS	U.S. Geological Survey
WCA	Water Conservation Area

Other Abbreviated Units

ka	kilo-annum
ky	kilo-year
mD	millidarcy
mg/L	milligram per liter
ppt	part per thousand
µS/cm	microsiemens per centimeter

A Cyclostratigraphic and Borehole-Geophysical Approach to Development of a Three-Dimensional Conceptual Hydrogeologic Model of the Karstic Biscayne Aquifer, Southeastern Florida

By Kevin J. Cunningham[1], Michael A. Wacker[1], Edward Robinson[2], Joann F. Dixon[1], and G. Lynn Wingard[3]

Abstract

A fundamental problem in the simulation of karst ground-water flow and solute transport is how best to represent aquifer heterogeneity as defined by the spatial distribution of porosity, permeability, and storage. Combined analyses of cyclostratigraphy, including lithofacies and depositional environments, and borehole-geophysical logs, has improved the conceptualization of porosity, permeability, and storage within the triple-porosity karstic Biscayne aquifer in an approximately 95-square-mile study area of Miami-Dade County in southeastern Florida. The triple porosity of the Biscayne aquifer is principally: (1) matrix of interparticle and separate-vug porosity, providing much of the storage, and under dynamic conditions, diffuse-carbonate flow; (2) touching-vug porosity creating stratiform ground-water flow passageways; and (3) less common conduit porosity composed mainly of bedding-plane vugs, thin solution pipes, and cavernous vugs. These three conduit porosity types are all pathways for conduit ground-water flow.

To develop an accurate three-dimensional conceptual hydrogeologic model of the Biscayne aquifer in the study area, a detailed analysis of data was conducted that include continuously drilled cores, digital borehole images, borehole-fluid conductivity and temperature logs, and borehole-flowmeter measurements from 25 wells that fully penetrate the Biscayne aquifer. Six depositional environments for major lithologic components of the Biscayne aquifer—the Tamiami Formation, Fort Thompson Formation, and Miami Limestone—include: (1) middle ramp, (2) platform margin-to-outer platform, (3) open-marine platform interior, (4) restricted platform interior, (5) brackish platform interior, and (6) freshwater terrestrial environments. High-frequency cycles form the fundamental building blocks of the rocks composing the Biscayne aquifer. Vertical lithofacies successions, which have stacking patterns that reoccur, fit within the high-frequency cycles. Upward-shallowing subtidal cycles, upward-shallowing paralic cycles, and aggradational subtidal cycles define three types of ideal high-frequency cycles that occur within the Fort Thompson Formation and Miami Limestone. Based on vertical cycle patterns, high-frequency cycles group into two cycle sets: an older progradational cycle set and an overlying younger aggradational cycle.

A primary observation is that a predictable vertical pattern of porosity and permeability commonly exists within the three ideal cycles because the porosity and permeability relate directly to lithofacies. Sixteen major lithofacies of the Fort Thompson Formation and Miami Limestone have been assigned to one of three pore classes (I, II, and III).

[1]U.S. Geological Survey, Florida Integrated Science Center—Water and Restoration Studies, Miami, Florida.
[2]University of West Indies, Kingston, Jamaica.
[3]U.S. Geological Survey, Reston, Virginia.

Touching-vug porosity and conduit porosity characterize pore class I, which commonly comprises the lower part of upward-shallowing cycles within the Fort Thompson Formation and an upper aggradational cycle of the Miami Limestone. Matrix porosity distinguishes pore class II, which commonly occurs in the upper part of the upward-shallowing subtidal cycles and middle part of the upward-shallowing paralic cycles. Micrite-dominated, leaky, low-permeability lithologies are characteristic of pore class III, which commonly caps upward-shallowing paralic cycles and occurs throughout much of a lower aggradational cycle of the Miami Limestone. These relations among lithofacies, cyclicity, and aquifer attributes (porosity, permeability, and storage) are crucial features of the architecture of a three-dimensional conceptual hydrogeologic model of the karstic Biscayne aquifer. This study shows that development of these relations is critical to producing a realistic cycle-based karstic aquifer framework for the Biscayne aquifer and for karst aquifers within other platform carbonates.

Introduction

During the past century, the Everglades and its watershed have been altered substantially by human activities, including the development of a highly managed hydrologic system in southern Florida. This hydrologic system of canals, levees, and pumping stations was developed to meet an increasing demand for water supply as a result of a rapidly growing urban population and intensive agricultural activities. As a consequence, much of the Everglades, the unconfined karstic Biscayne aquifer, and major estuarine systems in southern Florida presently do not receive sufficient quantity or distribution of water during times when it is needed most. An adequate water supply is essential to restoring the Everglades and its watershed and maintaining sustainable population growth.

In southeastern Florida, ground-water supply is augmented by surface-water storage in large-scale water-conservation areas (fig. 1) and Everglades National Park (ENP). Surface water seeps into the Biscayne aquifer from the wetlands and then moves as ground water beneath a system of levees and canals on the eastern perimeter of the wetlands, flowing toward agricultural, urban, and coastal areas to the east. Sustainable ground-water levels east of the wetlands are critical to maintaining water levels at water-supply wells, preventing saltwater intrusion along the coast, and restoring the quantity, quality, timing, and distribution of freshwater to Biscayne Bay.

To develop a water budget that meets natural, agricultural, and urban needs, it is necessary to accurately model the movement of ground water and associated loads from the surface-water storage areas to the coast ~~an~~ approach that involves numerical simulation of ground-water flow and solute transport in the Biscayne aquifer. Recent ground-water flow models for the Biscayne aquifer assume flow through porous media (Nemeth and others, 2000; Wilsnak and others, 2000; Langevin, 2001; Sonenshein, 2001); however, the Biscayne aquifer is a triple-porosity (matrix, touching-vug, and conduit porosity) karst aquifer (Vacher and Mylroie, 2002; Cunningham and others, 2004b; 2004c). As a consequence, rates of flow within the conduit pore system can be more rapid than within the matrix, as demonstrated by a tracer test conducted by the U.S. Geological Survey (USGS) at the Northwest Well Field (NWWF) in Miami-Dade County (Renken and others, 2005). Results of this test indicated that the apparent mean advective flow velocity of the tracer was one order of magnitude or greater than predictions by model simulations assuming only porous media. A realistic conceptual hydrogeologic model of the Biscayne aquifer, especially its karst limestone, is needed for development of numerical simulations that can reliably predict ground-water flow and solute transport through the aquifer's triple-porosity hydrogeologic framework.

A fundamental problem in the simulation of karst ground-water flow and solute transport is how best to represent aquifer heterogeneity as defined by the spatial distribution of porosity, permeability, and storage. By definition, karst carbonate aquifers contain dissolution-generated conduits that allow rapid movement of ground water, often as turbulent flow (White, 2002). Carbonate conduit flow systems pose a unique problem because of the complex variations in lithofacies and diagenetic history that contribute to their heterogeneity. Existing karst flow models can be improved if conceptual hydrogeologic models accurately delineate the distribution of conduits and aquifer matrix (White, 1999). This is especially true of Paleozoic karst aquifers that can include pipe-like conduits; these may be single caves or have a complex "branchwork pattern" (White and White, 2001). In younger Cretaceous and Cenozoic karst aquifers, zones of high porosity have been shown to occur within, or as equivalent to, small-scale depositional cycles (Edwards aquifer—Hovorka and others, 1996, 1998; Floridan aquifer—Budd, 2001; Ward and others, 2003; Budd and Vacher, 2004; Biscayne aquifer—Cunningham and others, 2004b; 2004c; 2006, in press), indicating a well-defined cyclostratigraphic framework that can be used to map the three-dimensional aspects of karst ground-water flow.

In 1998, the USGS, in cooperation with the South Florida Water Management District (SFWMD), initiated a study that identified and characterized candidate preferential ground-water flow zones in the upper part of the shallow karst limestone of the Biscayne aquifer in north-central Miami-Dade County using cyclostratigraphy, ground-penetrating radar, borehole-geophysical logs, continuously drilled cores, and paleontology (Cunningham and others, 2004b). This application of cyclostratigraphy has proven critical to development of a new conceptual hydrogeologic framework within the upper part of the Biscayne aquifer (Cunningham and others, 2004b; 2004c). In 2002, the USGS, in cooperation with the SFWMD, initiated the current study, which extends the shallow high-resolution hydrostratigraphic framework to the base of the Biscayne aquifer. The purpose of the current study is to define and map the spatial variations in the hydrogeology of the karstic

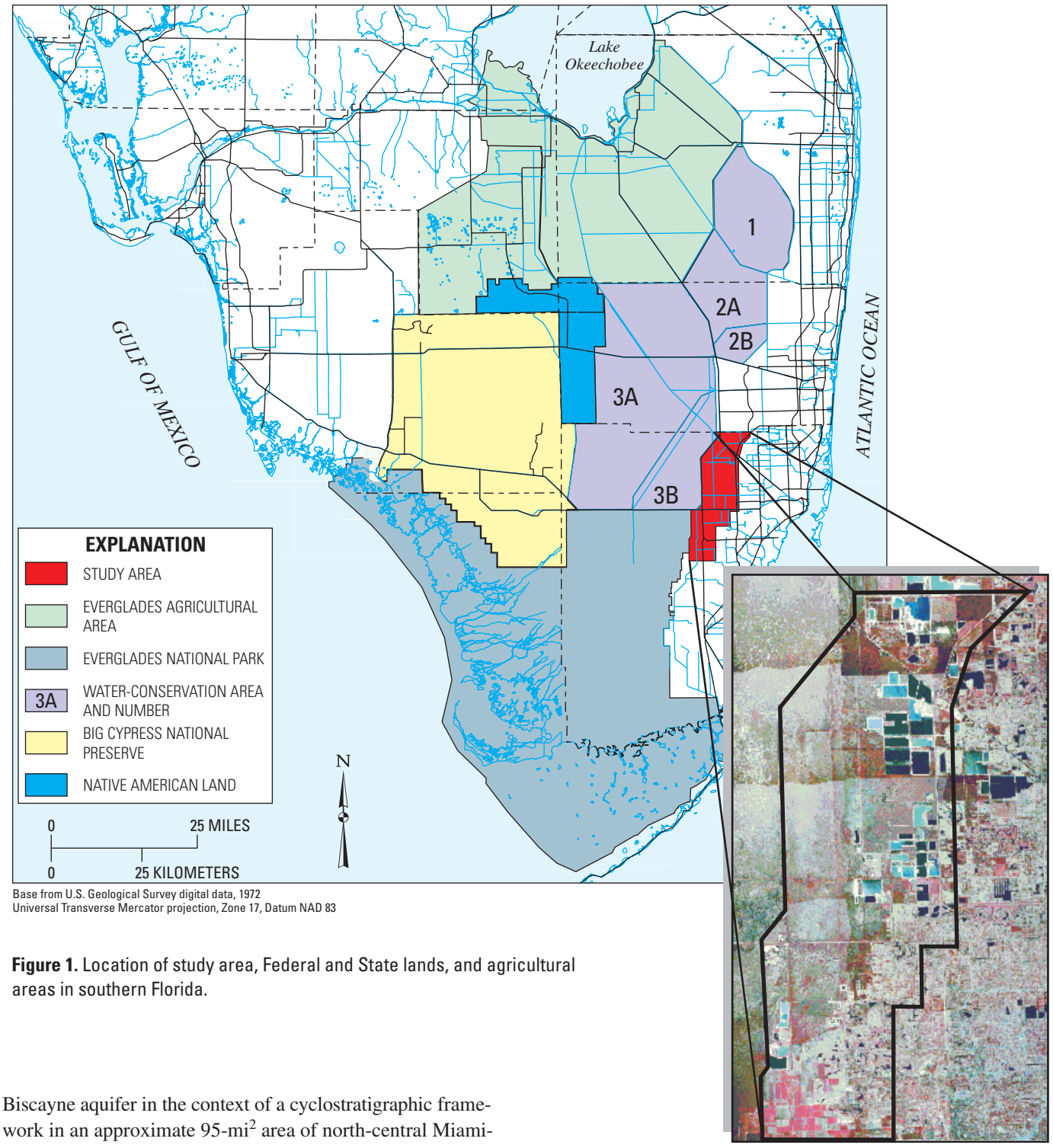

Figure 1. Location of study area, Federal and State lands, and agricultural areas in southern Florida.

Biscayne aquifer in the context of a cyclostratigraphic framework in an approximate 95-mi^2 area of north-central Miami-Dade County (fig. 1). The resulting conceptual hydrogeologic framework is critical in the development of procedures for reliable simulation of ground-water flow and solute transport in the triple-porosity Biscayne aquifer. This study shows that development of the methods used herein is critical to producing a realistic cycle-based karstic aquifer framework for the Biscayne aquifer and for karst aquifers within other platform carbonates. The current effort also incorporates borehole data from a recently completed study (Renken and others, 2005) done in cooperation with the USGS, Miami-Dade County Water and Sewer Department, and American Water Works Research Foundation at the municipal NWWF (fig. 2). That study assessed the transport of pathogenic protozoa within the Biscayne aquifer and examined the importance of straining or filtration mechanisms that could impede their advective movement.

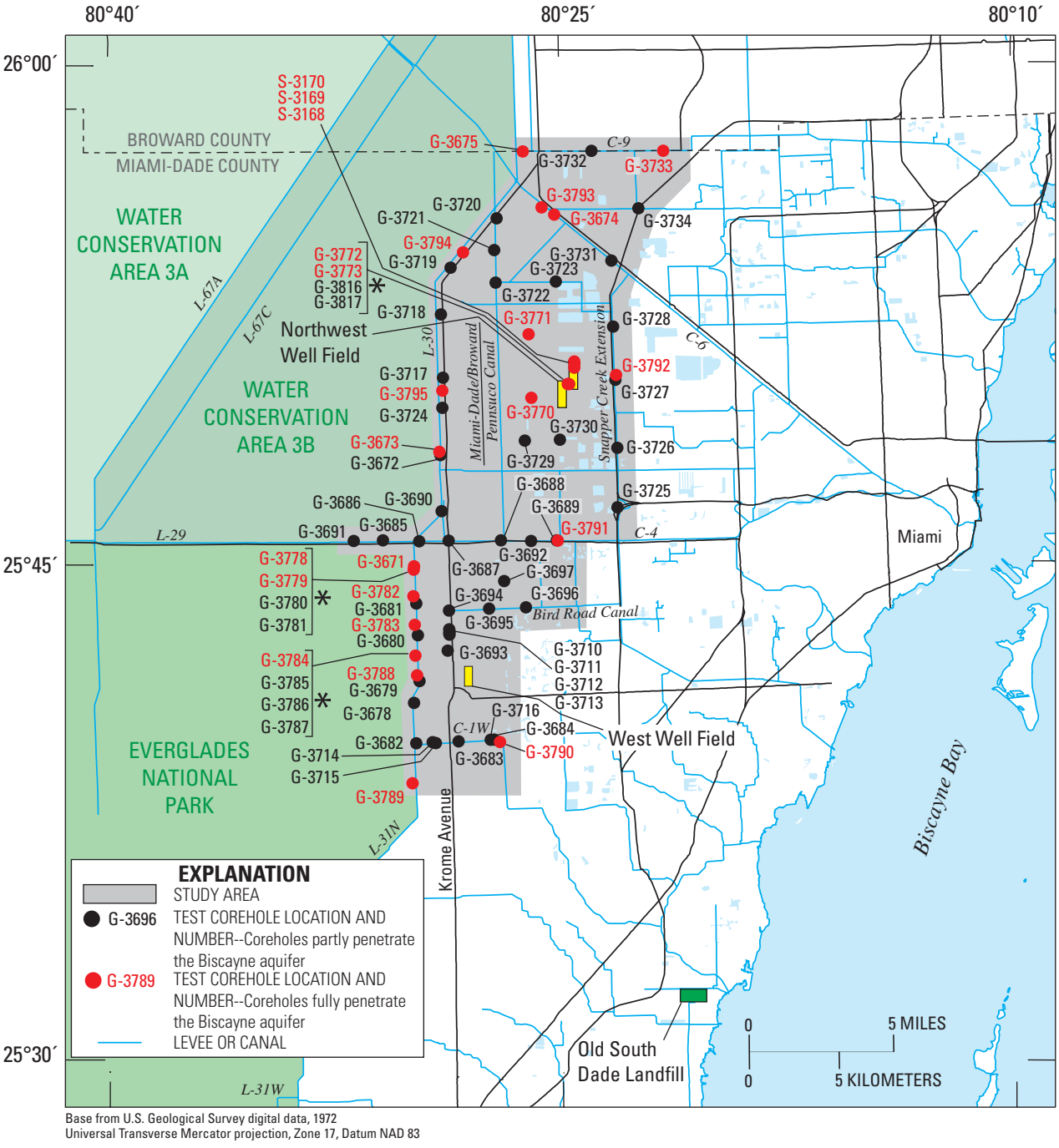

Figure 2. Study area in Miami-Dade County showing location of major canals and levees, Northwest Well Field, Old South Dade Landfill, and test coreholes used in this study. Asterisk indicates that some test coreholes are grouped together at the same location, and partly or fully penetrate the Biscayne aquifer.

Purpose and Scope

The purpose of this report is to document the second phase of the study, which applies cyclostratigraphic concepts to a database that includes borehole-geophysical logs, core-sample analyses, molluscan and foraminiferal paleontology, and borehole-flowmeter measurements. Specifically, this report demonstrates how carbonate cyclostratigraphy was crucial for defining the spatial distribution of porosity, permeability, and storage within a triple-porosity (matrix, touching-vug, and conduit porosity) karst aquifer.

Integrated analysis of the database resulted in delineation of vertical lithofacies successions, depositional environments, porosity, and permeability of the Pleistocene karst limestone of the Biscayne aquifer in the context of a cyclostratigraphic framework in north-central Miami-Dade County, Florida (figs. 1 and 2). A high-resolution cyclostratigraphic model is used throughout the entire thickness of the Biscayne aquifer over a wide area to select consistent correlable ground-water flow zones, diffuse flow zones, and zones of leaky, low permeability in the study area. That part of the Biscayne aquifer included in the upper part of the Pliocene Tamiami Formation by Fish and Stewart (1991) is not a major focus of this study.

Description of Study Area

The study area of Cunningham and others (2004b) was the approximate extent of the 89-mi^2 Lake Belt area (fig. 2), an up to 6-mi-wide region that separates urban Miami-Dade County from natural wetlands of ENP and Water Conservation Area (WCA) 3B. The Lake Belt area primarily is used for rock mining and public-water supply and as an environmentally protective freshwater wetland (Miami-Dade County Lake Belt Plan Implementation Committee, 1998). The current effort expands the study locale of Cunningham and others (2004b) southward by about 1.5 mi or 6 mi^2. (Compare fig. 2 in Cunningham and others (2004b) with fig. 2 in this report.)

Previous Studies

The goals of this study have been addressed by a wide range of studies that encompass different geologic disciplines. The disciplines include those that characterize: (1) ground-water flow in the Biscayne aquifer; (2) variability in porosity, permeability, and storage within the Biscayne aquifer; and (3) the hydrogeology of the Biscayne aquifer or the physical properties of carbonate strata using geophysical methods and other techniques.

Numerous studies that have investigated the presence of low-permeability zones in the Biscayne aquifer indicate the existence of one or more semiconfining units. The presence of low-permeability zones near the top of the Biscayne aquifer was first suggested by Klein and Sherwood (1961), who proposed that two thin layers of dense limestone retard downward infiltration of surface water in WCA 3A and WCA 3B (fig. 2), causing a high head differential across Levee 30 (L-30) at the edge of WCA 3B (fig. 2). Several studies that evaluated permeability from the top of the Fort Thompson Formation to the base of the Miami Limestone presented evidence for a dense low-permeability unit that spans this zone; some reports also identified other low-permeability units limiting ground-water flow within the Biscayne aquifer (Shinn and Corcoran, 1988; Guardiario, 1996; Brown and Caldwell Environmental Engineers and Consultants, 1998; Cunningham and Wright, 1998; Genereux and Gaurdiario, 1998; Kaufman and Switanek, 1998; Nemeth and others, 2000; Sonenshein, 2001; Cunningham and others, 2004b, 2004c; Cunningham and others, 2006, in press; Krupa and Mullen, 2005).

Along the Levee 31W Canal at the eastern boundary of ENP, borehole-flowmeter measurements by Guardiario (1996) showed that the low-permeability unit spanning the upper Fort Thompson Formation and lower Miami Limestone (figs. 3 and 4) acts as a semiconfining unit, supporting vertical head differences and restricting the vertical movement of water. At a nearby site, canal drawdown experiments were used with borehole-flowmeter measurements to establish a high-resolution hydraulic conductivity profile of the Biscayne aquifer (Genereux and Guardiario, 1998). Results indicated the presence of a low hydraulic conductivity zone at the top of the Fort Thompson Formation (Genereux and Guardiario, 1998), which presumably is equivalent to the low hydraulic conductivity zone that spans the upper Fort Thompson Formation and lower part of the Miami Limestone in north-central Miami-Dade County. The zone also has been identified as a semiconfining unit at the Old South Dade Landfill (fig. 2) in Miami-Dade County (Shinn and Corcoran, 1988; Brown and Caldwell Environmental Engineers and Consultants, 1998; Cunningham and Wright, 1998). Vertical head differences measured by Sonenshein (2001) indicated that this zone can restrict vertical flow between surface water and ground water in the wetlands west of L-30 in Miami-Dade County (fig. 2). Recent ground-water simulations by Nemeth and others (2000) along Levee 31N (L-31N) and Sonenshein (2001) near L-30 have modeled this zone as a low-permeability unit. This low-permeability unit and a deeper unit are shown in cross sections and a three-dimensional conceptual hydrogeologic model of the upper part of the Biscayne aquifer (Cunningham and others, 2004b, plates 1-5 and fig. 39, respectively) throughout most of the Lake Belt area.

Cunningham and others, (2004c; 2006, in press) mapped several low-permeability units throughout the Biscayne aquifer along L-31N and in a small area of the NWWF. Cunningham and others (2004c) also presented evidence for vertical head differences between three zones of high permeability within the lower, middle, and uppermost part of the Biscayne aquifer, providing evidence for the retardation of vertical leakance of ground water in the aquifer at two or more levels. Cunningham and others (2006, in press) and Renken and others (2005) conducted a forced-gradient convergent tracer test using

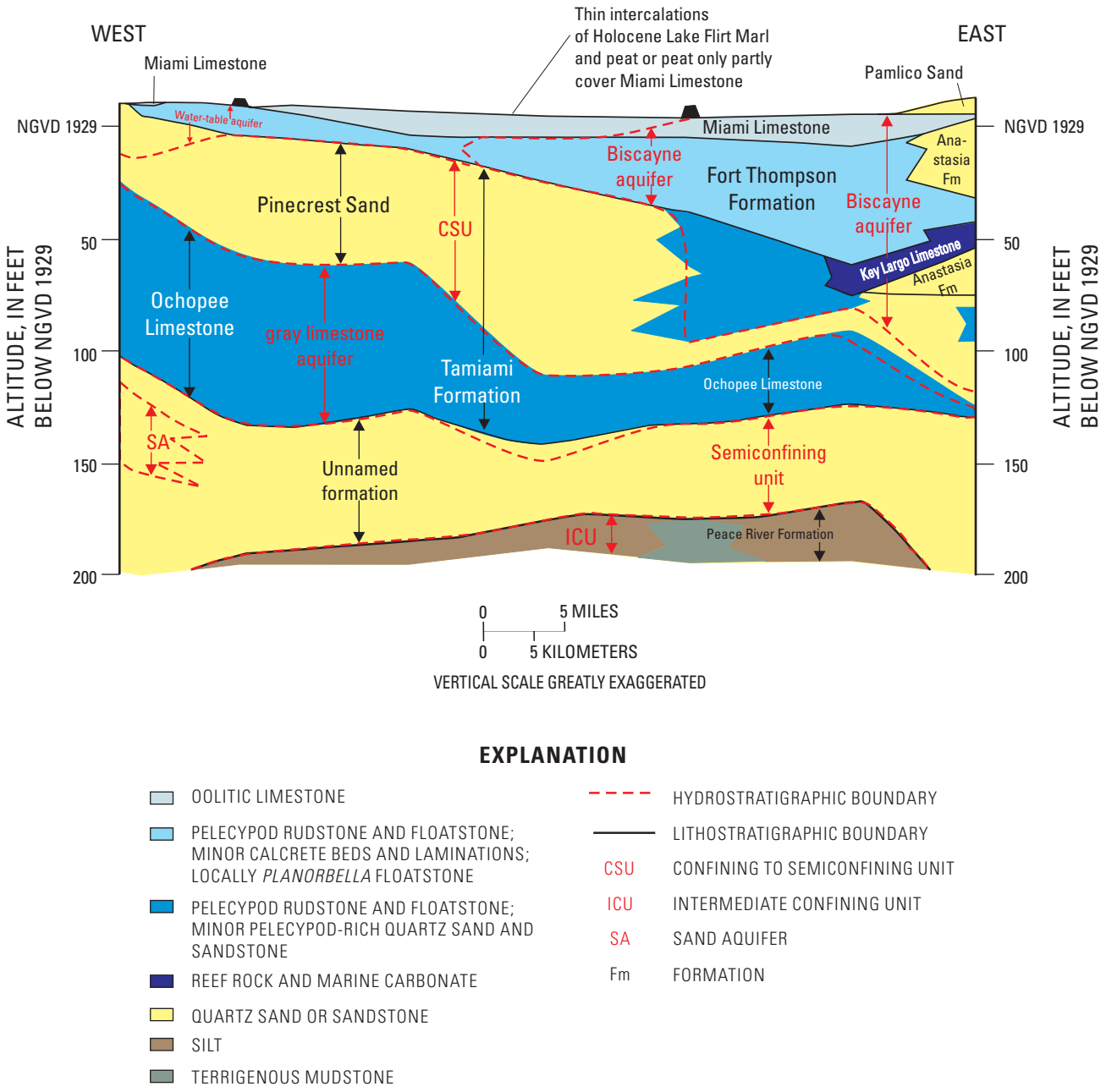

Figure 3. Relation of geologic and hydrogeologic units of the surficial aquifer system across central Miami-Dade County (modified from Reese and Cunningham, 2000).

Rhodamine WT and deuterated water and made borehole-fluid temperature and flowmeter measurements at an observation well. Results strongly suggested that ground water in the Biscayne aquifer in the area of the well field preferentially moves along stratiform zones of touching-vug porosity; typically, these zones are located at the base of high-frequency cycles, which can be mapped in three dimensions. Krupa and Mullen (2005) presented a detailed hydrogeologic study of the low-permeability unit that spans the upper Fort Thompson Formation and lower Miami Limestone.

Many recent studies have verified that digital electronic images of borehole walls can be useful for quantifying vuggy porosity (Hickey, 1993; Newberry and others, 1996; Hurley and others, 1998; 1999) in petroleum reservoirs and fractures in aquifers (Williams and Johnson, 2000). By quantifying vuggy porosity in borehole images, these researchers were able to identify fluid-flow zones. Cunningham and others (2004a) reported in detail the development of a method for quantifying vuggy porosity seen in digital borehole images of limestone in the Biscayne aquifer. Cunningham and others

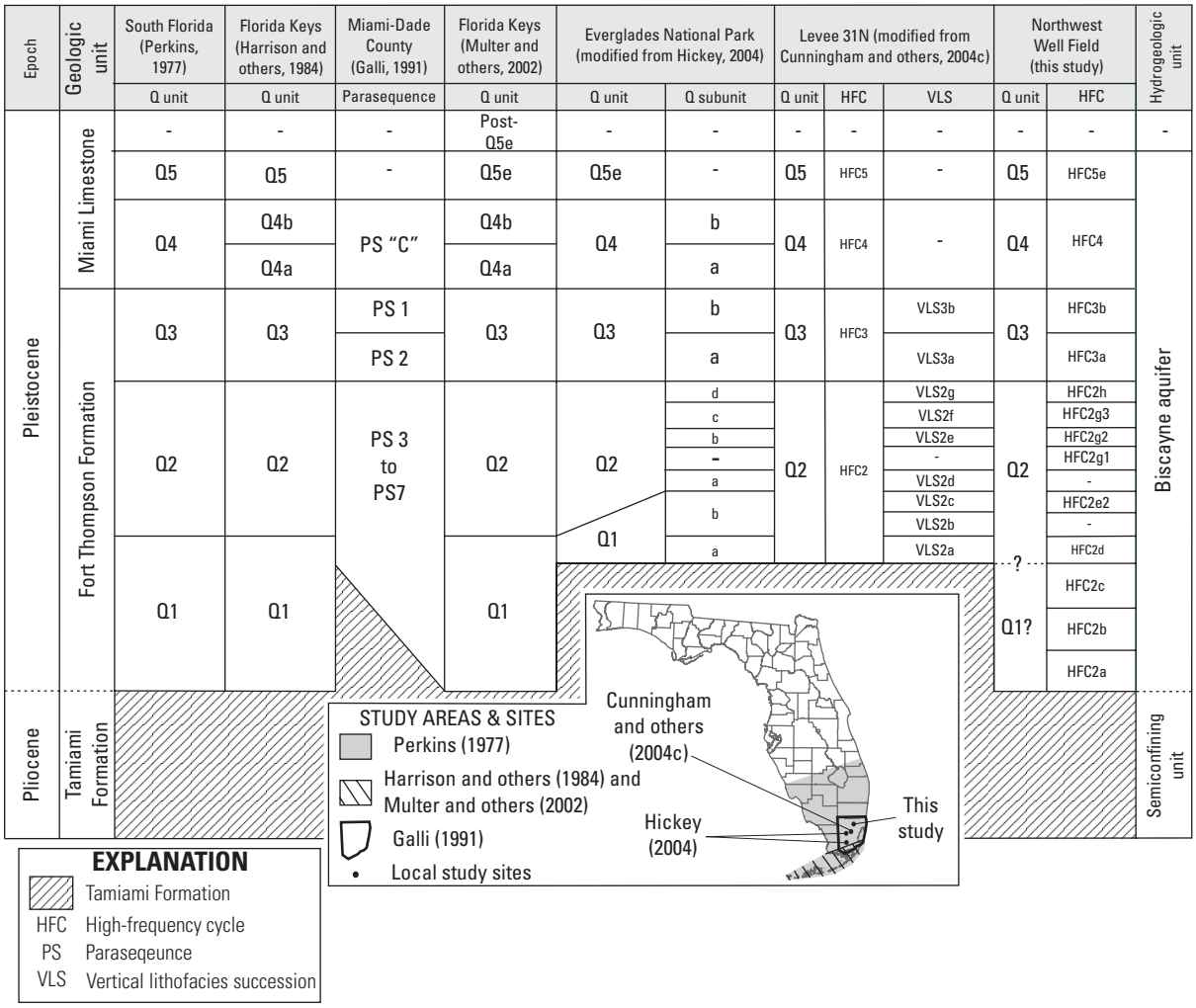

Figure 4. Correlation of ages, formations, stratigraphy, and hydrogeologic units of the Tamiami Formation, Fort Thompson Formation, and Miami Limestone from this and other studies.

(2004b; 2004c) also presented numerous digital borehole images from the Biscayne aquifer, which were used to calculate the percentage of vuggy porosity.

Acknowledgments

Cynthia Gefvert and Steven Krupa at the SFWMD gave useful advice and logistical support during the study. Gene Shinn and Barclay Shoemaker of the USGS and Pamela Hallock Muller of the University of South Florida provided technical reviews, and Mike Deacon and Rhonda Howard provided editorial reviews. Borehole data collected as part of a cooperative project funded by the USGS, Miami-Dade County Water and Sewer Department, and American Water Works Research Foundation at the Northwest Well Field were included in this study.

Methods of Investigation

A multidisciplinary approach was used to characterize the pore system within a cyclic hydrogeologic framework of the entire Biscayne aquifer. This approach involved integrating data from core analyses and borehole-geophysical logs and from cyclostratigraphic and paleontologic analyses.

Drilling, Well Completion, Core Analysis, and Borehole-Geophysical Logging

Twenty-five continuously cored wells that fully penetrate the Biscayne aquifer form the foundation of this study (table 1 and fig. 2). Other partially penetrating wells (fig. 2) from studies by Cunningham and others (2004b; 2004c; 2006,

in press) were used in support of interpretations. In 1998, the Miami-Dade County Water and Sewer Department directed the drilling of 3 of the 25 wells as test coreholes adjacent to production wells S-3168, S-3169, and S-3170 at the NWWF (fig. 2). The USGS supervised the drilling of the remaining 22 wells. Four wells were drilled as test coreholes (G-3671, G-3673, G-3674, and G-3675) in 1998 by Cunningham and others (2004b). Two test coreholes (G-3770 and G-3771) located about 1 mi east of the Miami-Dade-Broward/Pennsuco Canal (fig. 2), were completed in 2002. Another two of the 25 wells were completed in 2003, one as a monitoring well (G-3772) and the other as an injection well (G-3773); both wells were constructed for a tracer study (Cunningham and others, 2006, in press; Renken and others, 2005). Seven test coreholes (G-3778, G-3779, G-3782, G-3783, G-3784, G-3788, and G-3789) were drilled in 2003 on top of the L-31N berm or along its east side (Cunningham and others, 2004c). An additional seven test coreholes (G-3733 and G-3790 to G-3795) were completed between late 2003 and early 2004. Test corehole G-3733 was originally completed in the middle part of the Biscayne aquifer (Cunningham and others, 2004b), but redrilled as fully penetrating the Biscayne aquifer for this study.

Continuously drilled 3.4-in.-diameter cores from the four test coreholes (G-3671, G-3673, G-3674, and G-3675) that fully penetrate the Biscayne aquifer and completed in 1998 were collected using a wireline coring method to the total depth of each test corehole. Continuously drilled 4-in.-diameter cores were collected from the injection (G-3773) and monitoring (G-3772) wells at the NWWF using the same wireline coring method down to the first depth that quartz sands were penetrated; the remaining depths of both wells were then cored using a split-barrel sampler and standard penetration test (SPT) methodology (Shuter and Teasdale, 1989). All other test coreholes drilled under the supervision of the USGS (G-3733, G-3770, G-3771, G-3778, G-3782 to G-3784, G-3788 to G-3795) were drilled using a conventional hydraulic rotary coring method with freshwater as a drilling fluid (Shuter and Teasdale, 1989) to a depth where quartz sands were first encountered; the remaining depths of each test corehole were then drilled using a split-barrel sampler and SPT methodology (table 1). The exception was well G-3779 (fig. 2), which was drilled only using the conventional hydraulic rotary coring method to a short depth where the first quartz sands were encountered.

Seventeen test coreholes that fully penetrate the Biscayne aquifer and drilled under the supervision of the USGS were completed as open-hole stratigraphic tests with a short length of solid polyvinyl chloride (PVC) casing at the uppermost part of the well (table 1). The monitoring wells (G-3778, G-3779, and G-3784) that fully penetrate the Biscayne aquifer on top of the L-31N berm were completed with 2-in.-diameter solid PVC with a 2-ft-long screened interval in limestone of the Biscayne aquifer or underlying semiconfining unit (fig. 3). The injection (G-3773) and monitoring (G-3772) wells at the NWWF (fig. 2 and table 1) were constructed with solid PVC casing from land surface to near their base and with an open-hole interval at their base. The three test coreholes (S-3168, S-3169, and S-3170) drilled next to production wells at the NWWF (fig. 2 and table 1) were abandoned after cores were acquired.

Geophysical logs were collected in all 22 wells (app. I) drilled under the supervision of the USGS, but no logs were collected in the test coreholes adjacent to production wells S-3168, S-3169, and S-3170 (fig. 2). The types of logs collected by the USGS include the following: electromagnetic induction, three-arm caliper, borehole-fluid resistivity and temperature, full waveform sonic, heat pulse and spinner flowmeter, ALT OBI-40 Mark III™ digital optical televiewer (RAAX™ Borehole Imaging Processing System [BIPS] digital optical televiewer in the G-3671, G-3673, G-3674, and G-3675 test coreholes only), and Laval™ video (except for the G-3671, G-3673, G-3674, and G-3675 test coreholes). Vuggy porosity logs (Cunningham and others, 2004a) also were created for each of the wells logged by the USGS.

To construct hydrogeologic cross sections, data from nine test coreholes that only partly penetrate the Biscayne aquifer also are included in this study (G-3696, G-3720, G-3723, G-3725, G-3728, G-3730, G-3731, G-3732, and G-3734). Cunningham and others (2004b) describe the details of the drilling, completion, and geophysical logging for these test coreholes.

For this study, an analysis was conducted of core samples (either 3.4-. or 4.0-in.-diameter) obtained from the 25 wells that fully penetrate the Biscayne aquifer in the study area (fig. 2). Most of the core samples were slabbed and visually analyzed using a 10X-magnification hand lens and binocular microscope. Standard transmitted-light petrography was used to examine 215 thin sections. Cores and thin sections were analyzed to help determine lithofacies, vertical trends in lithofacies, sedimentary structures, cycle boundaries, and assess how features laterally varied and correlated. Lithofacies were defined by allochem types, fabric, sedimentary structures, bedding type, and diagenetic features using a combination of classification schemes and terminology from Dunham (1962), Embry and Klovan (1971), and Lucia (1999). The rock color of dry core samples was recorded by comparing them to a Munsell rock-color chart (Geological Society of America, 1991). Core Laboratories, Inc., measured horizontal and vertical permeability, porosity, and grain density of 267 whole-core samples collected from 13 wells (app. II). All continuous cores collected for this study were archived at the USGS Florida Integrated Science Center for Water and Restoration Studies (FISC-WRS) in Fort Lauderdale, Fla. Relations between lithofacies and petrophysical properties (porosity and permeability) were assessed using methods prescribed by Lucia (1995; 1999).

Table 1. List of all test coreholes drilled during this study.

[Well locations are shown in figure 2. All wells are located in Miami-Dade County, Florida. Latitudes and longitudes referenced to North American Datum of 1983. Altitude of measuring point is land surface referenced to the National Geodetic Vertical Datum of 1929 (NGVD 1929). All wells are test coreholes unless otherwise noted. Drilling method: AR, air rotary; CC, conventional core; MR, mud rotary; SPT, split barrel sampler using standard penetration test methodology. Other acronyms: NA, not applicable; NWWF, Northwest Well Field; PVC, solid polyvinyl chloride; WLC, wireline core]

Local well identifier	USGS site identification number	Drilling contractor	Drilling method	Latitude	Longitude	Altitude of measuring point (feet)	Total depth drilled (feet)	Well construction material	Depth of bottom of casing (feet)	Well fully penetrates Biscayne aquifer	End date of construction	Comments
G-3671	254456080295301	Amdrill	WLC	254456	802953	7.5	150	3.5-in. PVC	10	Yes	8-7-98	Open interval to 55.5 feet
G-3672	254822080290201	Amdrill	WLC	254822	802902	20	45	3.5-in. PVC	18	No	8-8-98	Abandoned-redrilled at G-3673
G-3673	254822080290202	Amdrill	WLC	254822	802902	20	160	3.5-in. PVC	18	Yes	8-10-98	--
G-3674	255529080251101	Amdrill	WLC	255529	802511	10	160	3.5-in. PVC	10	Yes	8-16-98	Destroyed
G-3675	255723080261301	Amdrill	WLC	255723	802613	8	90	No casing set	NA	Yes	8-21-98	--
G-3678	254050080295401	Amdrill	WLC	254050	802954	9	35	3.5-in. PVC	10	No	5-22-99	--
G-3679	254129080294301	Amdrill	WLC	254129	802943	9	40	3.5-in. PVC	10	No	5-23-99	--
G-3680	254252080294601	Amdrill	WLC	254252	802946	9	40	3.5-in. PVC	11	No	5-23-99	--
G-3681	254349080294901	Amdrill	WLC	254349	802949	9	45	3.5-in. PVC	11	No	5-23-99	--
G-3682	253937080295001	Amdrill	WLC	253937	802950	10	30	3.5-in. PVC	11	No	5-24-99	--
G-3683	253940080282601	Amdrill	WLC	253940	802826	8	35	3.5-in. PVC	11	No	5-24-99	Destroyed
G-3684	253943080272201	Amdrill	WLC	253943	802722	8	35	3.5-in. PVC	10	No	5-24-99	Destroyed
G-3685	254543080305501	Amdrill	WLC	254543	803055	8	30	3.5-in. PVC	11	No	5-25-99	Destroyed
G-3686	254541080294301	Amdrill	WLC	254541	802943	10	30	3.5-in. PVC	10	No	5-25-99	Destroyed
G-3687	254542080284401	Amdrill	WLC	254542	802844	10	30	3.5-in. PVC	11	No	5-25-99	--
G-3688	254542080270001	Amdrill	WLC	254542	802700	9.5	30	3.5-in. PVC	10	No	5-26-99	Destroyed
G-3689	254542080259001	Amdrill	WLC	254542	802590	9	30	3.5-in. PVC	10	No	5-26-99	Destroyed
G-3690	254635080285801	Amdrill	WLC	254635	802858	9	30	3.5-in. PVC	11	No	5-26-99	--
G-3691	254542080315301	Amdrill	WLC	254542	803153	8	35	3.5-in. PVC	10	No	5-27-99	Destroyed
G-3692	254541080260001	Amdrill	WLC	254541	802600	9	30	3.5-in. PVC	NA	No	5-27-99	Casing fell to borehole bottom
G-3693	254224080284701	Amdrill	WLC	254224	802847	10.5	35	3.5-in. PVC	NA	No	6-2-99	Casing fell to borehole bottom. Destroyed
G-3694	254336080284401	Amdrill	WLC	254336	802844	10	35	3.5-in. PVC	10	No	6-2-99	Destroyed
G-3695	254339080272401	Amdrill	WLC	254339	802724	9.5	35	3.5-in. PVC	11	No	6-3-99	--
G-3696	254341080261101	Amdrill	WLC	254341	802611	10	35	3.5-in. PVC	10	No	6-3-99	Lower borehole collapsed
G-3697	254429080265401	Amdrill	WLC	254429	802654	9	30	No casing set	NA	No	6-3-99	Well abandoned
G-3710	254310080284801	U.S. Drilling	CC	254310	802848	10	33	5-in.PVC	8	No	4-20-00	--
G-3711	254300080284701	U.S. Drilling	CC	254300	802847	10	37	5-in. PVC	7	No	4-20-00	--
G-3712	254250080284601	U.S. Drilling	CC	254250	802846	10	28	5-in. PVC	7	No	5-1-00	--
G-3713	254245080284501	U.S. Drilling	CC	254245	802845	10	32.5	5-in. PVC	7	No	5-2-00	--
G-3714	253937080292901	U.S. Drilling	CC	253937	802929	9	23	5-in. PVC	7	No	5-3-00	--
G-3715	253938080292301	U.S. Drilling	CC	253938	802923	9	23	5-in. PVC	5	No	5-3-00	--
G-3716	253943080272301	U.S. Drilling	CC	253943	802723	8	28	5-in. PVC	9	No	5-4-00	Destroyed
G-3717	255039080290101	U.S. Drilling	CC	255039	802901	9	43	5-in. PVC	7	No	5-8-00	--
G-3718	255220080290301	U.S. Drilling	CC	255220	802903	9	30	5-in. PVC	8	No	5-9-00	--

Table 1. List of all test coreholes drilled during this study. (Continued)

Local well identifier	USGS site identification number	Drilling contractor	Drilling method	Latitude	Longitude	Altitude of measuring point (feet)	Total depth drilled (feet)	Well construction material	Depth of bottom of casing (feet)	Well fully penetrates Biscayne aquifer	End date of construction	Comments
G-3719	255355080284301	U.S. Drilling	CC	255355	802843	9	30	5-in. PVC	6.5	No	5-10-00	--
G-3720	255530080271301	U.S. Drilling	CC	255530	802713	9	31	5-in. PVC	5	No	5-11-00	--
G-3721	255424080271201	U.S. Drilling	CC	255424	802712	10	30	5-in. PVC	9	No	5-12-00	--
G-3722	255326080270901	U.S. Drilling	CC	255326	802709	10	32	5-in. PVC	8	No	5-12-00	--
G-3723	255328080251201	U.S. Drilling	CC	255328	802512	8	45	5-in. PVC	-	No	5-15-00	Casing fell to borehole bottom
G-3724	254942080285801	U.S. Drilling	CC	254942	802858	9	30	5-in. PVC	7	No	5-16-00	Destroyed
G-3725	254655080231201	U.S. Drilling	CC	254655	802312	6	31.5	5-in. PVC	6	No	5-17-00	Destroyed
G-3726	254825080231201	U.S. Drilling	CC	254825	802312	7	33	5-in. PVC	10	No	5-18-00	Borehole collapsed to 16 feet below land surface
G-3727	255033080231301	U.S. Drilling	CC	255033	802313	8	43	5-in. PVC	8.7	No	5-30-00	Destroyed
G-3728	255154080231301	U.S. Drilling	CC	255154	802313	7	38	5-in. PVC	6	No	5-31-00	Destroyed
G-3729	254843080261101	U.S. Drilling	CC	254843	802611	6	36	5-in. PVC	6	No	6-1-00	--
G-3730	254842080250801	U.S. Drilling	CC	254842	802508	6	40	5-in. PVC	7	No	6-2-00	Casing fell to borehole bottom
G-3731	255408080231801	U.S. Drilling	CC	255408	802318	10	43	5-in. PVC	7.5	No	6-5-00	--
G-3732	255724080235401	U.S. Drilling	CC	255724	802354	6	48	5-in. PVC	5	No	8-21-00	--
G-3733	255724080213401	U.S. Drilling	CC	255724	802135	6	43	5-in. PVC	9.8	No	9-8-00	--
G-3733	255724080213401	MACTEC	CC/SPT	255724	802135	6	63	10-in. PVC	3	Yes	12-19-03	Original well deep-ened; 6.5-in. diameter hole below 10-in. casing. Open interval to 57 feet below land surface
G-3734	255540080222501	U.S. Drilling	CC	255540	802225	8	33	5-in. PVC	6	No	9-8-00	--
G-3770	254957080260101	U.S. Drilling	CC/SPT	254957	802601	6.7	80	6-in. PVC	8.6	Yes	11-06-02	Open interval to 58 feet below land surface
G-3771	255159080260501	U.S. Drilling	CC/SPT	255159	802605	6.0	80	6-in. PVC	8.2	Yes	11-18-02	Open interval to 58 feet below land surface
G-3772	255029080245001	Intercounty	WLC/ SPT	255029	802450	8.0	100	2-in. PVC	33.5	Yes	01-14-03	Monitoring well, open interval to 64 feet below land surface
G-3773	255029080245304	Intercounty	WLC/ SPT	255029	802453	8.1	100	6-in. PVC	33.5	Yes	01-29-03	Injection well, open interval to 66 feet below land surface
G-3778	254447080295201	MACTEC	CC/ SPT/ MR	254447	802952	16.4	111.4	2-in. PVC	103.3	Yes	09-24-03	Monitoring well, screened interval 101.3 to 103.3 feet below land surface
G-3779	254447080295202	MACTEC	CC	254447	802952	16.2	65	2-in. PVC	54.2	Yes	09-18-03	Monitoring well, screened interval 52.2 to 54.2 feet below land surface
G-3780	254447080295203	MACTEC	MR	254446	802952	16.4	34	2-in. PVC	33.4	No	09-22-03	Monitoring well, screened interval 31.4 to 33.4 feet below land surface
G-3781	254447080295204	MACTEC	MR	254446	802952	16.5	19	2-in. PVC	18.6	No	10-01-03	Monitoring well, screened interval 16.6 to 18.6 feet below land surface
G-3782	254351080295001	MACTEC	CC/SPT	254351	802950	8.9	70	6-in. PVC	9.2	Yes	07-27-03	Open interval to 57 feet below land surface
G-3783	254257080294801	MACTEC	CC/SPT	254257	802948	9.1	71	6-in. PVC	10	Yes	08-05-03	Open interval to 47 feet below land surface

Table 1. List of all test coreholes drilled during this study. (Continued)

Local well identifier	USGS site identification number	Drilling contractor	Drilling method	Latitude	Longitude	Altitude of measuring point (feet)	Total depth drilled (feet)	Well construction material	Depth of bottom of casing (feet)	Well fully penetrates Biscayne aquifer	End date of construction	Comments
G-3784	254207080294601	MACTEC	CC/SPT/MR	254207	802946	15.7	113.7	2-in. PVC	100.5	Yes	10-07-03	Monitoring well, screened interval 98.5 to 100.5 feet below land surface
G-3785	254207080294602	MACTEC	MR	254207	802946	15.8	45	2-in. PVC	44.4	No	10-15-03	Monitoring well, screened interval 42.4 to 44.4 feet below land surface
G-3786	254207080294603	MACTEC	MR	254207	802946	15.6	29	2-in. PVC	28.4	No	10-03-03	Monitoring well, screened interval 26.4 to 28.4 feet below land surface
G-3787	254207080294604	MACTEC	MR	254207	802946	15.9	19	2-in. PVC	19	No	10-02-03	Monitoring well, screened interval 16.9 to 18.9 feet below land surface
G-3788	254128080294401	MACTEC	CC/SPT	254128	802944	8.6	70	6-in. PVC	9.4	Yes	08-22-03	Open interval to 48 feet below land surface
G-3789	253813080295001	MACTEC	CC/SPT	253813	802950	8.0	70	6-in. PVC	9.6	Yes	08-25-03	Open interval to 58 feet below land surface
G-3790	253944080265801	MACTEC	CC/SPT	253944	802658	8.0	76	10-in. PVC	3	Yes	11-21-03	6.5-in. diameter hole below 10-in. casing. Open interval to 68 feet below land surface
G-3791	254541080250301	MACTEC	CC/SPT	254541	802503	8	79	10-in. PVC	5.8	Yes	12-03-03	6.5-in. diameter hole below 10-in. casing. Borehole bridged at 47 feet below land surface
G-3792	255036080231301	MACTEC	CC/SPT	255036	802313	8	90	10-in. PVC	9.3	Yes	01-07-04	6.5-in. diameter hole below 10-in. casing. Open interval to 84 feet below land surface
G-3793	255552080253901	MACTEC	CC/SPT	255552	802539	10	76	10-in. PVC	5.3	Yes	12-17-03	6.5-in. diameter hole below 10-in. casing. Open interval to 74 feet below land surface
G-3794	255420080282201	MACTEC	CC/SPT	255420	802822	9	70	10-in. PVC	4.8	Yes	01-13-04	6.5-in. diameter hole below 10-in. casing. Borehole bridged at 48 feet below land surface
G-3795	255015080290001	MACTEC	CC/SPT	255015	802900	9	90.5	10-in. PVC	3.5	Yes	01-17-04	6.5-in. diameter hole below 10-in. casing. Open interval to 88 feet below land surface
G-3816	255029080245302	Hydrologic Associates	AR	255029	802453	8.1	75	6-in. PVC	59.1	No	10-10-03	Injection well, open 59 to 74 feet below land surface
G-3817	255029080245303	Hydrologic Associates	AR	255029	802453	8.1	45	6-in. PVC	32.9	No	10-11-03	Injection well, open 33 to 43 feet below land surface
NWWF Corehole No. 13	--	Professional Services Industries	CC	--	--	8	85	No casing set	N/A	Yes	8-13-98	Core was taken adjacent to municipal water-supply well. S-3168. Abandoned
NWWF Corehole No. 14	--	Professional Services Industries	CC	--	-	8	76	No casing set	N/A	Yes	8-12-98	Core was taken adjacent to municipal water-supply well. S-3169. Abandoned
NWWF Corehole No. 15	--	Professional Services Industries	CC	--	--	8	95	No casing set	N/A	Yes	8-11-98	Core was taken adjacent to municipal water-supply well. S-3170. Abandoned

Collection of Borehole-Fluid Flow Data

To delineate borehole-fluid flow in the study area, digital optical borehole images, computed vuggy porosity data, caliper data, borehole-flowmeter data, fluid-conductivity data, and fluid-temperature data were collected for this study. These data were measured within uncased open-hole intervals in test coreholes that fully penetrate the Biscayne aquifer. Digital optical borehole images, computed vuggy porosity, and caliper logs were useful for selecting candidate high-permeability zones where fluid is flowing into or out of a borehole. Borehole flowmeters were used to measure vertical flow within a single well, and the data were used to identify areas of inflow or outflow to or from the borehole, respectively. Differences in hydraulic head between two transmissive hydrogeologic units produce vertical flow within a borehole, which was measured using vertical flowmeter logs. Ground water enters the borehole at the unit with the higher head and flows toward and out of the borehole at the unit with the lower head. If the heads of different transmissive zones are the same, no vertical flow will occur in the borehole.

Either a heat-pulse flowmeter, spinner flowmeter, or both were used to measure vertical borehole ground-water flow under ambient borehole conditions in the wells drilled under supervision by the USGS. The accuracy of the heat-pulse flowmeter measurements is limited because of the uncertainty concerning the amount of fluid flow bypassing the flexible-disk diverter on the flowmeter (Paillet, 2004). Cunningham and others (2006, in press) discussed measurements acquired with an electromagnetic flowmeter at wells G-3772 and G-3773 in the NWWF (fig. 2).

Logs of fluid conductivity, the reciprocal of fluid resistivity, can be used to assess changes in concentration of dissolved solids in the borehole fluid column (Keys, 1990). Fluid conductivity logs were useful to identify areas of the borehole that produce or receive water. Intervals of the borehole where there is inflow or outflow can be identified by sharp changes in borehole-fluid conductivity. Similarly, borehole-fluid temperature logs can be useful for delineation of zones contributing water to (or losing water from) the borehole by linking sharp changes in temperature to these intervals of inflow or outflow. Fluid-temperature logs, when used with flowmeter and fluid-conductivity data to define the movement of water through the wells, best allowed for delineation of intervals with inflow or outflow from the borehole; thus, these logs provide information on formation permeability.

Flowmeter data were used to observe vertical ground-water flow under existing hydraulic conditions in 16 wells during a period from December 20, 2002, to April 6, 2004. Stationary heat-pulse flowmeter measurements within the limestone of the Biscayne aquifer were obtained from wells G-3671, G-3733, G-3770, G-3771, G-3778, G-3782, G-3783, G-3784, and G-3788 to G-3795, and spinner flowmeter measurements were collected from wells G-3782, G-3783,G-3788, G-3789, G-3790, and G-3792 to G-3795. Heat-pulse flowmeter measurements were attempted at wells G-3772 and G-3773; however, both wells are within the West Well Field and flow velocities were higher than the resolution limits of the flowmeter (0.03 to 1.0 gal/min).

Fluid-temperature, fluid-conductivity, and flowmeter measurements were conducted in 13 wells for which the synoptic or quasi-synoptic measurements were collected for flowmeter data, conductivity, and temperature. Synoptic data were measured on the same day, and quasi-synoptic data were collected within a period ranging from 2 to 8 days. Borehole-fluid and fluid-temperature logs are reported for a period from March 28, 2003, to April 6, 2004. Fluid-conductivity and fluid-temperature logs were collected from wells G-3671, G-3733, G-3770, G-3771, G-3778, G-3782,G-3783, G-3784, and G-3788 to G-3795.

Molluscan and Benthic Foraminiferal Paleontology

Taxonomy of mollusks and foraminifera from selected lithofacies was determined to assist in interpretation of paleoenvironments. Mollusks from 13 core samples obtained from the test coreholes adjacent to the S-3168 and S-3170 production wells (fig. 2) were prepared and identified at the USGS Paleontology Laboratory in Reston, Va. Core samples were initially examined under a binocular microscope to observe diagnostic characteristics of the molluscan taxonomy and to compare the samples with those from previous studies (Mansfield, 1939; Olsson and Harbison, 1953; DuBar, 1958; Olsson and Petit, 1964; Abbott, 1974; Portell and others, 1992). Where appropriate, clay squeezes or latex casts were made of the molluscan molds to aid in their identification. Many molluscan species present in the Pleistocene units of southern Florida are extant or represented by close relatives, thus, living fauna are used to interpret paleoenvironmental settings. Publications by Perry and Schwengel (1955), Warmke and Abbott (1962), Abbott (1974), Andrews (1977), and Brewster-Wingard and others (2001) supported paleoenvironmental interpretations.

Benthic foraminifera were identified to the genus level, where possible, for 215 thin sections. Seven biofacies were recognized; one was distinguished by its absence of benthic foraminifera, and six were classified based on data from Bock and others (1971) and on biofacies suggested by Poag (1981) adapted to thin section analysis. The classification of biofacies by Poag (1981) is based on the predominant genera of benthic foraminifera present in a sample. Poag (1981) suggested counting 200 to 300 free specimens to establish the presence of a particular biofacies; however, the number of recognizable genera in samples used here is substantially less, thus, the interpreted assignments of biofacies are somewhat speculative. Data presented in Bock and others (1971), Rose and Lidz (1977), Poag (1981), and Lidz and Rose (1989) aided in the interpretation of paleoenvironmental conditions based on foraminiferal taxonomy.

Multidisciplinary Approach—Characterizing the Geologic Framework of the Biscayne Aquifer

Lithostratigraphy, molluscan and foraminiferal paleontology, lithofacies, depositional environments, and cyclostratigraphy were used to define a unique geologic framework for the rocks that compose the Biscayne aquifer in north-central Miami-Dade County. Lithostratigraphy is the description and systematic organization of rocks and sediments into distinctively named units based on the lithologic character of the rocks and sediments and their stratigraphic relations (Jackson, 1997). Molluscan and foraminiferal paleontology were useful in helping to establish paleoenvironments and environmental facies. Lithofacies is a mappable subdivision based on the mineralogic, petrographic, and paleontologic characteristics of rocks and sediments (Jackson, 1997). Depositional environments are: (1) geographically restricted areas where a sediment accumulates (or has accumulated), (2) described in geomorphic terms, and (3) characterized by physical, chemical, and biological conditions; for example, a marsh, lagoon, or shallow-marine shelf. Cyclostratigraphy is defined here as the analysis of several-foot-scale depositional cycles, defined similarly by James (1979) as upward-shallowing cycles (but herein including aggrading cycles), and deposited on ancient carbonate shelves and ramps. Even though some of the cycles reported herein have a chronostratigraphic significance (Perkins, 1977; Multer and others, 2002; Hickey, 2004), "cyclostratigraphy" is generally used herein to describe any regular repetition of lithofacies in a carbonate succession (Harris and others, 1999, p. 3) and not in the strict sense as to its application to geochronology as defined by Hilgen and others (2004).

Lithostratigraphy

Lithostratigraphic units of interest in this study (fig. 3) are contained in the Biscayne aquifer and include the Tamiami Formation, Anastasia Formation, Key Largo Limestone, Fort Thompson Formation, Miami Limestone, Pamlico Sand, and Lake Flirt Marl (Parker and Cooke, 1944; Causaras, 1987; Fish and Stewart, 1991). In the present study area, the Biscayne aquifer was interpreted to comprise mostly the Fort Thompson Formation, Miami Limestone, and Holocene peats and marls. These lithostratigraphic units and the uppermost Tamiami Formation are the focus of this study. The lithology, limiting extent, and thickness of lithostratigraphic units were determined by examination of continuously drilled cores and borehole-geophysical logs (especially digital optical borehole images). Graphical displays of lithologic core descriptions prepared for this study are presented in appendix I.

Molluscan Paleontology

The stratigraphic age of the Tamiami Formation was assessed in the one sample collected from the test corehole adjacent to well S-3170 (fig. 2), and the paleoenvironments and stratigraphic age of the Fort Thompson Formation were evaluated in the 13 samples collected for molluscan paleontology from two test coreholes adjacent to wells S-3168 and S-3170 (fig. 2). The test coreholes near production wells S-3168 and S-3170 were drilled as part of a separate project conducted by the Miami-Dade Water and Sewer Department in 1998 at the NWWF (fig. 2); earlier, Cunningham and others (2004b) evaluated additional samples in the general study area. The subsequent discussions summarize results from the two test coreholes, and appendix III presents detailed information on the mollusks found in specific samples.

Stratigraphic Age and Paleoenvironments from Test Corehole near S-3168

The samples from the test corehole near well S-3168 contain few diagnostic molluscan species. All of the identified species range in age from Pliocene to Holocene. The invertebrate assemblages in the core indicate an outer estuarine or shallow shelf paleoenvironment, with salinities ranging from 25 to 36 ppt (for example, figs. 5A-C and 6A). *Turbo castanea* (fig. 6B) and *Astralium phoebium*? indicate the presence of seagrass in the samples from 56 ft 10 in. to 56 ft 6 in. and from 57 ft 3 in. to 57 ft (Abbott, 1974). The images and description of selected Pelecypoda and Gastropoda species are shown in figures 5 and 6, respectively.

Stratigraphic Age and Paleoenvironments from Test Corehole near S-3170

The lowermost sample (95 ft 7 in. to 95 ft) of the test corehole near well S-3170 seems to be Pliocene in age on the basis of the few mollusks that can be positively identified. *Terebra aclinica* has been reported to be present only in the Pinecrest beds of the Tamiami Formation (Olsson, 1967). *Cymatoica marcottae*, a rare and distinctive clam found in the sample, was named from a "St. Petersburg fossil bed" by Olsson and Petit (1964); however, the formation was not identified. Numerous *Cyclocardia* are present in the sample that bears a strong resemblance to *Cyclocardia granulata* (Pliocene to early Pleistocene age), but the coarse granular texture of the sample prevented a positive identification. *Chione* specimens present in the sample do not seem to be typical *Chione cancellata*, common in the overlying sediments of the core, but bear a closer resemblance to *Chione procancellata* reported from the "*Cancellaria* Zone" by Mansfield (1932). These samples correspond to the lowermost lithologic samples collected at the G-3773 test corehole (fig. 1) and suggest that the uppermost part of the Tamiami Formation sampled in test coreholes in the study area is equivalent to the Pinecrest Sand Member of the Tamiami Formation (fig. 3) reported as Pliocene age by Scott (2001). Samples from 70 ft 5 in. to 70 ft and from 58 ft 6 in. to 58 ft 4 in. do not contain any mollusks that would be useful in distinguishing a Pleistocene verses a Pliocene age.

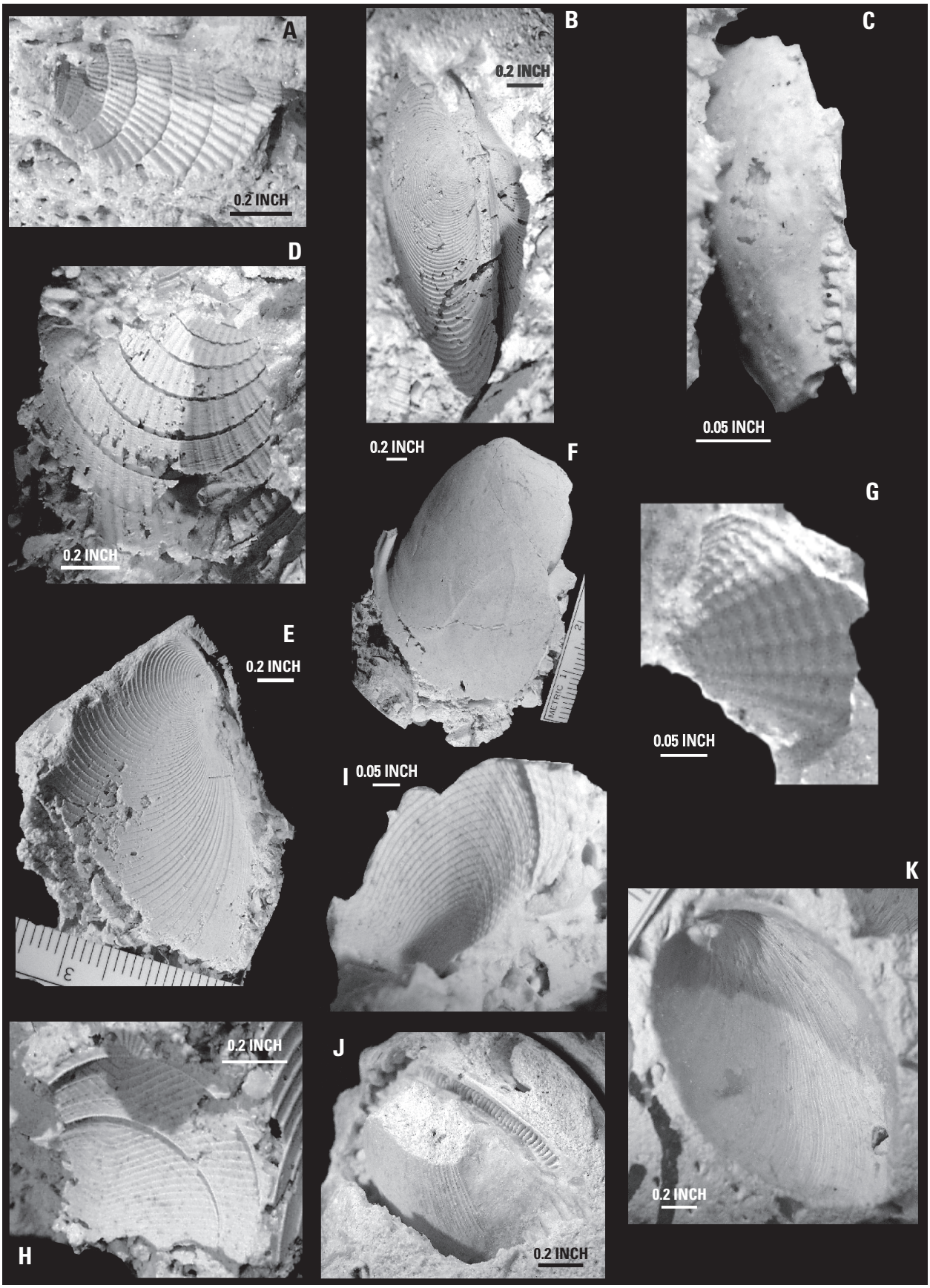
A
0.2 INCH
B
0.2 INCH
C
0.05 INCH
D
0.2 INCH
0.2 INCH
F
G
0.05 INCH
E
0.2 INCH
I
0.05 INCH
K
0.2 INCH
H
0.2 INCH
J
0.2 INCH

A	*Chione cancellata* (Linnaeus, 1767). External mold from sample collected at 56 feet 10 inches to 56 feet 6 inches in a test corehole adjacent to well S-3168, HFC2c2.
B	*Dosinia* sp. cf. Dosinia elegans (Conrad, 1843). Articulated external mold from sample collected at 56 feet 10 inches to 56 feet 6 inches in a test corehole adjacent to well S-3168, HFC2c2.
C	*Nuculana* sp. External mold from sample collected at 72 feet 5 inches to 72 feet 0 inches in a test corehole adjacent to well S-3168, HFC2a.
D	*Chione cancellata* (Linnaeus, 1767). External mold from sample collected at 52 feet 9 inches to 52 feet 5 inches in a test corehole adjacent to well S-3170, HFC2c2.
E	*Dosinia* sp. cf. *Dosinia elegans* (Conrad, 1843). External mold from sample collected at 52 feet 9 inches to 52 feet 5 inches in a test corehole adjacent to well S-3170, HFC2c2.
F	*Dosinia* sp. cf. *Dosinia elegans* (Conrad, 1843). Internal mold from sample collected at 52 feet 9 inches to 52 feet 5 inches in a test corehole adjacent to well S-3170, HFC2c2.
G-H	*Divaricella compsa* (Dall, 1903). External molds from sample collected at 52 feet 9 inches to 52 feet 5 inches in a test corehole adjacent to well S-3170, HFC2c2.
I	*Anadara aequalitas* (Tucker and Wilson, 1932). Internal mold from sample collected at 47 feet 4 inches to 46 feet 6 inches in a test corehole adjacent to well S-3170, HFC2c2.
J	*Phacoides (Bellucina) waccamawensis* (Dall, 1903). External mold from sample collected at 40 feet 4 inches to 39 feet 6 inches in a test corehole adjacent to well S-3170, HFC2e2.
K	*Anodontia alba* (Link, 1807). Articulated eternal mold from sample collected at 40 feet 4 inches to 39 feet 6 inches in a test corehole adjacent to well S-3170, HFC2e2.

Figure 5 (left). Selected Pelecypoda from core samples. Scale bars are shown with each specimen.

The sample from 52 ft 9 in. to 52 ft 5 in. contains relatively diverse molluscan fauna. The identified specimens range in age from Pliocene to Holocene. Several species (*Chione cancellata* (fig. 5 D), *Dosinia elegans* (fig. 5E-F), and *Phacoides* (*Bellalucina*) *waccamawensis* (fig. 5J) have been reported from the Caloosahatchee, Bermont, and Fort Thompson Formations (for example, DuBar, 1958; Portell and others, 1992). Conversely, *Divaricella compsa* (fig. 5G-H) ranges only from Pliocene to Pleistocene, and *Turritella apicalis* (fig. 6C) is reported only from Pliocene age beds presumably from the Caloosahatchee Formation (Mansfield, 1939; DuBar, 1958). The occurrence of *Turritella apicalis* seems to restrict this sample to the Pliocene; however, it is possible that either the sample needs to be reworked or the range of the species needs to be extended. The latter seems probable because data reported by Cunningham and others (2004b) indicate that its highest occurrence within the Fort Thompson Formation is in HFC2g3 at test corehole G-3732, an occurrence presumably well within the Pleistocene (Multer and others, 2002). The occurrence of *Anadara aequalitas* (fig. 5I) at 47 ft 4 in. to 46 ft 6 in. within HFC2d may place this sample in the lower Pleistocene because it has not been reported from above the Bermont formation (informal) (DuBar, 1958; Olsson and Harbison, 1953; Olsson and Petit, 1964). This occurrence suggests the lower part of the Fort Thompson Formation below HFC2d1 could be assigned to the lower Pleistocene, contrary to assignment of the Fort Thompson Formation to the late Pleistocene (Scott, 2001; Multer and others, 2002). There are no chronostratigraphic data (for example, microfossil taxonomy) herein, however, to corroborate an early Pleistocene age assignment to the lower Fort Thompson Formation.

Most molluscan species that occur in the samples from 40 ft 4 in. to 39 ft 6 in. and from 28 ft 4 in. to 27 ft range in age from Pliocene to Holocene (fig. 5J-K and 6D-F). The exception is *Lithopoma americanum* (fig. 6G) in the sample from 40 ft 4 in. to 39 ft 6 in. No published records of fossil occurrence of this species could be found, indicating its range needs to be extended. The two uppermost samples in the test corehole adjacent to well S-3170 (27 ft to 26 ft 10 in. and 20 ft 3 in. to 19 ft 6 in.) contain very few recognizable species, ranging in age from Pliocene or Pleistocene to Holocene.

The molluscan species present indicate an outer estuarine to shallow shelf paleoenvironment with a salinity range of 25 to 35 ppt. Beginning with the sample at about 70 ft 5 in. to 70 ft to the uppermost sample in the test corehole adjacent to well S-3170 (app. III), the mollusks are evidence of a very shallow, sandy or muddy bottom. *Parastarte triquetra* commonly are found on mudbanks and sandbars (Warmke and Abbott, 1962; Abbott, 1974). As noted in the present study and by Perry and Schwengel (1955), the presence of seagrass is indicated by *Turbo castanea* in the sample from 52 ft 9 in. to 52 ft 5 in. The assemblages in the samples from 46 ft 6 in. to 26 ft 10 in. indicate mixed hard-bottom communities with infaunal sand dwellers (*Anodontia alba*, *Codakia orbicularis*); mollusks that live in or on sponges, corals, or ascidians

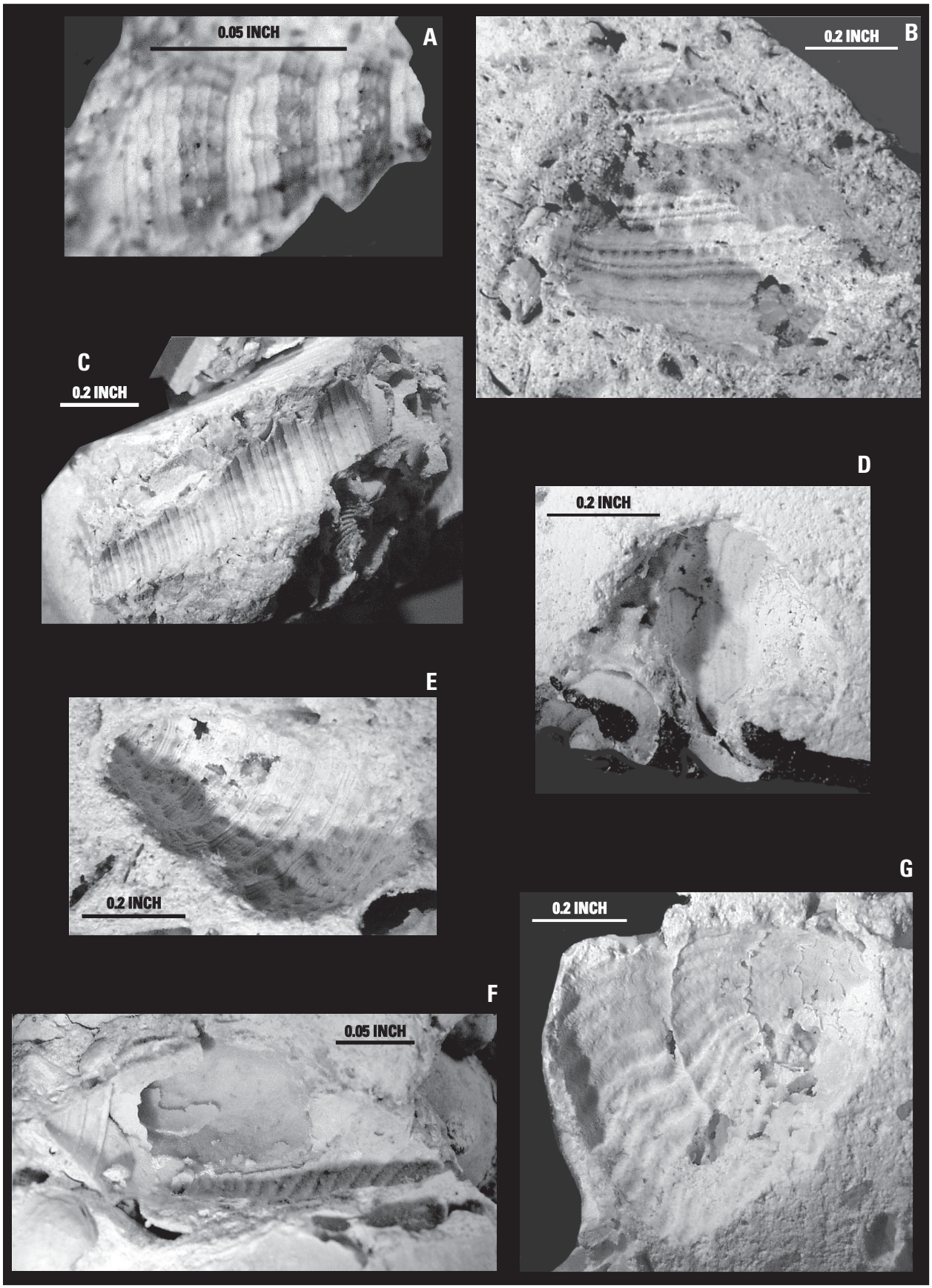
A
0.05 INCH
B
0.2 INCH
C
0.2 INCH
D
0.2 INCH
E
0.2 INCH
F
0.05 INCH
G
0.2 INCH

(arcids, *Lithopoma americanum*, *Vermicularia spirata*); and epiphytic mollusks (*Turbo castanea*, *Modulus modulus*, *Cerithium* sp.) that indicate the presence of seagrass as noted in the present study and by Abbott (1974).

Foraminiferal Paleontology

The occurrence of stratigraphically important foraminiferal taxa and other allochems (mollusks, ostracodes, echinoids, red algae, and charophytes) identified in the 215 thin sections obtained from the Tamiami Formation, Fort Thompson Formation, and Miami Limestone is presented in table 2. From these thin sections, seven major foraminiferal biofacies (table 3) were recognized that assisted in definition in depositional environments. Key foraminiferal taxa are shown in figure 7.

A	*Turritella subannulata* (Heilprin, 1887). External mold from sample collected at 72 feet 5 inches to 72 feet 0 inches in a test corehole adjacent to well S-3168, HFC2a.
B	*Turbo castanea* (Gmelin, 1791). External mold from sample collected at 56 feet 10 inches to 56 feet 6 inches in a test corehole adjacent to well S-3168, HFC2c2.
C	*Turritella apicalis* (Heilprin, 1886). External mold from sample collected at 52 feet 9 inches to 52 feet 5 inches in a test corehole adjacent to well S-3170, HFC2c2.
D	*Modulus modulus* (Linnaeus, 1758). External mold from sample collected at 40 feet 4 inches to 39 feet 6 inches in a test corehole adjacent to well S-3170, HFC2e2.
E	*Cerithium* sp. cf. *Cerithium vicinia* (Olsson and Harbison, 1953). External mold from sample collected at 40 feet 4 inches to 39 feet 6 inches in a test corehole adjacent to well S-3170, HFC2e2.
F	*Oliva* sp. External mold from sample collected at 40 feet 4 inches to 39 feet 6 inches in a test corehole adjacent to well S-3170, HFC2e2.
G	*Lithopoma americanum* (Gmelin, 1791). External mold from sample collected at 40 feet 4 inches to 39 feet 6 inches in a test corehole adjacent to well S-3170, HFC2e2.

Figure 6 (left). Selected Gastropoda from core samples. Scale bars are shown with each specimen.

Lithofacies and Depositional Environments

Lithofacies and vertical lithofacies successions (Kerans and Tinker, 1997) are the two principal lithostratigraphic elements identified in this study. A lithofacies is a lateral mappable subdivision of a designated stratigraphic unit, distinguished from adjacent subdivisions on the basis of lithology, including all mineralogic and petrographic characters and those paleontologic characters that influence the appearance, composition, or texture of the rock (Jackson, 1997). A vertical lithofacies succession is a distinct stack of lithofacies that records upward shallowing or an amalgamation of a persistent environment as accommodation fills within a cycle-scale relative sea-level rise (Kerans and Tinker, 1997). Lithofacies were arranged into vertical lithofacies successions that represent either upward-shallowing units or units composed entirely or mostly of a distinct lithofacies representative of a single prevailing depositional water depth. Assessment of sedimentary characteristics and paleontology of lithofacies, their vertical arrangement within vertical lithofacies successions, and their relation to bounding surfaces of the successions produced inferred major depositional environments.

Lithofacies

Lithofacies are the fundamental descriptive rock components of this study. Sixteen lithofacies delineate the sedimentary rocks that form the Fort Thompson Formation and Miami Limestone in the study area. Many of the lithofacies may be composed of a substantial amount of quartz sand grains (generally less than 50 percent). In this case, “sandy” is added as a prefix to the lithofacies type on plates 1 to 4. “Touching vugs,” a prefix to a lithofacies type, refers to vuggy porosity that forms an interconnected pore system (Lucia, 1999).
The 16 lithofacies include: (1) peloid packstone and grainstone, (2) peloid wackestone and packstone, (3) *Planorbella* floatstone and rudstone, (4) gastropod floatstone and rudstone, (5) conglomerate, (6) autobreccia, (7) pedogenic limestone (laminated calcrete, massive calcrete, and root-mold limestone), (8) mudstone and wackestone, (9) laminated peloid packstone and grainstone, (10) skeletal packstone and grainstone, (11) coral framestone, (12) pelecypod floatstone and rudstone, (13) touching-vug pelecypod floatstone and rudstone, (14) vuggy wackestone and packstone, (15) quartz sandstone and skeletal quartz sandstone, and (16) quartz sand (table 4). Cunningham and others (2004b) provide detailed descriptions of most of these lithofacies and inferred environments of deposition, although some lithofacies terminology and definition of depositional environments are modified herein (table 4). For example, *Planorbella* floatstone and rudstone is added to the present study. The three principal lithofacies that typically have the relatively highest yield of ground-water flow into or out of wellbores are peloid packstone and grainstone, laminated peloid packstone and grainstone, and touching-vug pelecypod floatstone and rudstone.

Table 2. Occurrence of stratigraphically important benthic foraminiferal taxa and other allochems in selected test coreholes.

[Sample depth, in feet below land surface. Biofacies 1, foraminifera absent (commonly contains smoothed-walled ostracods, commonly together with gastropods); biofacies 2, *Ammonia* predominant; biofacies 3, *Elphidium* predominant; biofacies 4, miliolids predominant; biofacies 5, archaiasinids, soritids, and peneroplids predominant; and biofacies 6, amphisteginids predominant. Annotations: X, present; ?, presence is questionable; **X**, predominant foraminiferal taxa; HFC, high-frequency cycle; TF, Tamiami Formation; forams, foraminifers]

Local well identifier	Sample depth	HFC/Fm	Lithofacies	Biofacies	Rotaliform forams	*Rotalia*	*Ammonia*	*Elphidium*	Miliolids	Soritids	*Sorites*	*Parasorites*	Archaiasinids	*Archaias*	*Androsina*	*Cyclorbiculina*	*Cycloputeolina*	Peneroplids	*Peneroplis*	Bolivinids	*Bolivina*	*Gypsina*	*Nonion*	Amphisteginids	Globigerinids	*Spaerogypsina*	Agglutinating forams	Mollusks	Gastropods	Bivalves	Ostracods	Echinoids	Red Algae	Bryozoans	Charophytes
G-3678	23.4	HFC3a	*Planorbella* floatstone/rudstone	1																								X			X				
	24.80	HFC2h	Mudstone/wackestone	1-2			X																						X		X				X
	33.3	HFC2g3	Mudstone/wackestone	1																											X				
G-3679	15.6	HFC3a	Mudstone/wackestone	1																								X?			X				
	27.1	HFC2h	Mudstone/wackestone	3?			X	X																							F				
	35.7	HFC2g3	Mudstone/wackestone	1																									X		X				
G-3681	14.9	HFC3b	Mudstone/wackestone	2-3			X	X																					X		X				
G-3683	13.1	HFC4	Peloid wackestone/packstone	-																								X							
G-3684	16.0	HFC4	Peloid wackestone/packstone	-																															
	16.4	HFC4	Peloid wackestone/packstone	5					X				X					X																	
	17.4	HFC3b	Mudstone/wackestone	2			F	F																							X				
	19.8	HFC3b	Skeletal packstone/grainstone	5									X					X																	
	22.0	HFC3a	Mudstone/wackestone	1?-2			**X**?	X																							X				
	23.2	HFC3a	Pelecypod floatstone/rudstone	5									**X**					**X**																	
	27.2	HFC3a	Pelecypod floatstone/rudstone	5									X					X																	
	30.7	HFC3a	Touching-vug pelecypod floatstone/rudstone	-																										X					
	31.5	HFC2h	Skeletal packstone/grainstone	5														X													X				
G-3685	28.5	HFC2h	Skeletal packstone/grainstone	1?																											X				
G-3687	14.2	HFC3a	Mudstone/wackestone	4-5			X		X				X																						
	15.5	HFC3a	Skeletal packstone/grainstone	4-5					X				X																						
	16.5	HFC3a	Skeletal packstone/grainstone	4-5					X									X																	
	17.5	HFC3a	Skeletal packstone/grainstone	5														X																	
	18.8	HFC3a	Touching-vug pelecypod floatstone/rudstone	1?																											X				
	21.1	HFC3a	*Planorbella* floatstone/rudstone	-																								X			X?				
	24.1	HFC2h	Skeletal packstone/grainstone	2			X																												
	25.6	HFC2h	Pelecypod floatstone/rudstone	2			X																												
G-3733	49.94	HFC2c2	Very sandy pelecypod floatstone/rudstone	4-5					X									X																	
	53.28	HFC2c2	Skeletal quartz sandstone	6?																				X											
G-3770	71.00	Tamiami Fm	Mudstone/wackestone	2-3			X	X																					X		**X**				
G-3772	11.89	HFC3b	Pedogenic limestone	5					X	**X**			**X**						X														X		
	14.03	HFC3a	*Planorbella* floatstone/rudstone	1			X																						**X**		**X**				X
G-3772	14.95	HFC3a	*Planorbella* floatstone/rudstone	1																									X		X				X
	15.60	HFC3a	Mudstone/wackestone	5					X	X								X																	

Table 2. Occurrence of stratigraphically important benthic foraminiferal taxa and other allochems in selected test coreholes. (Continued)

Local well identifier	Sample depth	HFC/Fm	Lithofacies	Biofacies	Rotaliform forams	*Rotalia*	*Ammonia*	*Elphidium*	Miliolids	Soritids	*Sorites*	*Parasorites*	Archaiasinids	*Archaias*	*Androsina*	*Cyclorbiculina*	*Cycloputeolina*	Peneroplids	*Peneroplis*	Bolivinids	*Bolivina*	*Gypsina*	*Nonion*	Amphisteginids	Globigerinids	*Spaerogypsina*	Agglutinating forams	Mollusks	Gastropods	Bivalves	Ostracods	Echinoids	Red Algae	Bryozoans	Charophytes
	16.06	HFC3a	Conglomerate	4?				X?	X	X																			X						
	16.36	HFC3a	Mudstone/wackestone	3?				X?	X																										
	17.20	HFC3a	Skeletal packstone/grainstone	3-5?	X		X	X	X				X															X				X			
	18.03	HFC3a	Pelecypod floatstone/rudstone	5			X	X	X	X			X					X				X?						X				X			
	19.70	HFC3a	Pelecypod floatstone/rudstone	4-5					X	X																		X							
	21.47	HFC3a	Touching-vug pelecypod floatstone/rudstone	5					X	X			X																						
	22.30A	HFC3a	*Planorbella* floatstone/rudstone	1																									X		X				X
	22.30B	HFC3a	*Planorbella* floatstone/rudstone	1																									X		X				X
	22.89	HFC2h	Skeletal packstone/grainstone	5	X		X						X					X										X							
	23.14	HFC2h	Skeletal packstone/grainstone	3-4	X			X	X									X										X				X	X		
	23.55	HFC2h	Skeletal packstone/grainstone	3-5				X	X				X															X				X	X		
	25.35	HFC2h	Pelecypod floatstone/rudstone	4-5	X				X	X																		X				X	X		X	
	27.35	HFC2g3	Pelecypod floatstone/rudstone	5	X				X				X															X					X		
	28.27	HFC2g3	Pelecypod floatstone/rudstone	4?-5?	X				X	X																				X	X			X	
	28.77	HFC2g3	Pelecypod floatstone/rudstone	5	X		X?		X	X			X															X				X	X		X	
	29.69	HFC2g3	Pelecypod floatstone/rudstone	3-5?	X			X	X				X					X																	
	30.47	HFC2g2	Sandy skeletal packstone/grainstone	3-5?	X			X	X									X										X				X			
	31.15	HFC2g2	Skeletal packstone/grainstone	3	X			X	X									X										X					X		
	31.65	HFC2g2	Skeletal packstone/grainstone	3-4	X		X	X	X																			X					X		
	31.98	HFC2g2	Skeletal packstone/grainstone	3-5?	X			X	X									X										X					X		
	32.90	HFC2g2	Pelecypod floatstone/rudstone	5	X				X	X			X															X					X		
	33.73	HFC2g1	*Planorbella* floatstone/rudstone	3-5?				X	X										X									X					X		
	33.95	HFC2g1	*Planorbella* floatstone/rudstone	1?-5?														X										X				X			
	34.32	HFC2g1	Pelecypod floatstone/rudstone	4				X	X									X															X		
	34.49	HFC2g1	Pelecypod floatstone/rudstone	3			X	X	X																			X				X			
	34.53	HFC2g1	Pelecypod floatstone/rudstone	3-5	X			X	X					X					X									X					X		
	36.49	HFC2e2	Sandy pelecypod floatstone/rudstone	3-5				X	X	X																									
	37.57	HFC2e2	Sandy pelecypod floatstone/rudstone	3-5	X			X	X				X															X					X		
	38.24	HFC2e2	Sandy pelecypod floatstone/rudstone	3-5				X	X									X										X							
	41.97	HFC2d	Skeletal packstone/grainstone	1?-3?-5?	X			X		X																		X				X	X		
	42.26	HFC2d	Skeletal packstone/grainstone	5	X			X	X	X			X																X				X		
	42.65	HFC2d	Skeletal packstone/grainstone	1-4?	X				X				X															X				X	X		
	42.98	HFC2d	Skeletal packstone/grainstone	5	X				X				X					X										X				X	X		
	43.98	HFC2d	Skeletal packstone/grainstone	4-5	X				X	X																							X		
	44.90	HFC2d	Skeletal packstone/grainstone	5					X				X						X														X		
	46.13	HFC2d	Sandy *Planorbella* floatstone/rudstone	2-3			X	X																				X				X			

Table 2. Occurrence of stratigraphically important benthic foraminiferal taxa and other allochems in selected test coreholes. (Continued)

Local well identifier	Sample depth	HFC/Fm	Lithofacies	Biofacies	Rotaliform forams	*Rotalia*	*Ammonia*	*Elphidium*	Miliolids	Soritids	*Sorites*	*Parasorites*	Archaiasinids	*Archaias*	*Androsina*	*Cyclorbiculina*	*Cycloputeolina*	Peneroplids	*Peneroplis*	Bolivinids	*Bolivina*	*Gypsina*	*Nonion*	Amphisteginids	Globigerinids	*Spaerogypsina*	Agglutinating forams	Mollusks	Gastropods	Bivalves	Ostracods	Echinoids	Red Algae	Bryozoans	Charophytes
G-3772	46.88	HFC2d	Skeletal sandstone	2-3			X	X																					X				X			
	47.20	HFC2d	Skeletal sandstone	2			X		X																			X				X			
	51.60	HFC2c2	Sandy pelecypod floatstone/rudstone	2-4			X	X	X				X															X				X			
	51.89	HFC2c2	Sandy pelecypod floatstone/rudstone	2-5			X	X					X															X				X			
	52.49	HFC2c2	Sandy pelecypod floatstone/rudstone	3-5				X					X										X?					X				X			
	52.99	HFC2c2	Sandy pelecypod floatstone/rudstone	4-5	X		X		X				X															X				X			
	54.66	HFC2c2	Sandy pelecypod floatstone/rudstone?	4	X		X		X													X						X				X	X		
	57.85	HFC2c2	Sandy pelecypod floatstone/rudstone	5									X					X						X				X				X			
	58.29	HFC2c2	Sandy pelecypod floatstone/rudstone	2			X	X																				X							
	58.62	HFC2c2	Sandy pelecypod floatstone/rudstone	2	X		X	X																				X				X			
	58.90	HFC2b	Sandy pelecypod floatstone/rudstone	2			X																					X				X			
	59.20	HFC2b	Sandy skeletal packstone/grainstone	2-3	X		X	X																				X				X			
	60.12	HFC2b	Sandy skeletal packstone/grainstone	4					X																										
	60.43	HFC2b	Sandy pelecypod floatstone/rudstone	4?					X	X																		X				X			
	61.51	HFC2b	Sandy pelecypod floatstone/rudstone	5					X	X								X										X				X			
	64.69	HFC2a	Sandy pelecypod floatstone/rudstone	5					X	X				X				X										X				X			
	65.77	HFC2a	Sandy pelecypod floatstone/rudstone	5					X	X				X				X										X				X			
	66.90	HFC2a	Sandy skeletal packstone/grainstone	3-5			X	X	X	X				X				X										X				X			
	67.31	HFC2a	Sandy skeletal packstone/grainstone	5/3	X			X	X	X			X															X							
	67.70	HFC2a	Sandy skeletal packstone/grainstone	5?	X		X		X				X															X				X			
	67.86	HFC2a	Sandy skeletal packstone/grainstone	5					X				X					X						X?											
	68.61	HFC2a	Sandy skeletal packstone/grainstone	5			X		X	X												X												X	
	70.20	HFC2a	Sandy conglomerate	2-5			X		X	X													X?					X				X			
	70.87	HFC2a	Sandy conglomerate	6?			X	X																X											
	70.9	HFC2a	Sandy conglomerate	3	X			X																							X	X			
	71.6	HFC2a	Sandy conglomerate	3-4	X				X																							X			
	72.88	HFC2a	Sandy conglomerate	?	X																			X?				X							
	73.03	HFC2a	Sandy conglomerate	?	X																							X							
	73.86	HFC2a	Sandy conglomerate	6?	X		X																	X?				X				X			
	74.2	Tamiami Fm	Sandy conglomerate	3	X			X																								X			
	75.00	Tamiami Fm	Sandy conglomerate?	6																				X	X			X				X			
G-3779	16.17	HFC5	Peloid packstone/grainstone	4					X																		X				X				
	17.17	HFC5	Peloid packstone/grainstone	4					X																									X	
	18.20	HFC5	Peloid packstone/grainstone	4					X																				X		X			X	
	21.87	HFC3b	Mudstone/wackestone	2	X		X																						X		X				
	21.93	HFC3b	Mudstone/wackestone	2?				X?	X																				X		X				

Table 2. Occurrence of stratigraphically important benthic foraminiferal taxa and other allochems in selected test coreholes. (Continued)

Local well identifier	Sample depth	HFC/Fm	Lithofacies	Biofacies	Rotaliform forams	*Rotalia*	*Ammonia*	*Elphidium*	Miliolids	Soritids	*Sorites*	*Parasorites*	Archaiasinids	*Archaias*	*Androsina*	*Cyclorbiculina*	*Cycloputeolina*	Peneroplids	*Peneroplis*	Bolivinids	*Bolivina*	*Gypsina*	*Nonion*	Amphisteginids	Globigerinids	*Spaerogypsina*	Agglutinating forams	Mollusks	Gastropods	Bivalves	Ostracods	Echinoids	Red Algae	Bryozoans	Charophytes
	22.41	HFC3b	Mudstone/wackestone	2-5?	X		X	X					X															X	X						
	23.45	HFC3b	Pedogenic limestone (crumbly mudstone)	2-3			X	X	X																										
	24.30	HFC3b	Skeletal packstone/grainstone	2-4?			X		X									X													X				
G-3779	25.45	HFC3b	Skeletal packstone/grainstone	4-5					X				X					X														X			
	26.53	HFC3b	Pelecypod floatstone/rudstone	5					X				X					X									X	X				X			
	26.70	HFC3b	Pelecypod floatstone/rudstone	5			X		X	X?			X																						
	27.50	HFC3a	*Planorbella* floatstone/rudstone	1																									X		X				X
	29.74	HFC3a	Laminated peloid packstone/grainstone	3-4?				X	X				X																						
	30.80	HFC3a	Pelecypod floatstone/rudstone	3-4	X			X	X				X																						
	34.98	HFC3a	*Planorbella* floatstone/rudstone	1																									X		X				X
	36.10	HFC3a	*Planorbella* floatstone/rudstone	1																									X		X				X
	38.55	HFC2h	Skeletal packstone/grainstone	2			X	X		X?			X					X											X			X			
	39.30	HFC2h	Pelecypod floatstone/rudstone	3-5	X		X?	X	X				X																	X		X			
	40.43	HFC2h	Pelecypod floatstone/rudstone	5	X		X	X	X				X																	X	X	X			
	43.60	HFC2g3	Touching-vug pelecypod floatstone/rudstone	5	X				X	X			X											X				X				X			
	46.72	HFC2g2	Skeletal packstone/grainstone	3-5			X	X	X									X										X				X			
	47.31	HFC2g2	Skeletal packstone/grainstone	5	X				X				X					X										X				X			
	47.52	HFC2g2	Skeletal packstone/grainstone	5/1-1a	X				X				X															X			X	X			
	48.58	HFC2g2	Touching-vug pelecypod floatstone/rudstone	1-2			X	X	X																			X	X		X	X			X
	49.02	HFC2f	Skeletal wackestone/packstone	1																											X				X
	49.71	HFC2f	Skeletal wackestone/packstone	1																											X				X
	51.94	HFC2f	*Planorbella* floatstone/rudstone	1/3-6	X			X																X							X	X			X
	52.11	HFC2e2	Mudstone/wackestone	1																											X				X
	52.65	HFC2e2	Mudstone/wackestone	1-2/3			X	X																					X		X				X
	53.97	HFC2e2	Touching-vug pelecypod floatstone/rudstone	3-5	X			X	X				X					X											X	X		X			
	54.76	HFC2d	Mudstone/wackestone	1																											X				
	55.19	HFC2d	*Planorbella* floatstone/rudstone	1/2-4?																											X	X			X
	58.50	HFC2d	Sandy pelecypod floatstone/rudstone	4-6	X				X	X														X			X								
	59.51	HFC2d	Sandy pelecypod floatstone/rudstone	3?				X	X																				X						
	60.25	HFC2d	Sandy pelecypod floatstone/rudstone	6?	X		X		X	X											X			X											
G-3782	43.30	HFC2e2	Mudstone/wackestone	1																											X				X
G-3784	31.00	HFC3a	*Planorbella* floatstone/rudstone	1																											X				X
G-3788	37.66	HFC2f	Mudstone/wackestone	1																											X				X
	43.60	HFC2e1	Laminated calcrete	1					X																						X				

Table 2. Occurrence of stratigraphically important benthic foraminiferal taxa and other allochems in selected test coreholes. (Continued)

Local well identifier	Sample depth	HFC/Fm	Lithofacies	Biofacies	Rotaliform forams	*Rotalia*	*Ammonia*	*Elphidium*	Miliolids	Soritids	*Sorites*	*Parasorites*	Archaiasinids	*Archaias*	*Androsina*	*Cyclorbiculina*	*Cycloputeolina*	Peneroplids	*Peneroplis*	Bolivinids	*Bolivina*	*Gypsina*	*Nonion*	Amphisteginids	Globigerinids	*Spaerogypsina*	Agglutinating forams	Mollusks	Gastropods	Bivalves	Ostracods	Echinoids	Red Algae	Bryozoans	Charophytes
G-3789	40.67	HFC2f	Mixed mudstone/wackestone and gastropod floatstone/rudstone	1																									X		X					X
	48.80	HFC2e1	Skeletal packstone/grainstone	5?				X	X				X															X					X		
	53.90	HFC2d	Touching-vug pelecypod floatstone/rudstone with sandstone matrix	3?				X																				X						X	
G-3790	40.97	HFC2g2	*Planorbella* floatstone/rudstone	1																									X		X				X
	44.50	HFC2f	Mudstone/wackestone	1/2-3			X	X																					X		X				
	50.02	HFC2e2	Mudstone/wackestone	1																											X				X
	55.70	HFC2d	Sandy pelecypod floatstone/rudstone	3				X																					X						
G-3791	16.60	HFC3b	Mudstone/wackestone	2-3			X	X																					X		X				
	28.10	HFC3a	Touching-vug pelecypod floatstone/rudstone	4					X																		X			X					
	29.90	HFC3a	*Planorbella* floatstone/rudstone	1																									X	X	X				X
	35.55	HFC2h	Sandy pelecypod floatstone/rudstone	1/2-3?	X																								X		X				X
	35.63	HFC2h	Sandy pelecypod floatstone/rudstone	1																									X		X				X
	43.20	HFC2f	Mudstone/wackestone	1/5?					X				X					X											X		X				
	51.25	HFC2d	Mudstone/wackestone	1/2-3?																								X			X				
	53.50	HFC2d	Sandy mudstone/wackestone	3			X	X																							X				
	58.30	HFC2c2	Mudstone/wackestone	1?/3?				X																				X	X		X				
	58.50	HFC2c2	Mudstone/wackestone	1																									X		X				
	58.60	HFC2c2	Mudstone/wackestone	1-4					X																						X				X
	63.35	Tamiami Fm	Sandy gastropod floatstone	2			X	X																					X		X				
	75.60	Tamiami Fm	Sandy pelecypod floatstone/rudstone	1																											X				
	75.70	Tamiami Fm	Sandy pelecypod floatstone/rudstone	5					X	X														X?				X			X	X		X	
	76.30	Tamiami Fm	Sandy pelecypod floatstone/rudstone	6?				X	X																			X			X			X	
	76.60	Tamiami Fm	Sandy pelecypod floatstone/rudstone	3?				X	X	X?																		X	X		X		X	X	
G-3793	6.19	HFC3b	*Planorbella* floatstone/rudstone	1																									X		X				X
	17.19	HFC2h	Skeletal packstone	5					X	X																									
	21.25	HFC2h	Laminated calcrete and skeletal packstone	3/4-5?	X		X	X	X	X								X																	
	59.57	HFC2a	Auto breccia wackestone	mixed			X		X	X																X					X	X			
	63.92	Tamiami Fm	Sandy pelecypod floatstone/rudstone	6																			X	X	X										
	65.40	Tamiami Fm	Sandy pelecypod floatstone/rudstone	6					X															X	X										
G-3794	19.35	HFC2h	Skeletal packstone/grainstone	3-5				X	X	X																		X			X	X			
	63.10	Tamiami Fm	Sandy pelecypod floatstone/rudstone	6																				X	X			X				X			
G-3795	17.57	HFC3a	Burrowed wackestone	2-5			X	X	X	X																					X				
	35.00	HFC2f	*Planorbella* mudstone	1-3				X																							X				X
	59.00	Tamiami Fm	Skeletal packstone/grainstone	2-3			X	X	X																			X				X			

Table 2. Occurrence of stratigraphically important benthic foraminiferal taxa and other allochems in selected test coreholes. (Continued)

Local well identifier	Sample depth	HFC/Fm	Lithofacies	Biofacies	Rotaliform forams	*Rotalia*	*Ammonia*	*Elphidium*	Miliolids	Soritids	*Sorites*	*Parasorites*	Archaiasinids	*Archaias*	*Androsina*	*Cyclorbiculina*	*Cycloputeolina*	Peneroplids	*Peneroplis*	Bolivinids	*Bolivina*	*Gypsina*	*Nonion*	Amphisteginids	Globigerinids	*Spaerogypsina*	Agglutinating forams	Mollusks	Gastropods	Bivalves	Ostracods	Echinoids	Red Algae	Bryozoans	Charophytes
	59.70	Tamiami Fm	Skeletal packstone/grainstone	2-3			X	X	X																			X							
	61.54	Tamiami Fm	Pelecypod floatstone/rudstone and skeletal packstone/grainstone	5	X				X	X								X						X				X							
	63.92	Tamiami Fm	Pelecypod floatstone/rudstone	4?	X				X																X			X				X			
S-3169[1]	8.3	HFC5	Peloid packstone/grainstone	5										X																					
	9.6	HFC5	Peloid packstone/grainstone	?																								X			X				
	12.21	HFC3b	Massive calcrete	-																															
S-3169[1]	13.52	HFC3a	*Planorbella* floatstone/rudstone	1-2				X																					X		X				
	14.9	HFC3a	*Planorbella* floatstone/rudstone	1																									X		X				
	20.2	HFC3a	Mudstone/wackestone	3?				X	X																							X				
	22.5	HFC3a	Mudstone/wackestone	1					X																				X	X	X				
	23.9	HFC3a	Mudstone/wackestone	1																															
	25.75	HFC2g3	Autobreccia	3-4					X				X?							X								X			X	X			
	27.7	HFC2g3	Pelecypod floatstone/rudstone	4?	X		X?		X			X?													X			X				X			
	28.9	HFC2g3	Skeletal wackestone/packstone	2-3	X			X																				X			X	X			
	29.24	HFC2g3	Sandy skeletal packstone/grainstone	3-5				X				X?				X?												X				X			
	30.3	HFC2g2	Skeletal wackestone/packstone	3-5				X	X				X?				X?	X											X	X		X			
	31.5	HFC2g2	Pelecypod floatstone/rudstone	3-5				X	X				X						X										X	X					
	33.27	HFC2e2	Laminated calcrete and skeletal wackestone/packstone	2-5			X?	X				X?																		X		X			
	35.2	HFC2e2	Sandy pelecypod floatstone/rudstone	3-5				X				X?																X				X			
	36.3	HFC2e2	Sandy pelecypod floatstone/rudstone	4-5					X			X																	X	X	X	X			
	37.9	HFC2e2	Sandy pelecypod floatstone/rudstone	5?								X?																X				X			
	40.2	HFC2d	Sandy skeletal packstone	2-5?			X					X?																	X	X		X			
	42.1	HFC2d	Sandy skeletal packstone	5?								X?							X?									X				X			
	43.0	HFC2d	Sandy skeletal packstone	5					X				X				X?											X				X			
	47.0	HFC2d	Sandy touching-vug pelecypod floatstone/rudstone	5?					X				X																			X			
	47.2	HFC2c2	Sandy skeletal packstone	3	X			X																				X				X			
	48.1	HFC2c2	Sandy skeletal packstone	4-5					X				X															X				X			
	50.2	HFC2c2	Sandy touching-vug pelecypod floatstone/rudstone	4					X																			X				X			
	51.45	HFC2c2	Sandy skeletal grainstone	3-5				X					X															X				X			
	52.45	HFC2c2	Sandy skeletal packstone	5						X							X?											X				X			
	54.45	HFC2c2	Sandy pelecypod floatstone/rudstone	5?	X				X				X											X?				X							
	55.5	HFC2c2	Sandy pelecypod floatstone/rudstone	3-5	X			X	X									X			X							X				X			

Local well identifier	Sample depth	HFC/Fm	Lithofacies	Biofacies	Rotaliform forams	*Rotalia*	*Ammonia*	*Elphidium*	Miliolids	Soritids	*Sorites*	*Parasorites*	Archaiasinids	*Archaias*	*Androsina*	*Cyclorbiculina*	*Cycloputeolina*	Peneroplids	*Peneroplis*	Bolivinids	*Bolivina*	*Gypsina*	*Nonion*	Amphisteginids	Globigerinids	*Spaerogypsina*	Agglutinating forams	Mollusks	Gastropods	Bivalves	Ostracods	Echinoids	Red Algae	Bryozoans	Charophytes
	64.75	HFC2b	Sandy pelecypod floatstone/rudstone	5									X															X				X			
	68.0	HFC2b	Sandy pelecypod floatstone/rudstone	5?	X				X						X?	X	X											X							
	69.08	HFC2a	Sandy skeletal packstone/grainstone	5								X?					X?	X										X							
	70.09	HFC2a	Sandy skeletal wackestone/packstone	5?			X		X			X?				X?								X				X			X				
	70.9	HFC2a	Sandy pelecypod floatstone/rudstone	5								X?				X?								X				X							
	73.35	HFC2a	Conglomerate	5	X		X?		X															X				X				X			
	73.4	HFC2a	Conglomerate	4?					X																			X				X			
	76.0	Tamiami Fm	Sandy pelecypod floatstone/rudstone	4?																								X				X			
	76.1	Tamiami Fm	Sandy pelecypod floatstone/rudstone	4-6																				X				X				X			
	76.2	Tamiami Fm	Sandy pelecypod floatstone/rudstone	2																	X?			X	X			X				X			

[1]Test corehole adjacent to well S-3169.

Table 3. Foraminiferal biofacies and associated interpretive paleoenvironments.

Biofacies	Principal foraminiferal genera	Paleoenvironment
1	Foraminifera absent	Freshwater; commonly contains smooth-walled ostracods and freshwater gastropods
2	*Ammonia* predominant	Inner shelf and nearshore, in coastal bays, lagoons, and lower reaches of estuaries, having variable salinity values, commonly tidally influenced
3	*Elphidium* predominant	Inner shelf and nearshore, in coastal bays, lagoons, and lower reaches of estuaries, having variable salinity values, but more normal salinity, open ocean
4	Miliolids predominant	Marine shelf environments of normal to mildly hypersalinity, typically with grassy meadows and associated with areas of significant biogenic carbonate production. Depths can vary from about 3 to about 130 feet
5	Archaiasinids, soritids, peneroplids predominant	Marine shelf environments of normal to mildly hypersalinity, typically with grassy meadows and associated with areas of significant biogenic carbonate production. Depths can vary from about 3 to about 130 feet
6	Amphisteginids predominant	Amphisteginids range throughout shelf deposits to about 328 feet, but also on the margins of Holocene or relict Pleistocene carbonate buildups and platforms
7	Planktic foraminifera significant	Indicative of open ocean conditions, possibly at the platform margin or over deeper parts of the shelf

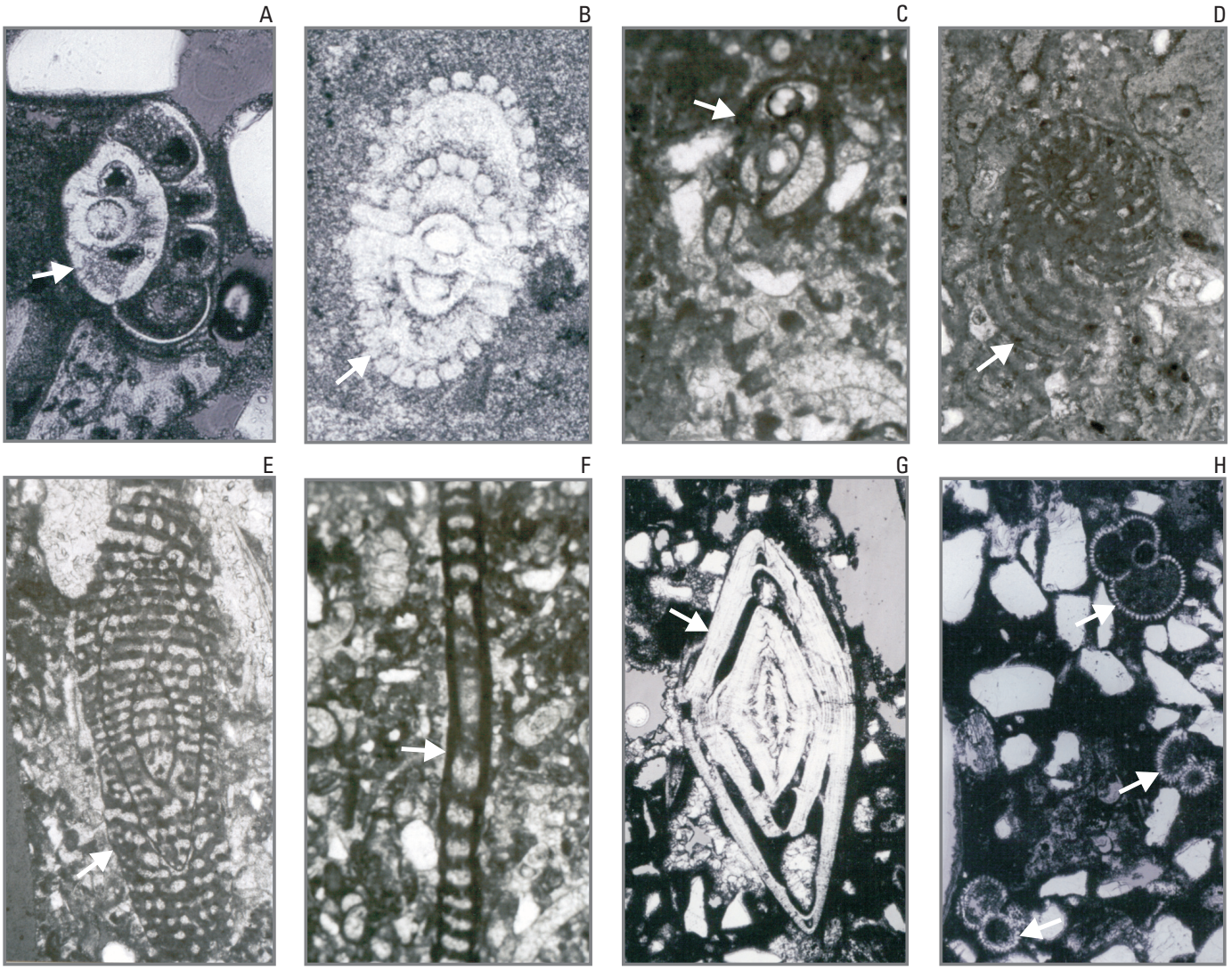

A	*Ammonia* sp. of biofacies 2
B	*Elphidium* sp. of biofacies 3
C	Miliolid of biofacies 4
D	*Peneroplis* sp. of biofacies 5
E	*Archaias* sp. of biofacies 5
F	Soritid of biofacies 5
G	*Amphistegina* sp. of biofacies 6
H	Planktics of biofacies 7

Figure 7. Thin-section photomicrographs of foraminifera characteristic of foraminiferal biofacies 2-7. An explanation of biofacies relation to foraminiferal taxonomy is provided in table 3.

Depositional Environments

Lithofacies are the preserved part of ancient depositional facies that are representative of ancient depositional environments. In the study area, evaluation of the lithofacies of the uppermost Tamiami Formation, Fort Thompson Formation, and Miami Limestone (figs. 3 and 4) are indicative of six major depositional environments. In a generally regressive succession, from bottom to top, these include: (1) middle ramp, (2) platform margin-to-outer platform, (3) open-marine platform interior, (4) restricted platform interior, (5) brackish platform interior, and (6) freshwater terrestrial environments (figs. 8 and 9). The presence of depositional environments 2 to 6 is inferred for the Fort Thompson Formation; however, only the middle ramp and the open-marine platform interior environments are representative of the uppermost Tamiami Formation and Miami Limestone, respectively. The lithofacies associated with the open-marine platform interior depositional environment typically have the relatively highest yield of ground-water flow into or out of wellbores.

Table 4. Summary of lithofacies of the Miami Limestone, Fort Thompson Formation, and selected lithofacies of the Tamiami Formation in north-central Miami-Dade County.

[NDA, No laboratory measurements available; *, lithology specific to Tamiami Formation]

Lithofacies	Description
Peloid packstone and grainstone	**Color:** Very pale orange 10YR 8/2, grayish orange 10YR 7/4 and pale yellowish orange 10YR 8/6 matrix **Depositional texture:** Burrow-mottled pelmold and peloid grainstone and packstone **Sedimentary structures/textures:** Highly burrowed, including minor callianassid shrimp burrows, very thickly bedded **Carbonate and accessory grains:** Mainly pelmolds and peloids; minor pelecypods, gastropods, oomolds, and *Schizoporella* bryozoans, miliolids, quartz grains, intraclasts, archaiasinids, agglutinating foraminifera **Helium porosity (percent):** Common pore types include pelmoldic, solution-enlarged burrow porosity, and root-mold porosity. Mean porosity is 44.5, n = 26, range from 37.2 to 49.4 **Air permeability (millidarcies):** Mean maximum horizontal is 9,187, n = 24, range from 1,116 to 25,764; mean vertical is 4,719, n = 26, range from 220 to 14,750 **Paleoenvironment:** Open marine platform interior
Peloid wackestone and packstone	**Color:** Very pale orange 10YR 8/2, dark yellowish orange 10YR 6/6, moderate yellowish brown 10YR 5/4, pale yellowish brown 10YR 6/2, and light brown 5YR 5/6 matrix **Depositional texture:** Mainly mud-dominated fabric characterized by pelecypod, benthic foram lime floatstone with a peloid lime wackestone to mud-dominated lime packstone matrix, but minor grain-dominated fabric characterized by peloid lime grainstone or skeletal grain-dominated lime packstone matrix; minor solution-enlarged burrows filled with peloid grainstone or packstone **Sedimentary structures/textures:** Highly burrowed, including minor callianassid shrimp burrows, common ~0.5-1-mm-diameter rhizoliths and less common up to 5-cm wide subvertical root molds, medium to very thickly bedded **Carbonate and accessory grains:** Mainly peloids, pelecypods (including *Chione*) and benthic foraminifers (including archaiasinids, soritids, miliolids, peneroplids, *Cyclorbiculina*), ostracods, and minor *Schizoporella* bryozoans, quartz grains, and intraclasts **Helium porosity (percent):** Common pore types include pelmoldic and skeletal moldic porosity, separate- and touching-vug porosity, root-mold porosity, and intraparticle porosity. Mean porosity is 18.4, n = 12, range from 11.0 to 27.3 **Air permeability (millidarcies):** Mean maximum horizontal is 2,611, n = 12, range from 13.8 to 11,017; mean vertical is 596, n = 12, range from 11 to 1,750 **Paleoenvironment:** Open-marine platform interior
***Planorbella* floatstone and rudstone**	**Color:** Pale yellowish brown 10YR 6/2, very pale orange 10YR 8/2, light gray N7 to medium dark gray N4 **Depositional texture:** Moldic gastropod floatstone and rudstone with skeletal wackestone and packstone matrix; local lime wackestone **Sedimentary structures/textures:** ~0.5-1-mm diameter rhizoliths, local desiccation cracks, very thinly to very thickly bedded **Carbonate and accessory grains:** Mainly gastropod molds including *Planorbella, Pomacea, Physa*, *Hydrobiida*e?, smooth-walled ostracods, and skeletal fragments; minor quartz sand, pelecypods, freshwater-algae *Charophyta,* uncommon benthic foraminifera (including *Ammonia*, *Elphidium*, peneroplids), echinoids **Helium porosity (percent):** Common pore types include skeletal-moldic separate vugs, solution-enlarged semivertical root molds, minor vertical or irregular vugs and local root-mold porosity. Mean porosity is 21.8, n = 31, range from 13.0 to 41.5 **Air permeability (millidarcies):** Mean maximum horizontal is 3,458, n = 31, range from 0.02 to 19,323; mean vertical is 5,354, n = 30, range from 1 to 17,428 **Paleoenvironment:** Freshwater terrestrial (mainly freshwater ponds or marshes)
Gastropod floatstone and rudstone	**Color:** Very pale orange 10YR 8/2 **Depositional texture:** Moldic gastropod floatstone and rudstone with skeletal wackestone and packstone matrix; local lime wackestone **Sedimentary structures/textures:** Thinly to medium bedded **Carbonate and accessory grains:** Mainly gastropods molds including skeletal fragments; minor quartz sand, pelecypods, ostracods **Helium porosity (percent):** Common pore types include skeletal-moldic separate vugs and minor irregular vugs. Mean porosity is 20.8, n = 4, range from 11.2 to 29.7 **Air permeability (millidarcies):** Mean maximum horizontal is 1,101, n =4, range from 43 to 2,350; mean vertical is 3,775, n = 4, range from 317 to 13,272 **Paleoenvironment:** Restricted platform interior

Table 4. Summary of lithofacies of the Miami Limestone, Fort Thompson Formation, and selected lithofacies of the Tamiami Formation in north-central Miami-Dade County. (Continued)

Lithofacies	Description
Conglomerate	**Color:** Very pale orange 10YR 8/2 and pale yellowish brown 10YR 6/2 matrix, and very pale orange 10YR 8/2, dark yellowish orange 10YR 6/6, moderate yellowish brown 10YR 5/4, pale yellowish brown 10YR 6/2, moderate brown 5YR 4/4, light brown 5YR 6/4, grayish orange pink 5YR 7/2 and dark gray N3 to light gray N7 intraclasts **Depositional texture:** Intraclast lime rudstone with quartz sandstone matrix or quartz sand-rich lime grainstone or mud-dominated lime packstone matrix **Sedimentary structures/textures:** Common ~0.5-1-mm diameter rhizoliths, thinly to medium bedded **Carbonate and accessory grains:** Mainly intraclasts and quartz grains; local minor peloids, pelecypods, gastropods, echinoids, and benthic foraminifera (including *Elphidium, Ammonia,* miliolids, soritids, rotaliforms, amphistiginids, *Nonion*) **Helium porosity (percent):** Common pore types include intergrain porosity, separate- and touching-vug porosity, and local root-mold porosity. Mean porosity is 15.5, n = 10, range from 6.9-26.0 **Air permeability (millidarcies):** Mean maximum horizontal is 968, n = 10, range from 1-3,813; mean vertical is 1,009, n = 10, range from 0-5,624 **Paleoenvironment:** Freshwater terrestrial (fluvial?), restricted platform interior (shoreface?), platform margin-to-outer platform
Autobreccia	**Color:** Very pale orange 10YR 8/2 and light gray N7 **Depositional texture:** Angualar clasts forming a rudstone **Sedimentary structures/textures:** Commonly thinly to medium bedded **Carbonate and accessory grains:** Mostly autoclasts, fossils include mollusks, ostracods, echinoids, benthic foraminifera (including *Ammonia,* archaiasinids?, miliolids, soritids, rotaliforms, bolvinids, *Spaerogypsina,* amphistiginids) **Helium porosity (percent):** Common pore types include minor microporosity; interclast porosity, and vuggy porosity. Mean porosity is NDA **Air permeability (millidarcies):** Mean maximum horizontal is NDA and mean vertical is NDA **Paleoenvironment:** Subaerial exposure
Pedogenic limestone	**Color:** (1) Very pale orange 10YR 8/2, dark yellowish orange 10YR 6/6, moderate yellowish brown 10YR 5/4, pale yellowish brown 10YR 6/2 and grayish orange 10YR 7/4; (2) very pale orange 10YR 8/2 and grayish orange 10YR 7/4; and (3) dark yellowish orange 10YR 6/6, grayish orange 10YR 7/4, pale yellowish brown 10YR 6/2, moderate yellowish brown 10YR 5/4 and very pale orange 10YR 8/2 **Depositional texture:** Three principal types: (1) laminated calcrete, (2) massive calcrete, and (3) root-mold limestone **Sedimentary structures/textures:** (1) Thinly to very thickly bedded and drapes over microtopography; (2) very finely laminated; and (3) thinly to very thickly bedded or poorly bedded, desiccation cracks **Carbonate and accessory grains:** (1) Minor quartz grains, uncommon miliolids, ostracods; (2) minor intraclasts, pelecypods, skeletal fragments, quartz grains, benthic foraminifera including *Ammonia*, *Elphidium,* miliolids, soritids, arachaiasinids, peneroplids, rotaliforms; and (3) skeletal fragments and local miliolids, minor quartz sand **Helium porosity (percent):** (1) Minor microporosity; (2) 20 to 30 percent root-mold porosity, 5 to 10 percent vuggy porosity, 5 percent pelmoldic and skeletal moldic porosity; and (3) 2 to 5 percent skeletal moldic porosity, 2 to 5 percent desiccation crack porosity **Air permeability (millidarcies):** (1) Low, (2) moderate to high, and (3) matrix very low to low **Paleoenvironment:** Subaerial exposure
Mudstone and wackestone	**Color:** Very pale orange 10YR 8/2, grayish orange pink 5YR 7/2, pale yellowish brown 10YR 6/2, grayish orange 10YR 7/4 **Depositional texture:** Lime mudstone and wackestone **Sedimentary structures/textures:** Common subvertical cracks, ~0.5 to 1 mm diameter rhizoliths, semivertical solution-enlarged vugs, thinly to thickly bedded **Carbonate and accessory grains:** (1) Brackish: mainly ostracods, skeletal fragments, gastropods (including *Planorbella* in the G-3679 test corehole), benthic foraminifers (including *Ammonia*, *Elphidium*, miliolids, soritids, archaiasinids, peneroplids, *Androsina,* rotaliforms); minor pelecypods quartz sand, charophytes; and (2) mud mound: peloids, pelecypods, benthic foraminifers (including miliolids), quartz sand, intraclasts, ostracods **Helium porosity (percent):** Common pore types include skeletal mold porosity, root-mold porosity, separate vug porosity, semivertical touching-vug porosity, and desiccation-crack porosity. Mean porosity is 15.7, n = 50, range from 5.5 to 31.1 **Air permeability (millidarcies):** Mean maximum horizontal is 2,292, n = 49, range from 0.001 to 20,592; mean vertical is 1,880, n = 50, range from 0 to 18,223 **Paleoenvironment:** Brackish platform interior

Table 4. Summary of lithofacies of the Miami Limestone, Fort Thompson Formation, and selected lithofacies of the Tamiami Formation in north-central Miami-Dade County. (Continued)

Lithofacies	Description
Laminated peloid packstone and grainstone	**Color:** Very pale orange 10YR 8/2 **Depositional texture:** Peloid grainstone and packstone **Sedimentary structures/textures:** Thinly laminated to very thinly bedded **Carbonate and accessory grains:** Mainly peloids; minor quartz grains, skeletal fragments, and benthic foraminifers (including miliolids, *Elphidium*, archaiasinids, *Androsina*, rotaliforms), mollusk fragments **Helium porosity (percent):** Common pore types include moldic porosity, intergrain porosity, and bedding plane vug porosity. Mean porosity is 20.2, n = 1 **Air permeability (millidarcies):** Mean maximum horizontal is 5,268, n = 1; mean vertical is 533, n = 1 **Paleoenvironment:** Restricted platform interior (tidal flat)
Skeletal packstone and grainstone	**Color:** Very pale orange 10YR 8/2, pale yellowish brown 10YR 6/2, grayish orange 10YR 7/4; light gray N7 to very light gray N8 **Depositional texture:** Skeletal grainstone and packstone **Sedimentary structures/textures:** Principally massive and highly burrowed, thickly to very thickly bedded **Carbonate and accessory grains:** Mainly skeletal fragments, benthic foraminifers (including archaiasinids, soritids, miliolids, peneroplids, *Elphidium*, *Ammonia*, *Androsina*, *Amphistegina,* rotaliforms, *Gypsina, Parasorites, Cyclorbiculina, Cycloputeolina),* peloids, mollusks (including *Chione, Modulus, Turritella, Codakia, Lucina, Trachycardium, Anodontia, Lirophora, Pyrazisinus, Tagelus, Anomalocardia, Melongena, Lucinisca, Carditimera, Codakia, Cerithium)*, skeletal fragments, peloids, ostracods, gastropods, echinoids; minor to abundant quartz grains; trace red algae, bryozoans, charophytes **Helium porosity (percent):** Common pore types include skeletal moldic porosity, intergrain porosity, pelmoldic porosity, root-mold porosity, and intraparticle. Mean porosity is 27.1, n = 85, range from 10.8 to 48.3 **Air permeability (millidarcies):** Mean maximum horizontal is 3,279, n = 84, range from 0.2 to 19,318; mean vertical is 3,102, n = 83, range from 0 to 20,140 **Paleoenvironment:** Mainly restricted platform interior, minor open-marine platform interior and platform margin-to-outer platform
Coral framestone	**Color:** Very pale orange 10YR 8/2, grayish orange 10YR 7/4, dark yellowish orange 10YR 6/6, moderate yellowish brown 10YR 5/4, pale yellowish brown 10YR 6/2 **Depositional texture:** Coral framestone **Sedimentary structures/textures:** Massive with borings and vugs **Carbonate and accessory grains:** Mainly *Monastrea* head coral, minor medium to large pebble-sized *Schizoporella*; trace to 5 percent quartz grains with peloids in boring and vug fill **Helium porosity (percent):** Common pore types include intragrain porosity, separate-vug porosity, and root-mold porosity. Mean porosity is NDA **Air permeability (millidarcies):** Mean maximum horizontal is NDA and mean vertical is NDA **Paleoenvironment:** Platform margin-to-outer platform
Pelecypod floatstone and rudstone	**Color:** Very pale orange 10YR 8/2, very light gray N8 **Depositional texture:** Pelecypod floatstone and rudstone with skeletal wackestone, packstone or grainstone matrix **Sedimentary structures/textures:** Thickly to very thickly bedded **Carbonate and accessory grains:** Mainly mollusks *(Chione*, *Turritella*, *Trachycardium*, *Bellucina*, *Cerithium, Diodora*, *Muricid*, *Brachidontes*, *Modulus*, *Anomalocardia*?*, Divaricella, Bulla,* pectenids, arcids, *Glycymeris,* muricids, ostreids, *Phacoides, Vermicularia, Anodontia, Codakia, Conus, Lithopoma, Oliva, Turbo, Anadara, Carolinapecten, Nuculana, Parastarte)* benthic foraminifers (including archaiasinids, peneroplids, miliolids, *Parasorites*, soritids, *Ammonia*, *Elphidium, Androsina,* rotaliforms, *Gypsina*?, *Nonion*?, amphistiginids, agglutinating foraminifera, *Bolivina, Cyclorbiculina, Cycloputeolina)*, peloids, ostracods; minor quartz grains; trace echinoids, red algae, charophytes, globigerinids **Helium porosity (percent):** Common pore types include moldic intergrain, irregular separate and touching vugs. Mean porosity is 26.8, n = 89, range from 10.0 to 50.2 **Air permeability (millidarcies):** Mean maximum horizontal is 6,922, n = 90, range from 0.3 to 27,411; mean vertical is 3,485, n = 90, range is 0 to 18,551 **Paleoenvironment:** Mainly restricted to open platform interior, minor platform margin-to-outer platform

Table 4. Summary of lithofacies of the Miami Limestone, Fort Thompson Formation, and selected lithofacies of the Tamiami Formation in north-central Miami-Dade County. (Continued)

Lithofacies	Description
Touching-vug pelecypod floatstone and rudstone	**Color:** Very pale orange 10YR 8/2, very light gray N8 **Depositional texture:** Pelecypod floatstone and rudstone with peloid and skeletal fragment wackestone and packstone matrix **Sedimentary structures/textures:** Medium to very thickly bedded **Carbonate and accessory grains:** Mainly peloids, mollusks (including *Chione*, *Modulus*, *Turritella*, *Codakia*, *Lucina*, *Cerithium*, *Trachycardium, Lucinisca, Pecten, Diplodonta, Strombus, Pleuromeris, Carditimera, Anadara, Glycymeris, Anodonita, Cardium, Dosinia, Nucula, Turbo, Glycymeris, Pecten*?, *Astralium, Nuculana, Phacoides, Divaricella)*, skeletal fragments, benthic foraminifers (including soritids, archaiasinids, miliolids, *Ammonia*, *Parasorites*, amphistiginids, *Elphidium*, peneroplids, rotaliforms, *Androsina*), ostracods, echinoids; trace *Porites* coral, red algae, bryozoans **Helium porosity (percent):** Common pore types include skeletal moldic porosity, 5 to 100 percent separate and touching vugs. Mean porosity is 36.4, n = 5, range from 32.0 to 42.1. **Air permeability (millidarcies):** Mean maximum horizontal is 8,358, n = 4, range from 2,731 to 16,478; mean vertical is 7,881, n = 7, range from 1,387 to 16,468 **Paleoenvironment:** Open-marine platform interior
Vuggy wackestone and packstone	**Color:** Very pale orange 10YR 8/2 **Depositional texture:** Peloid wackestone and packstone **Sedimentary structures/textures:** Thickly to very thickly bedded **Carbonate and accessory grains:** Mainly peloids, benthic foraminifers (including miliolids), gastropods; minor to abundant quartz grains **Helium porosity (percent):** Common pore types include irregular separate and touching vugs. Mean porosity is 27.0, n = 3, range from 24.9 to 30.8 **Air permeability (millidarcies):** Mean maximum horizontal is 8,358, n = 4, range from 2,731 to 16,478; mean vertical is 9,403, n = 3, range from 5,524 to 12,981 **Paleoenvironment:** Restricted platform interior (includes mud banks)
Quartz sandstone and skeletal quartz sandstone*	**Color:** Very pale orange 10YR 8/2, very light gray N8 **Depositional texture:** Skeletal sandstone **Sedimentary structures/textures:** Thickly to very thickly bedded **Carbonate and accessory grains:** Mainly quartz sand, peloids, pelecypods, skeletal fragments, gastropods, echinoids; foraminifera can include globigerinids, amphistiginids, *Ammonia, Elphidium,* miliolids **Helium porosity (percent):** Common pore types include interparticle and skeletal mold porosity. Mean porosity is 14.0, n = 5, range from 8.3 to 19.7 **Air permeability (millidarcies):** Mean maximum horizontal is 609, n = 4, range from 0.67to 1,736; mean vertical is 1,088, n = 5, range from 0 to 3,333 **Paleoenvironment:** Mainly middle ramp of the Tamiami Formation
Quartz sand*	**Color:** Very pale orange 10YR 8/2, very light gray N8 **Depositional texture:** Quartz sand **Sedimentary structures/textures:** Thickly to very thickly bedded **Carbonate and accessory grains:** Mainly quartz sand, peloids, pelecypods, skeletal fragments, gastropods; foraminifera include globigerinids and amphistiginids **Helium porosity (percent):** Common pore types include interparticle and skeletal mold porosity. Mean porosity is NDA **Air permeability (millidarcies):** Mean maximum horizontal is NDA and mean vertical is NDA **Paleoenvironment:** Mainly middle ramp of the Tamiami Formation

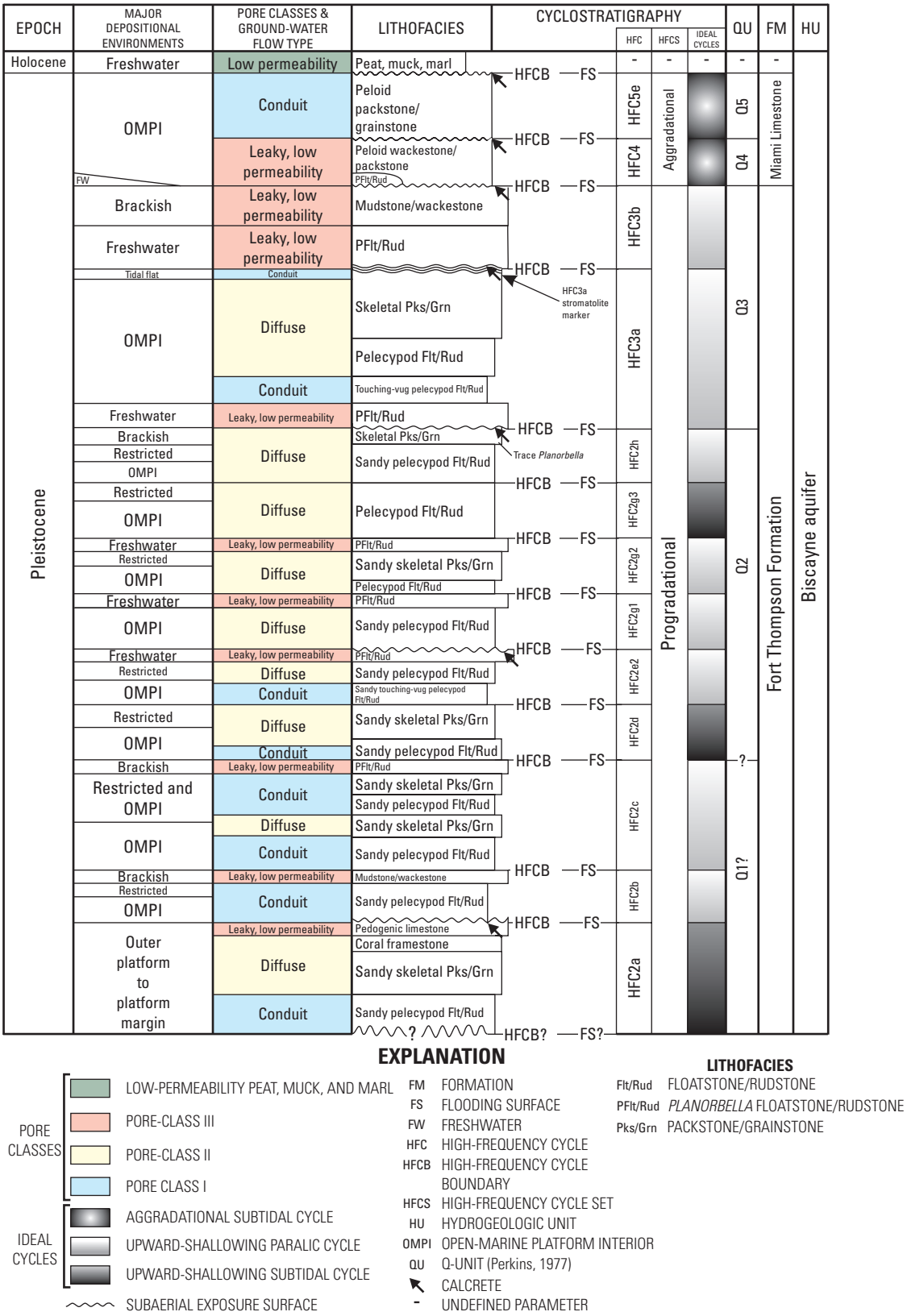

Figure 8. Conceptual hydrogeologic column for the northern part of the study area that includes ages, major depositional environments, ground-water flow types, pore classes, lithofacies, cyclostratigraphy, Q-units of Perkins (1977), formations, and hydrogeologic units.

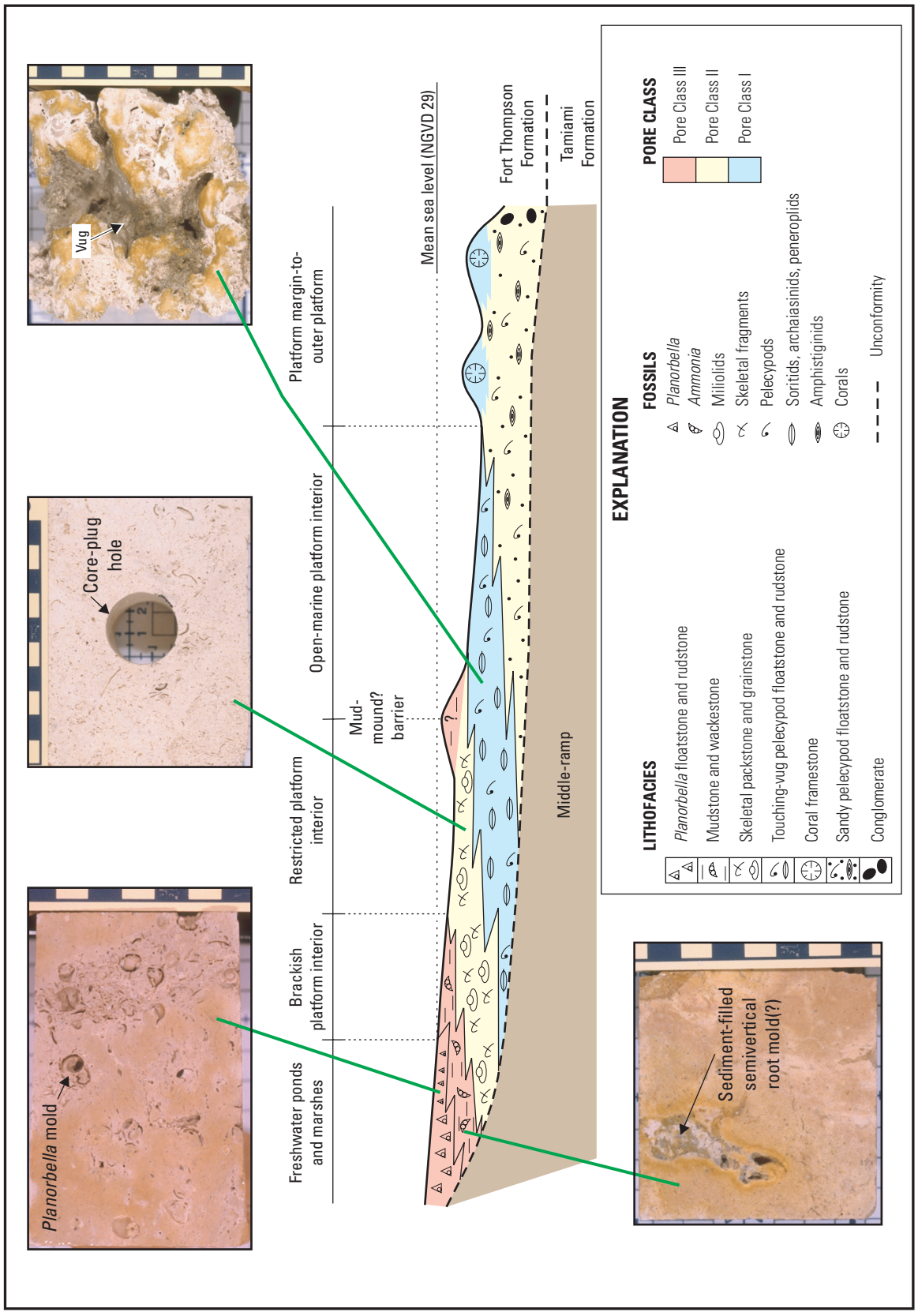

Figure 9. Conceptual facies model showing relations between major lithofacies, depositional environments, and pore classes for the study area. The four photographs of characteristic slabbed-core samples from the Fort Thompson Formation illustrate some of the carbonate textures and diagenetic features associated with key lithofacies. Each incremental color change represents 1 cm (0.394 in.) on the scale bars.

Middle Ramp

A middle ramp is characteristic of parts of the Pinecrest Sand Member of the Tamiami Formation. Lithofacies common to the middle ramp or Pinecrest Sand Member of the Tamiami Formation in the study area include pelecypod floatstone and rudstone, quartz sandstone and skeletal quartz sandstone, quartz sand, and unconsolidated pelecypod rudstone. Mollusks, amphistiginids, and globigerinids are common to these rocks of the Pinecrest Member of the Tamiami Formation. Less common, but present in a few samples representative of this depositional environment, are echinoids, miliolids, rotaliform foraminifera, soritids, and peneroplids. The amphistiginid and globigerinid foraminifera are indicative of deposition in relatively deep marine water. Rose and Lidz (1977) found these foraminiferal groups to be important on the upper slope of the Florida and Bahama Platforms, where they reported approximate water depths ranging from 131 to 656 ft. The shallow depth of this 131- to 656-ft range, however, is most probable because the uncommon foraminiferal occurrence of soritids and peneroplids is consistent with deposition in an open-marine platform interior, where water depths are reported to range from about 0 to 98 ft by Rose and Lidz (1977) on the Florida and Bahama Platforms. The limestone assigned to a middle ramp environment is commonly pelecypod rudstone with a well-washed, grain-dominated matrix (Lucia, 1995) and lime mud-rich pelecypod floatstone. The mixture of these grain-dominated and mud-dominated carbonates and a lack of shallow-water indicators or exposure suggest deposition below fair-weather wave base (FWWB) but above storm wave base (SWB). This zone between FWWB and SWB defines the "mid-ramp" depositional environment (Burchette and Wright, 1992).

Platform Margin-to-Outer Platform

The four lithofacies from limestone of the Fort Thompson Formation that distinguish the platform margin-to-outer platform environments include coral (*Montastrea*) framestone, conglomerate, sandy skeletal packstone and grainstone, and sandy pelecypod floatstone and rudstone lithofacies. The grainy lithofacies contain amphistiginids, which prefer areas of reef growth at the platform margin of the modern southern Florida platform, and patch reefs and nearby environments not far (possibly about 2 mi) from the platform margin (Rose and Lidz, 1977). Rose and Lidz (1977) estimated that water depths of the platform margin-to-outer platform environments range from 0 to 131 ft. The *Montonastrea* equivocally have a flat morphology, suggesting growth in water depths of about 82 ft or greater (Pamela Hallock Muller, University of South Florida, oral commun., 2005). The platform margin-to-outer platform environments are a notable exception because they are present only at the base of the Fort Thompson Formation in the study area. Rocks or sediments of the uppermost Pinecrest Member of the Tamiami Formation underlying the four lithofacies representative of the platform margin-to-outer platform environment include: (1) quartz sands, (2) shallowing-upward limestone cycles of the Tamiami Formation, and (3) pelecypod floatstone and rudstone. Uncommon calcrete separating the Fort Thompson Formation from the Tamiami Formation suggests that an irregular subaerial unconformity separates the two formations.

Open-Marine Platform Interior

Overlying the platform margin-to-outer platform depositional facies in the lowermost Fort Thompson Formation are open-marine platform interior depositional facies, suggesting upward shallowing and platform progradation within the lower Fort Thompson Formation (figs. 8 and 9). For the Fort Thompson Formation, lithofacies characteristic of the open-marine platform interior depositional environment include touching-vug pelecypod floatstone and rudstone, sandy touching-vug pelecypod floatstone and rudstone, skeletal packstone and grainstone, and sandy skeletal packstone and grainstone lithofacies. Common to these lithofacies are benthic foraminifers (soritids, archaiasinids, and peneroplids) that are consistent with deposition in an open-marine platform interior, similar to the modern platform interior of southern Florida that is seaward of the present-day islands of the Florida Keys (Rose and Lidz, 1977; Lidz and Rose, 1989). These lithofacies are commonly highly burrowed. The association of a soritid-, archaiasinid-, and peneroplid-dominated foraminiferal assemblage and preservation of a highly burrowed lithofacies is suggestive of deposition below FWWB in a lower shoreface zone. Mollusks present in samples from the pelecypod-rich lithofacies are suggestive of the outer estuary to shallow-marine platform interior environments of Florida Bay (app. III).

Two lithofacies, peloid wackestone and packstone and peloid packstone and grainstone, characterize the Miami Limestone (fig. 8). Burrowing of these lithofacies is pervasive and resembles many of the types of burrows described by Shinn (1968), Halley and Evans (1983), and Evans (1984). A benthic foraminiferal assemblage dominated by archaiasinids, soritids, and peneroplids in the peloid wackestone and packstone lithofacies is consistent with deposition in an open-marine platform interior (Rose and Lidz, 1977; Lidz and Rose, 1989). Alternatively, the archaiasinid, soritid, and peneroplid assemblage could be suggestive of shallow, somewhat restricted, possibly even somewhat hypersaline or euryhaline conditions (Hallock and Glenn, 1986). *Schizoporella* bryozoan is commonly present in both lithofacies. The two lithofacies correspond to the bryozoan facies of Hoffmeister and others (1967), which they interpreted to represent an open-marine shelf lagoon. Later, both Perkins (1977) and Evans (1984) indicated deposition of the bryozoan facies was on an open-marine platform. Presence of an open-marine platform interior foraminiferal assemblage and preservation of abundant burrowing suggest deposition below FWWB in a lower shoreface zone.

Restricted Platform Interior, Brackish Platform Interior, and Freshwater Terrestrial

Characteristic of the restricted platform interior environment is mainly highly burrowed, pelecypod floatstone and rudstone, sandy pelecypod floatstone and rudstone, skeletal packstone and grainstone, and sandy skeletal packstone and grainstone lithofacies. Miliolids commonly dominate the benthic foraminiferal assemblage of the lithofacies, which is consistent with deposition in a restricted platform interior. Rose and Lidz (1977) and Lidz and Rose (1989) noted that miliolid-dominated benthic foraminiferal assemblages are common in restricted areas of modern Florida Bay. The combined association of a miliolid-dominated foraminiferal assemblage and preservation of a highly burrowed lithofacies suggests deposition below FWWB in a lower shoreface zone.

The mudstone and wackestone lithofacies commonly distinguishes the brackish platform interior environment. This lithofacies is principally micrite and has an abundance of the benthic foraminifer *Ammonia* and smooth-shelled ostracodes. Charophytes, the benthic foraminifer *Elphidium*, and the freshwater gastropod *Planorbella* are less commonly present. Other types of benthic foraminifers are not common. Modern Florida Bay sediments with large populations of *Ammonia* and *Elphidium* and containing few other foraminiferal species are indicative of a brackish platform interior (Rose and Lidz, 1977; Lidz and Rose, 1989). Ishman and others (1997) and Brewster-Wingard and others (1997) found *Ammonia-Elphidium* assemblages to be present in hyposaline-influenced areas of modern Biscayne Bay and Florida Bay, respectively.

The *Planorbella* floatstone and rudstone lithofacies characterizes a freshwater terrestrial environment. This micrite-rich lithofacies commonly contains abundant *Planorbella*, smooth-shelled ostracodes, and charophytes. Interpretation indicates deposition of the *Planorbella*-rich beds in freshwater ponds or marshes (Galli, 1991).

Cyclostratigraphy

The cyclostratigraphy presented herein divides fundamental depositional cycles, high-frequency cycles (HFCs), into units defined by distinct vertical lithofacies successions bounded by surfaces across which there is evidence for a relative increase in sea level (Kerans and Tinker, 1997). Relative changes in sea level can have substantial control over the vertical stacking patterns of lithofacies on carbonate platforms (Kerans and Tinker, 1997). Although the concept of sea-level control on cycle production has been challenged (Drummond and Wilkinson, 1993; Miall, 1997), the systematic application of cyclostratigraphy has been shown to be an effective approach for defining spatial relations between stratigraphic and aquifer properties, especially porosity and permeability (Hovorka and others, 1996; 1998; Lucia, 1999; Budd, 2001; Ward and others, 2003; Budd and Vacher, 2004; Cunningham and others, 2004b; 2004c). It is beyond the scope of the present study to determine whether the HFCs in the Biscayne aquifer have a eustatic (for example, Perkins, 1977; Multer and others, 2002) or autocyclic origin because this study includes only part of the lateral extent of the uppermost Tamiami Formation, Fort Thompson Formation, and Miami Limestone.

Delineation of Cycles and Ideal Cycles

The HFCs form the fundamental building blocks of the rocks that constitute the Biscayne aquifer (fig. 4). The fitting of vertical lithofacies successions between substantial bounding surfaces (flooding surfaces) define these cycles. In some cases, a calcrete layer indicative of subaerial exposure delineates the flooding surface (fig. 8). A flooding surface is a boundary that separates younger from older strata, across which there is a sharp upward increase in paleowater depth (Van Wagoner and others, 1988). Flooding surfaces herein indicate a sharp upward deepening of paleomarine water depth or paleoflooding of a subaerial exposure surface by seawater or freshwater.

Three distinct recurring vertical assemblages of lithofacies translate into three ideal HFCs: an upward-shallowing subtidal cycle, an upward-shallowing paralic cycle, and an aggradational subtidal cycle (fig. 10 and table 5). Paralic environmental facies cap the upward-shallowing paralic cycles. The principal characteristic of paralic depositional environments is that they occur at the transition between marine and terrestrial realms—estuaries, coastal lagoons, marshes, and coastal zones subject to high freshwater input (Debenay and others, 2000). The vertical stacking of lithofacies and associated interpretive depositional environments within the ideal HFCs are shown in figure 10. The two upward-shallowing ideal cycles are present only within the Fort Thompson Formation and the aggradational subtidal cycle is present only within the Miami Limestone.

Cycle Hierarchy

In the Fort Thompson Formation and Miami Limestone, two hierarchical levels of cyclicity are recognized. The HFCs are the fundamental cycle type, but based on upward trends of progradation or aggradation, they group into two HFC sets (fig. 8 and table 6). The lower HFC set (Fort Thompson Formation) displays a broad uniform upward-shallowing trend indicative of carbonate shelf progradation based on a cycle-scale seaward progression of lithofacies tracts, shifting upward from deeper depositional environments to those that are shallower within the study area. The singular vertical lithofacies characteristics and general lack of any lateral or vertical shift in lithofacies tracts within the two HFCs of the upper HFC set (Miami Limestone) are suggestive of carbonate shelf aggradation (Kerans and Tinker, 1997) in the study area.

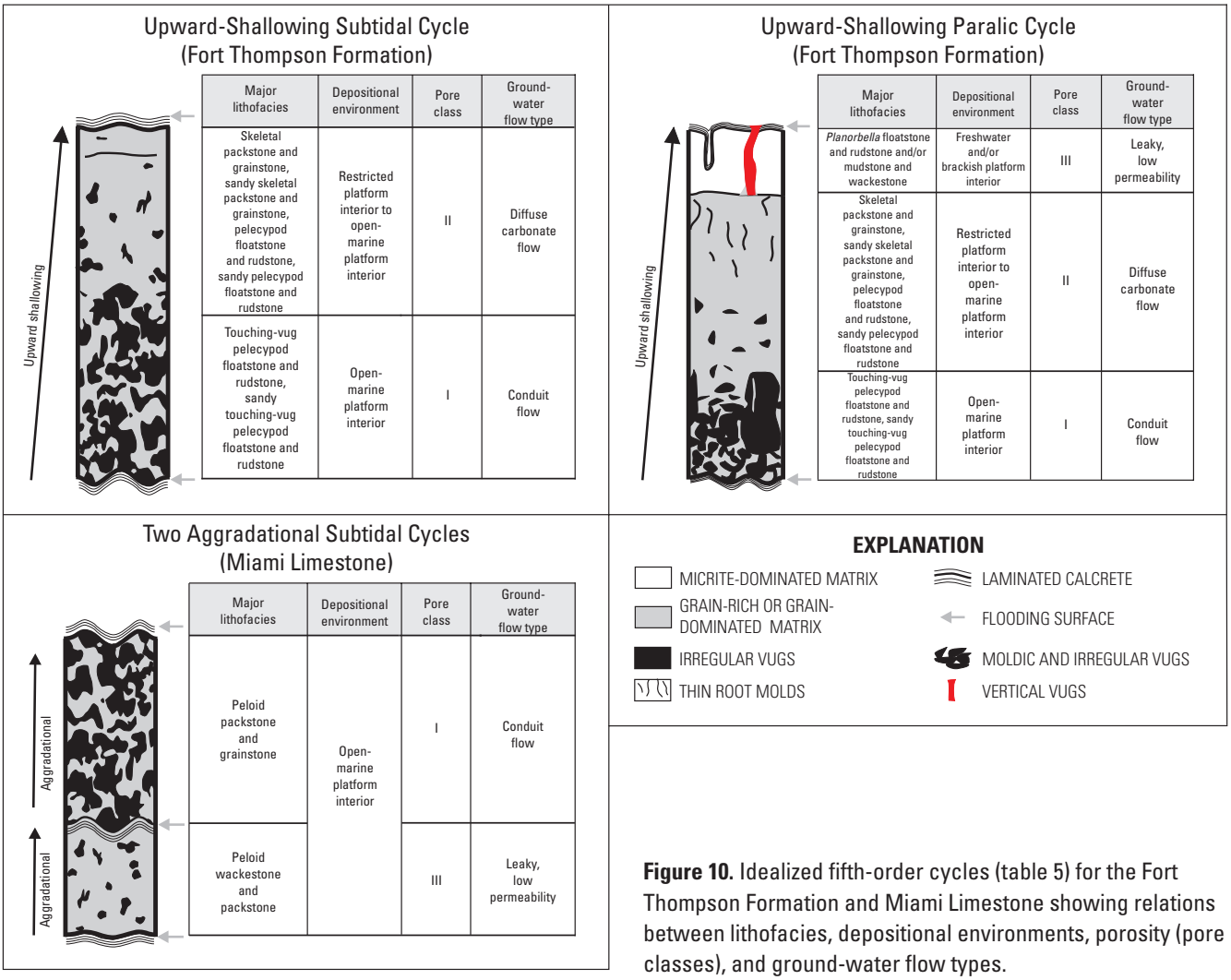

Figure 10. Idealized fifth-order cycles (table 5) for the Fort Thompson Formation and Miami Limestone showing relations between lithofacies, depositional environments, porosity (pore classes), and ground-water flow types.

Table 5. Ideal cycles of the Fort Thompson Formation and Miami Limestone.

Cycle type	Major depositional environments	Description
Aggradational subtidal	Open-marine platform interior	Cycle thickness ranges from 0.1 to 13.0 feet; mean is 4.2 feet. Little or no change. in grain size upward through succession. Mainly peloid packstone and grainstone or peloid wackestone and packstone lithofacies. Top of upper boundary is an exposure surface (calcrete)
Upward-shallowing paralic	Open-marine platform interior Restricted platform interior Brackish platform interior Freshwater terrestrial	Cycle thickness ranges from 1.0 to 13.8 feet; mean is 5.6 feet. Fining upward succession. Base typically burrowed peleypod-rich floatstone or rudstone lithofacies, which may be quartz sand rich, grading upward to mudstone and wackestone or *Planorbella* floatstone and rudstone cap. Commonly, upper boundary is an exposure surface (calcrete). *Planorbella* present in capping *Planorbella* floatstone and rudstone lithofacies, and local occurrence in mudstone and wackestone lithofacies
Upward-shallowing subtidal	Open-marine platform interior Restricted platform interior	Cycle thickness ranges from 0.3 to 13.2 feet; mean is 5.2 feet. Mostly fining upward succession. Base typically burrowed peleypod-rich floatstone or rudstone, which may be quartz sand rich, grading upward to packstone and grainstone. Upper boundary may be an exposure surface (calcrete)

Table 6. Terminology of stratigraphic cycle hierarchies and orders of cyclicity.

[Modified from Kerans and Tinker (1997). >, greater than the value]

Hierarchical order	Sequence stratigraphic unit	Duration (million years)
First	None	>100
Second	Supersequence	10–100
Third	Depositional sequence Composite sequence	1–10
Fourth	High-frequency sequence High-frequency cycle set	0.1–1
Fifth	High-frequency cycle	0.01–0.1
Sixth	Microcycle	<0.01

Orders of Cycles

Within the study area, a hierarchical order is proposed herein for the cyclicity recognized in the Fort Thompson Formation and Miami Limestone; HFCs are fifth-order scale or higher and HFC sets are fourth-order scale (table 6). The proposed scales for the cycle ordering are based on various ranges in ages proposed by Multer and others (2002) and Hickey (2004) for the five unconformity-bound Quaternary marine units or Q units defined by Perkins (1977). The Q1 to Q5 units of Perkins (1977) correlate to the new cyclostratigraphy (present study) shown in figures 4 and 8, based on comparisons of descriptions of lithofacies and unconformities by Perkins (1977) to those observed in the present study. No lithofacies or unconformity observed in the study area reliably correlate to the Q1 unit of Perkins (1977) shown in figure 4. Multer and others (2002) assumed a maximum age of 420 ka for the Q1 unit of Perkins (1977) in the basal Fort Thompson Formation (fig. 4) and reported that the Q5 unit of Perkins (1977) accumulated during the Marine Isotope Substage 5e, which terminated at about 114 ka (Shackleton and others, 2003). One model of the ordering of cyclicity, thus, assumes a maximum duration of about 306 ky for accumulation of the 13 HFCs identified in the study area, or average cycle duration of about 23.5 ky, which is consistent with fifth-order cyclicity (table 6). Fourth-order scaling of the HFC sets is in agreement with cycle-set durations based on Q-unit ages presented in Perkins (1977) and Multer and others (2002). Alternatively, a second model of the ordering of cyclicity suggests that the HFCs are fifth-order or higher. This model assumes a short-duration pulsed flooding of the Florida platform during the Pleistocene, as suggested by correlation of the Perkin's Q units to various marine isotope stages (Hickey, 2004). The HFCs bundled within the Q1?, Q2, and Q3 units of Perkins (1977) are possibly microcycles (Zühlke, 2004) with duration less than 10 ky. The single HFCs defined within the Q4 and Q5 units of Perkins (1977) could be composed of fifth-order cycles (table 6).

Hydrogeologic Framework for Model Representation of the Biscayne Aquifer

Geologic units of varying permeability that underlie southeastern Florida to depths between about 180 and 220 ft below NGVD 1929 are known as the surficial aquifer system, an unconfined aquifer system that is the source of much of the potable water used in the study area (Fish, 1988; Fish and Stewart, 1991). In Miami-Dade County, the upper, highly permeable part of the aquifer system is named the Biscayne aquifer (Parker, 1951; Parker and others, 1955). Underlying the Biscayne aquifer are two semiconfining units that occur above and below the gray limestone aquifer (Reese and Cunningham, 2000; fig. 3, this report). The geology and hydrology of the study area have been reported in numerous studies (Parker and Cooke, 1944; Parker and others, 1955; Perkins, 1977; Causaras, 1987; Labowski, 1988; Fish and Stewart, 1991; Galli, 1991; Solo-Gabriele and Sternberg, 1998; Nemeth and others, 2000; Sonenshein, 2001; Cunningham and others, 2004b; 2004c; Wilcox and others, 2004; Cunningham and others, 2006, in press).

Previous Interpretations

In Miami-Dade County, the surficial aquifer system includes all rock and sediment from land surface downward to the top of the intermediate confining unit (fig. 3). The rock and sediment are mostly composed of limestone, sandstone, sand, shell, and clayey sand and range in age from Holocene to Pliocene (Causaras, 1987). The top of the system is land surface, and a substantial decrease in permeability defines the base. The permeability of the rock and sediment of the surficial aquifer system is variable, allowing the system to be divided into one or more aquifers separated by less-permeable or semiconfining units. The uppermost part of these water-bearing units is the Biscayne aquifer, and the lowermost water-bearing unit is the gray limestone aquifer (Fish and Stewart, 1991; Reese and Cunningham, 2000).

The Biscayne aquifer is the primary aquifer in southeastern Florida and has been declared a sole-source aquifer (Federal Register Notice, 1979). Parker (1951) named and defined the Biscayne aquifer as a hydrologic unit of water-bearing rocks that carries unconfined ground water in southeastern Florida. Later, Fish (1988), defined the Biscayne aquifer more completely as:

> That part of the surficial aquifer system in southeastern Florida composed of (from land surface downward) the Pamlico Sand, Miami Oolite [Limestone], Anastasia Formation, Key Largo Limestone, and Fort Thompson Formation (all of Pleistocene age) and contiguous, highly permeable beds of the Tamiami Formation of Pliocene and late Miocene age where at least 10 ft of section is very highly permeable (a horizontal hydraulic conductivity of about 1,000 ft/d or more).

Fish (1988) provided further definition of the base of the Biscayne aquifer:

> If there are contiguous, highly permeable (having hydraulic conductivities of about 100 ft/d or more) limestone or calcareous sandstone beds of the Tamiami Formation, the lower boundary is the transition from these beds to subjacent sands or clayey sands. Where the contiguous beds of the Tamiami Formation do not have sufficiently high permeability, the base of highly permeable limestones or sandstones in the Fort Thompson Formation, Anastasia Formation, or Key Largo Limestone is the base of the Biscayne aquifer.

This study focuses on the part of the Biscayne aquifer that is composed of the uppermost part of the Tamiami Formation, the Fort Thompson Formation, and the Miami Limestone (fig. 3). The key wells used in this study fully penetrate the rocks of the Biscayne aquifer. Cunningham and others (2004b) concentrated on the uppermost part of the Biscayne aquifer.

Pore System of the Limestone of the Biscayne Aquifer

Traditionally, karst aquifers are characterized by three types of porosity: interparticle matrix porosity, fracture porosity, and large cavernous porosity (Martin and Screaton, 2001). This has led many researchers to view karst aquifers as two component systems, where much of the ground-water storage occurs in the matrix porosity or fractures or both, and much of the ground-water flow and transport takes place in the large dissolutional conduits (Martin and Screaton, 2001). In the young eogenetic karst that defines the Pleistocene limestone of the Biscayne aquifer, however, a fourth porosity type, touching-vug porosity, is especially important in terms of conveyance of ground water (Vacher and Mylroie, 2002; Cunningham and others, 2006, in press). The triple porosity of the Biscayne aquifer is typically: (1) matrix of interparticle and separate-vug porosity, providing much of the storage; (2) touching-vug porosity creating stratiform ground-water flow passageways; and (3) less common, conduit porosity composed mainly of bedding-plane vugs, thin solution pipes, and cavernous vugs (figs. 11 and 12). These three conduit porosity types are all pathways for conduit ground-water flow. Stratiform refers to the three-dimensional aspects of the porosity; that is, it is constrained to a layer, bed, or stratum with lateral continuity (Jackson, 1997).

Pore Classes

In the study area, the porosity, permeability, and storage of the limestone in the Biscayne aquifer relate directly to lithofacies and have a predictable vertical distribution within the upward-shallowing cycles of the Fort Thompson Formation and the aggradational subtidal cycles of the Miami Limestone (Cunningham and others, 2004b; 2006, in press). The 16 lithofacies of the Fort Thompson Formation and Miami Limestone (previously described) have been assigned to pore classes I, II, or III (figs. 11 and 12), as presented in table 7. These lithofacies have rather unique stratigraphic spatial distributions, and distinct porosity, permeability, and storage characteristics. Table 7 also describes how the three pore classes relate to three ground-water flow types defined by Cunningham and others (2004b).

Pore class I commonly comprises the lower part of many upward-shallowing cycles of the Fort Thompson Formation and the upper aggradational subtidal cycle of the Miami Limestone where porosity and permeability are highest (figs. 8 and 10). Characteristic lithofacies associated with pore class I are: (1) touching-vug pelecypod floatstone and rudstone, (2) peloid packstone and grainstone, (3) laminated peloid packstone and grainstone, (4) autobreccia, (5) coral framestone, and (6) vuggy wackestone and packstone (table 7). Pore types that can be associated with specific lithofacies include solution-enlarged fossil molds up to pebble size, molds of burrows or roots, irregular vugs surrounding casts of burrows or roots, bedding-plane vugs, and irregular vugs or cavities of uncertain textural association up to about 4 ft in height (figs. 11 and 12). Touching-vugs are the most common type of interconnected (effective) porosity in this class. A tabular, three-dimensional, stratiform geometry regionally characterizes the touching-vug flow zones, which are constrained between cycle boundaries, based on correlations of porous zones in the study area (pls. 1-5). An important point is that the touching vugs of the two upward-shallowing cycle types of the Fort Thompson Formation are typically most concentrated just above the flooding surface in the lower part of the cycles, and the upper aggradational cycle of the Miami Limestone has a generally regular vertical distribution of touching vugs throughout the cycle. Therefore, accurate cycle correlation can produce a realistic linkage of permeable or preferential ground-water flow zones. Typical ground-water flow in pore class I should not be conceptually viewed as movement of ground water through a system of pipes or underground stream conduits, but more of a stratiform passage formed by coalescence of touching vugs into a mostly tortuous path for the movement of conduit ground-water flow. Figure 13 exemplifies the stratiform distribution of pore class I locally within the NWWF (fig. 2), notably where the darkened area at the base of HFC2e2 in digital optical borehole images represents touching-vug porosity. Figure 14 shows how both molds of borrows and interburrow porosity in well G-3816 combine to create a stratiform zone of effective porosity at the base of HFC2e2 (fig. 13). Cunningham and others (2004b) showed that pore class I has the highest porosity and permeability of the three pore classes defined herein; however, the terminology they used for pore class I was “horizontal conduit ground-water flow class.”

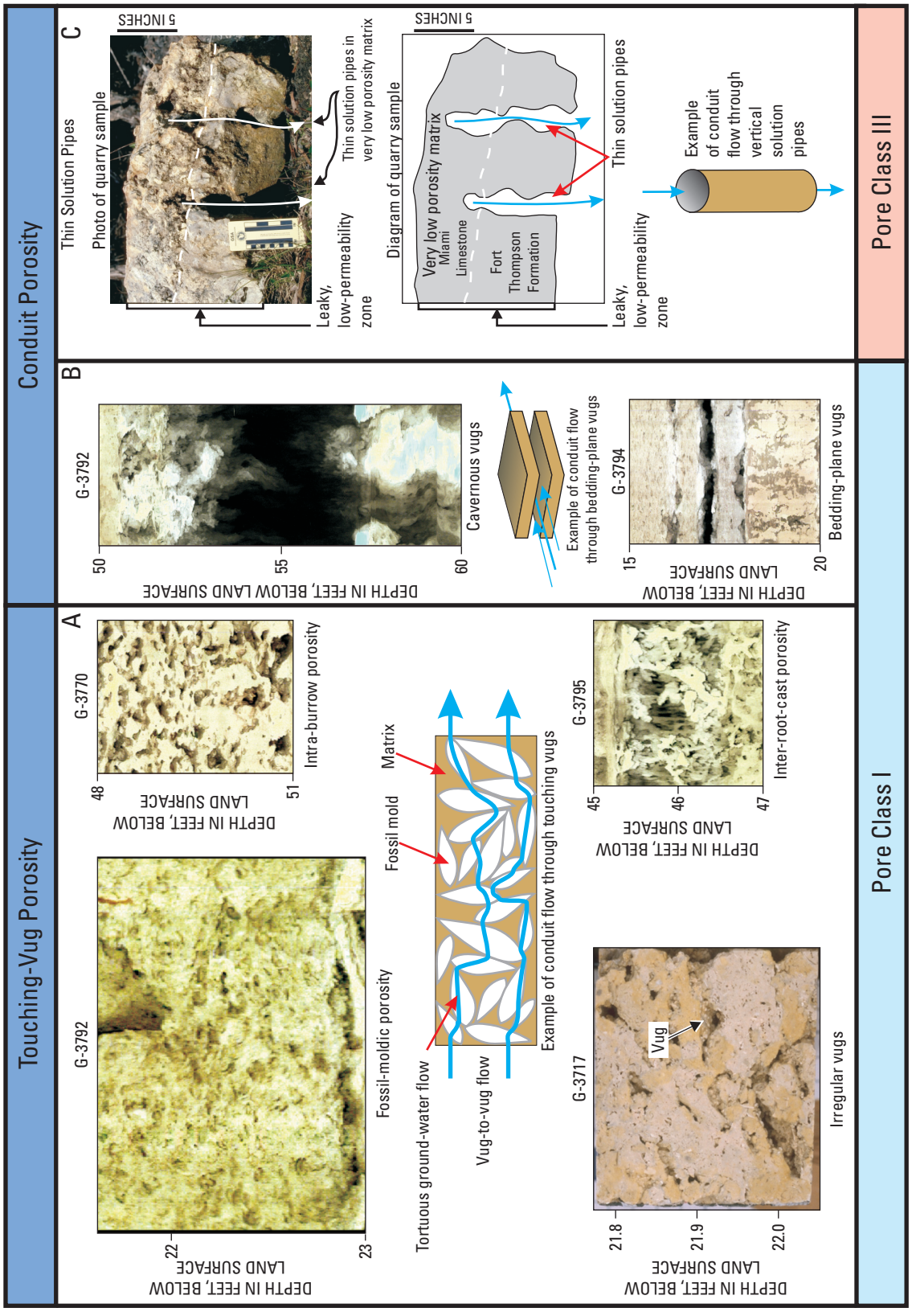

Figure 11. Relation between pore classes I and III and touching-vug and conduit pore types, respectively, for the Fort Thompson Formation and Miami Limestone of the Biscayne aquifer in the study area. (A) Four common types of touching-vug porosity: fossil moldic, intra-burrow, irregular vugs, and inter-root-cast porosity for pore class I; (B) Two types of conduit porosity (cavernous and bedding-plane vugs) that are rather untypical for pore class I; (C) Thin, vertical conduits that are a typical pore type of pore class III.

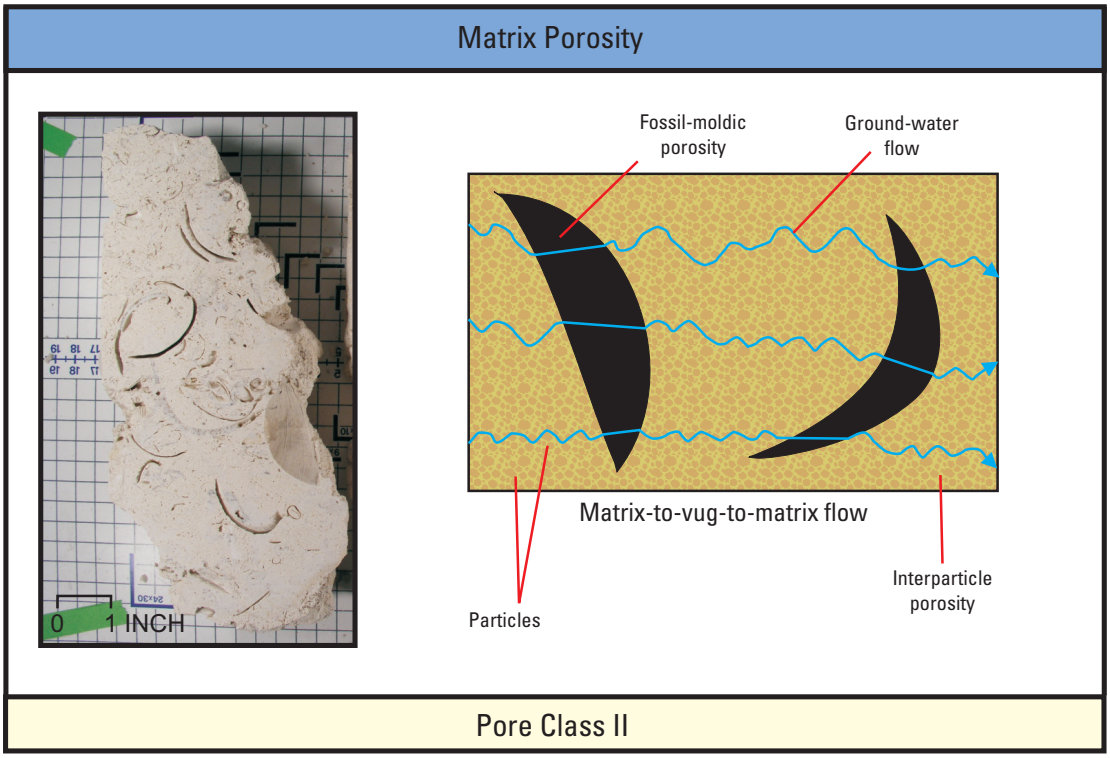

Figure 12. Relation between pore class II and matrix porosity. Ground-water flow through the matrix is general matrix-to-vug-matrix flow. Core sample of pelecypod floatstone and rudstone lithofacies shown in photo on left-hand side is from the Fort Thompson Formation in the G-3783 test corehole (fig. 2).

Table 7. Pore classes (I, II, and III) related to aquifer attributes of the Miami Limestone and Fort Thompson Formation in the study area.

[mD, millidarcies; HFC, high-frequency cycle; n, number of samples used to calculate median]

Pore class	Lithofacies	Major pore type	Median whole-core helium porosity	Median maximum horizontal air permeability	Major type ground-water flow type and relative permeability
I	Touching-vug pelecypod floatstone-rudstone, peloid packstone-grainstone, laminated peloid packstone-grainstone, autobreccia, coral framestone, and vuggy wackestone and packstone	Touching vugs including fossil-moldic, intra-burrow, and inter-root-cast porosity, and irregular vugs; and conduit porosity including bedding-plane-vugs and cavernous vugs	HFC5e aggradational subtidal cycle of Miami Limestone and lower part of upward shallowing cycles of Fort Thompson Formation is 33.4 percent; n = 54	HFC5e aggradational subtidal cycle of Miami Limestone and lower part of upward shallowing cycles of Fort Thompson Formation is 8,498 mD; n = 52	Conduit flow, high permeability
II	Skeletal packstone-grainstone, pelecypod floatstone-rudstone, quartz sandstone and skeletal quartz sandstone, and quartz sand	Matrix porosity including interparticle and separate vugs	Middle part of upward-shallowing paralic cycles and middle to upper part of upward-shallowing subtidal cycles is 25.0 percent; n = 110	Middle part of upward-shallowing paralic cycles and middle to upper part of upward-shallowing subtidal cycles is 2,784 mD; n = 113	Diffuse-carbonate flow, moderate permeability
III	Mudstone-wackestone, *Planorbella* floatstone-rudstone, peloid wackestone-packstone, conglomerate, pedogenic limestone, and gastropod floastsone-rudstone	Separate vugs including moldic porosity or thin vertical solution pipes or both	HFC4 aggradational subtidal cycle of Miami Limestone and commonly cycle top of upward-shallowing paralic cycles of Fort Thompson Formation (an exception is base of HFC3a) is 17.6 percent;n = 78	HFC4 aggradational subtidal cycle of Miami Limestone and commonly cycle top of upward-shallowing paralic cycles of Fort Thompson Formation (an exception is base of HFC3a) is 575 mD; n = 74	Leaky, low permeability

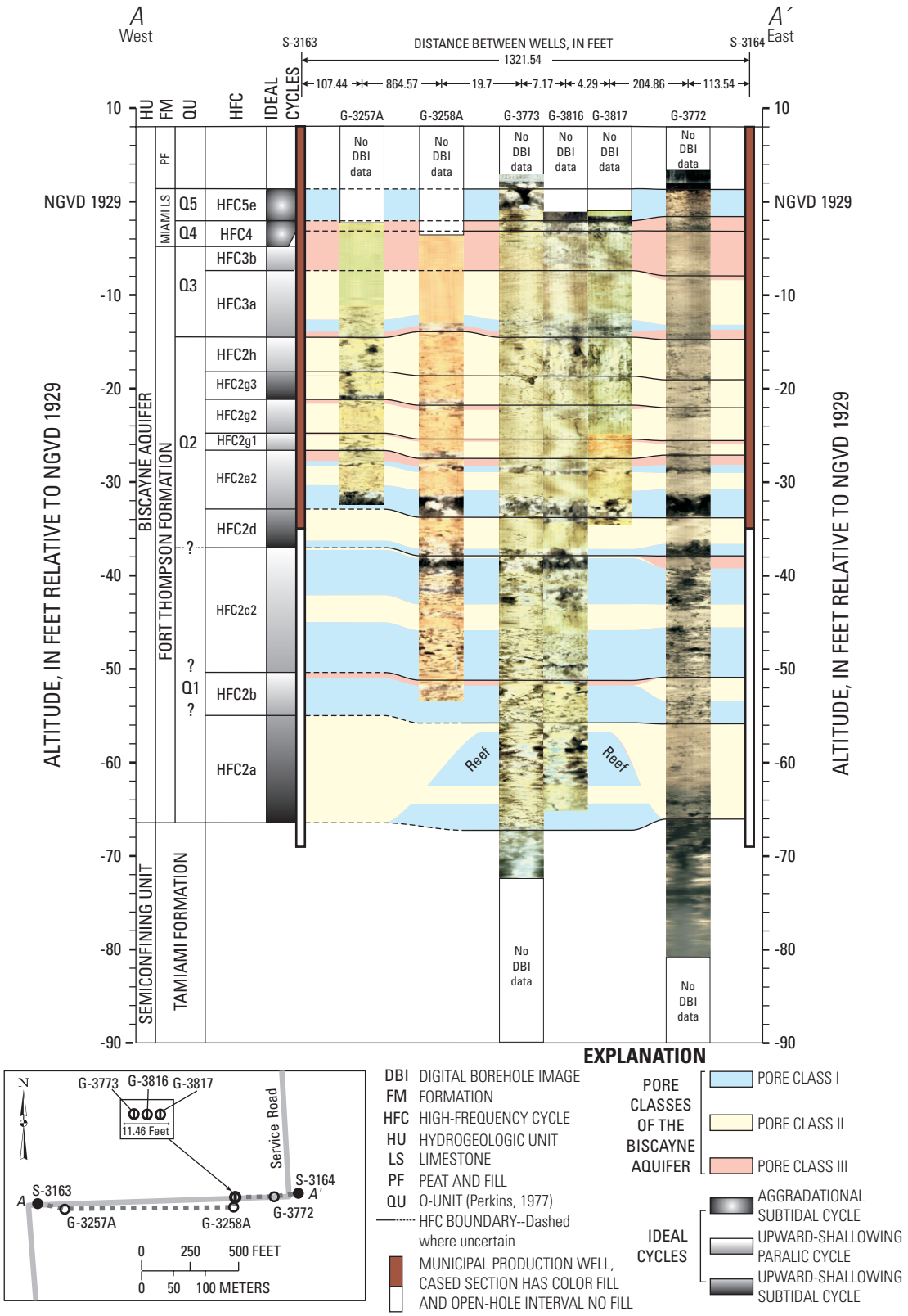

Figure 13. Hydrostratigraphic correlation section *A-A´* between the S-3163 and S-3164 production wells, including six digital image logs from observation and injection wells at the Northwest Well Field. Black or very dark areas on the digital optical image logs typically indicate large-scale vuggy porosity. Inset map shows location of section *A-A´* within a small area of the well field. Most of the highly porous areas of the aquifer are within stratiform touching-vug porosity zones of pore class I.

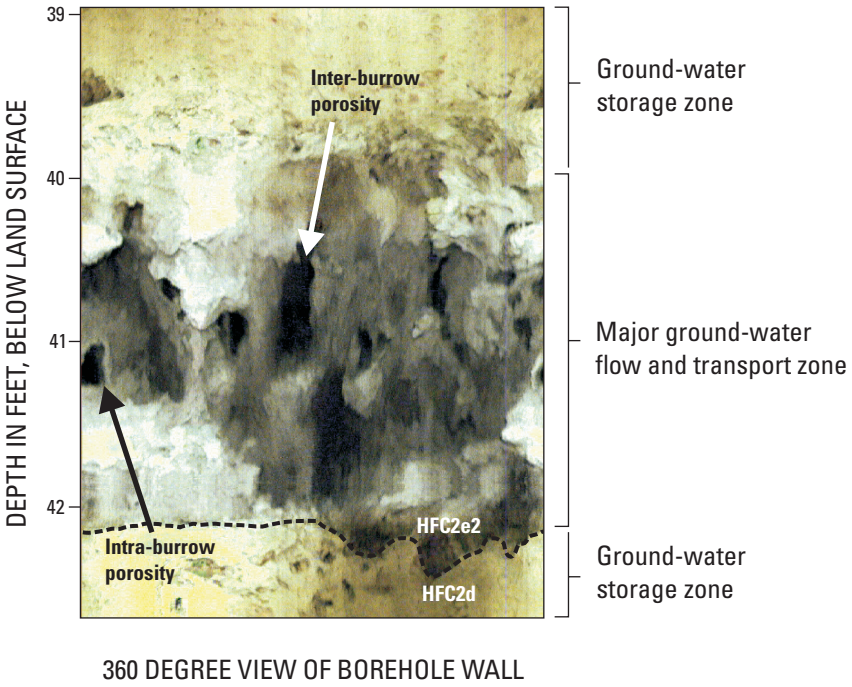

Figure 14. Digital image of a borehole wall that spans a highly porous and permeable stratiform ground-water flow zone at the base of high-frequency cycle HFC2e2 in well G-3816 (figs. 2 and 13. The dashed line represents the boundary and flooding surface that separates high-frequency cycles HFC2d and HFC2e2.

The following lithofacies are typically assigned to pore class II: (1) skeletal packstone and grainstone, (2) pelecypod floatstone and rudstone, (3) quartz sandstone and skeletal quartz sandstone, and (4) quartz sand (table 7). The skeletal packstone and grainstone and pelecypod floatstone and rudstone lithofacies commonly occur in the upper part of upward-shallowing subtidal cycles and the middle part of the upward-shallowing paralic cycles (fig. 10). The two quartzose lithofacies are most common in the Pinecrest Sand Member of the Tamiami Formation. Interparticle, intraparticle, very small moldic porosity, and irregular separate-vug (Lucia, 1999) pore spaces characterize most of these lithofacies, which typically yield ground-water movement through vug-to-matrix-to-vug connections. Diffuse-carbonate ground-water flow, compared with diffuse flow of Shuster and White (1971) and Thrailkill (1976), characterizes ground-water movement in areas of the Biscayne aquifer assigned to pore class II. Those parts of the aquifer that are principally quartz sand or quartz sandstone and that lack moldic or vuggy porosity also are dominated by diffuse ground-water flow.

The following lithofacies are usually assigned to pore class III: (1) mudstone and wackestone, (2) *Planorbella* floatstone and rudstone, (3) peloid wackestone and packstone, (4) conglomerate, (5) pedogenic limestone, and (6) gastropod floatstone and rudstone (table 7). The first two lithofacies commonly cap upward-shallowing paralic cycles, and the peloid wackestone and packstone lithofacies is representative of the lower aggradational subtidal cycle of the Miami Limestone (fig. 10). The conglomerate lithofacies is mostly uncommon, but typically occurs at or near the base of HFC4. The pedogenic limestone lithofacies is associated with cycle tops and is the product of diagenesis or deposition of calcrete during subaerial exposure. Porosity types common to this pore class include thin semivertical solution pipes and fossil molds, which are both typically separate vugs (fig. 12). The solution pipes have a bed-scale length, and as a result, convey only ground water effectively over very short distances. Mangrove roots are suspected as the origin for many of the solution pipes because they are similar to structures described as fossil mangrove roots by Hoffmeister and Multer (1965), Bain and Teeter (1975), and Galli (1991). The matrix of the six lithofacies assigned to pore class III is commonly micrite (microcrystalline limestone); consequently, the matrix porosity and permeability of these lithofacies are commonly low (table 7). Thus, these lithofacies tend to retard ground-water movement. On a local scale, however, lithofacies assigned to pore class III can contain bedding-plane vugs that have a sheet-like geometry and can represent major conduits that are highly permeable.

Generalized Layering Scheme of Pore Classes

The hydrogeologic framework of the Biscayne aquifer shown on plates 1 to 4 is a complex arrangement of the three types of pore classes mapped within a cyclostratigraphic framework. These two-dimensional views of the hydrogeologic framework were translated into an eight-layer, three-dimensional representation of the hydrogeologic framework for the study area (figs. 15 and 16). The uppermost layer represents peat, muck, marl, and/or fill, and the underlying seven layers delineate pore classes I, II, and III (figs. 15 and 16). Because of the interbedded, fine scale, and lateral complexity of some of the pore classes delineated on plates 1 to 4, it is unavoidable that many of the seven layers representing pore classes in the three-dimensional model include two or three different types of pore classes in the two-dimensional views. Therefore,

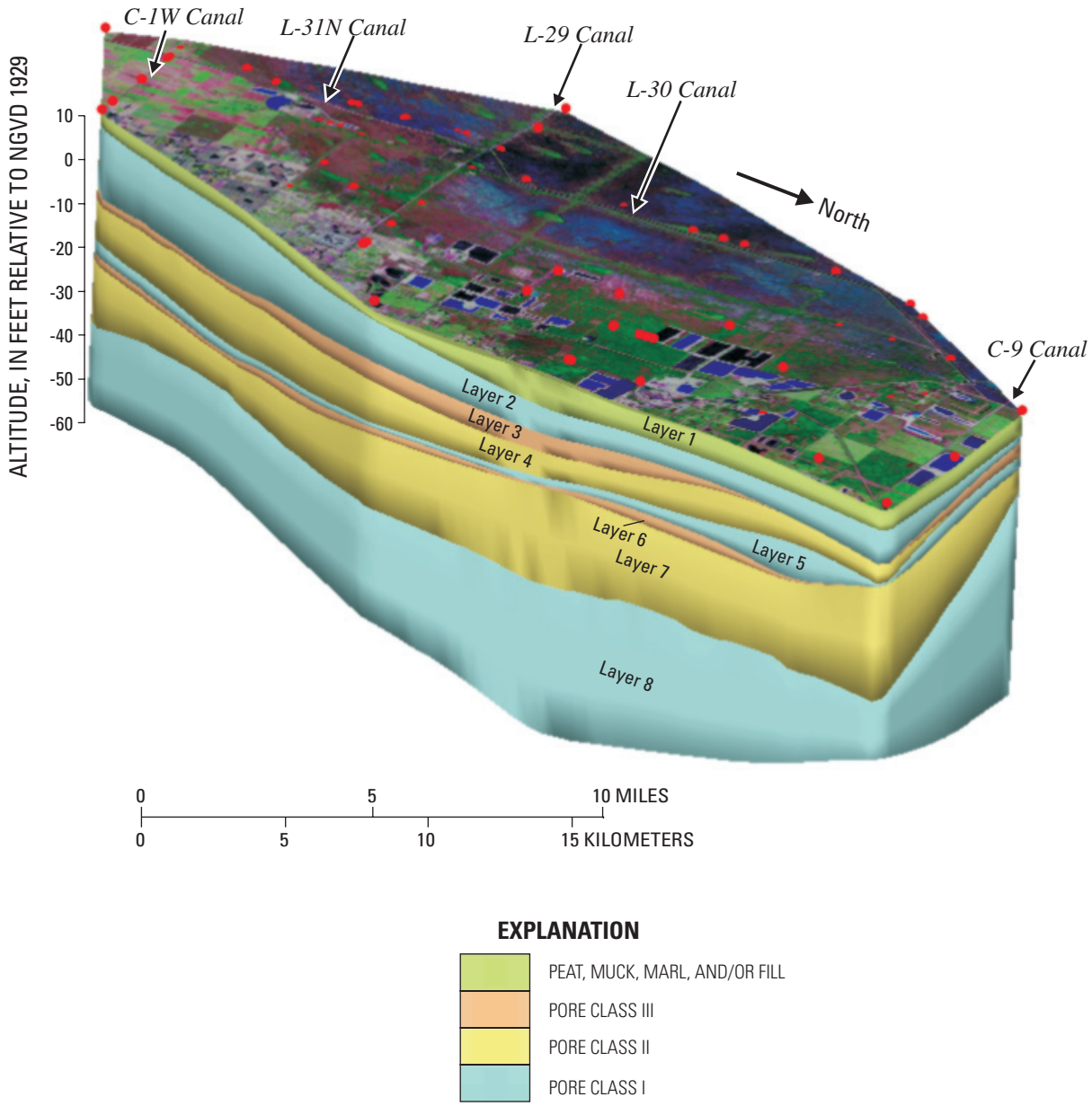

Figure 15. Three-dimensional conceptual hydrogeologic model of the Biscayne aquifer for the study area in north-central Miami-Dade County.

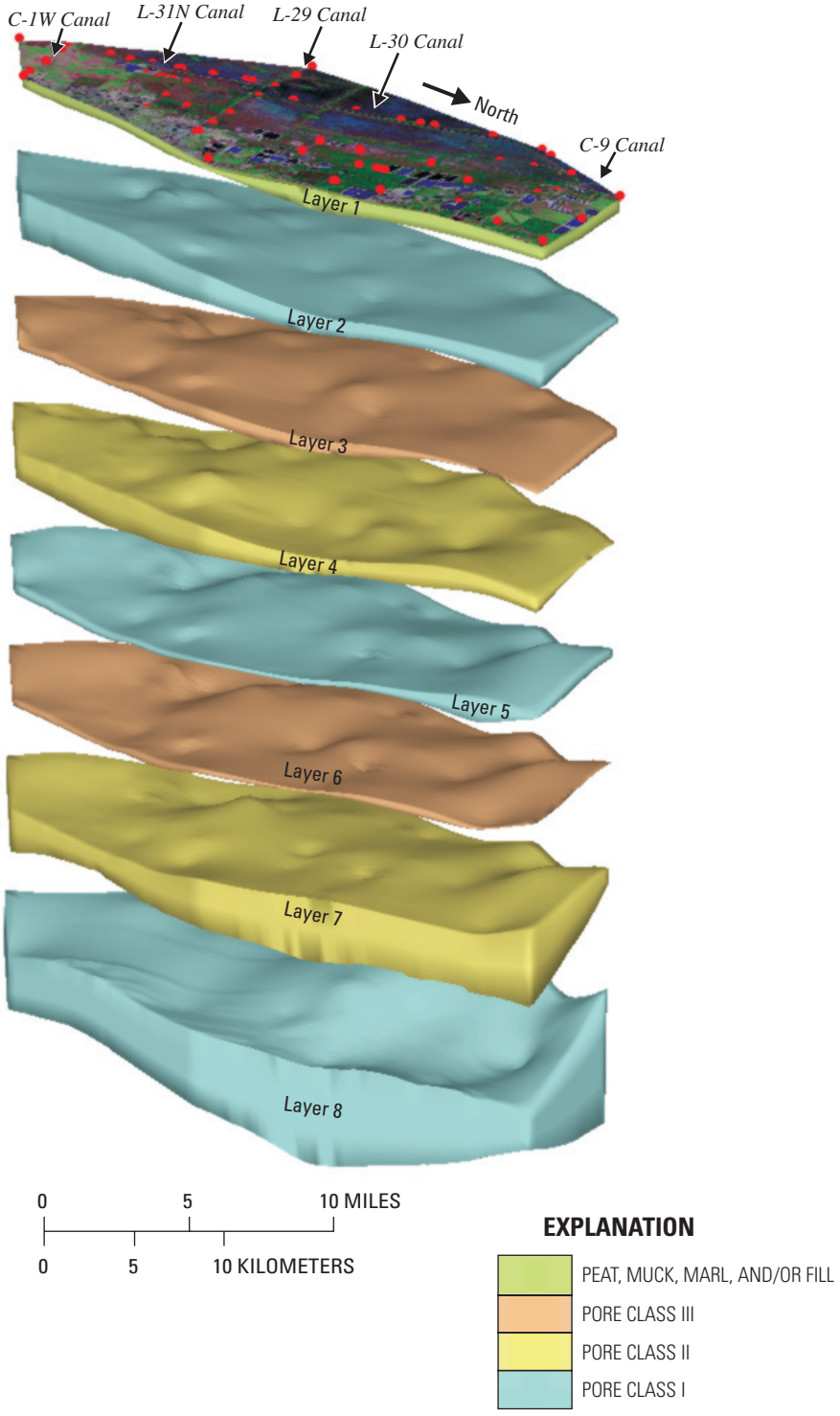

Figure 16. An exploded view showing much of the geometry of the upper surfaces of the three-dimensional conceptual hydrogeologic model of the Biscayne aquifer for the study area in north-central Miami-Dade County. Refer to figure 15 for vertical scale.

figures 15 and 16 are simplified interpretations of the two-dimensional framework shown on plates 1 to 4. For example, permeable zones representative of pore class I that seem to be more hydraulically connected laterally than isolated are combined into regional units. The delineation of three distinct relatively high-permeability layers (figs. 15 and 16, represented by pore class I) is supported by measured differences in vertical hydraulic gradient for permeable zones contained in HFC5e and HFC3a and permeable zones in the lower part of the Biscayne aquifer in the southwestern part of the study area (Cunningham and others, 2004c).

The Biscayne aquifer is conceptualized as three sub-aquifers of relatively high permeability (layers 2, 5, and 8), which are interlayered with two layers of relatively moderate permeability (layers 4 and 7) and two layers of relatively low permeability (layers 3 and 6) as shown in figures 15 and 16. The two uppermost relatively high-permeability layers (2 and 5) are approximately equivalent to HFC5e and HFC3a and have good physical connection in and around the study area. The two relatively moderate permeability layers (4 and 7) representing pore class II are conceptualized as containing mostly diffuse-carbonate ground-water flow. Both layers are hypothesized to contain much of the ground-water storage in the Biscayne aquifer and less important in terms of regional ground-water flow. Layers 3 and 6 representing pore class III are conceptualized as relatively low-permeability layers that generally include: (1) HFC4 and the top of HFC3b; and (2) the base of HFC3b, and locally, the top of HFC2h. Both layers are considered to leak vertically and inhibit horizontal movement of ground water and have only a minor role, if any, in the horizontal movement of ground water, except in areas where bedding-plane vugs are present. In summary, the mapping of the altitudes and thicknesses of pore-class layers within a simplified conceptual model of the Biscayne aquifer could be used as a template for more reliable numerical ground-water model layering than previously possible (figs. 15 and 16).

Altitudes and Thicknesses of Hydrogeologic Layers

Layer 1 is composed of peat, marl, muck, and fill and layers 2 to 8 are characterized by pore class I, II, or III. Pore class I is characteristic of layer 2 and generally corresponds to HFC5e, the Q5 unit of Perkins (1977) or Q5e of Multer and others (2002). In general, the upper surface of layer 2 is highest in the area of the NWWF (fig. 17). North of the well field, the surface dips slightly to the south; south of the well field, the surface generally dips northward. Layer 2 generally is thinnest in the northwest and thickens southeastward to more than 15 ft (fig. 18).

Layer 3 is characterized by the upper zone of pore class III, and mostly is inclusive of HFC4, the Q4 unit of Perkins (1977), and the uppermost part of HFC3b; that is, this layer can span the base of the Miami Limestone and uppermost part of the Fort Thompson Formation. The upper surface of layer 3 generally dips to the east or southeast, but also dips to the west, in an area to the southwest of the intersection of Krome Avenue and Tamiami Trail (fig. 19). Layer 3 generally is between 2 and 4 ft thick throughout the study area (fig. 20). This low-permeability layer has been evaluated in numerous studies (Klein and Sherwood, 1961; Shinn and Corcoran, 1988; Guardiario, 1996; Brown and Caldwell Environmental Engineers and Consultants, 1998; Genereux and Guardiario, 1998; Nemeth and others, 2000; Sonenshein, 2001; Cunningham and others, 2004b; Krupa and Mullen, 2005).

Layer 4 is characterized by the upper zone of pore class II, and generally is equivalent to the lower and middle parts of HFC3b and the middle and upper parts of HFC3a. The upper surface of layer 4 has a slight broad dip toward the southeast (fig. 21). The thickness of this layer varies throughout the study area, ranging from 0 to 15.4 ft (fig. 22). Layer 4 generally is thin in the northern and southwestern parts of the study area, however, and thickens to the northwestern and southeastern parts (fig. 22).

Layer 5 is characterized by the middle zone of pore class I, and generally corresponds to the base (or near the base) of HFC3a. The approximate direction of the dip of the upper surface of layer 5 is toward the south in the northern part of the study area and toward the southeast in the southern part of the study area (fig. 23). The layer is thickest (almost 10 ft) in the northeastern part of the study area, but generally is between 1 and 3 ft thick over much of the study area and locally absent (fig. 24).

Layer 6 is characterized by the lower zone of pore class III and occurs at the base of HFC3a and locally at the uppermost part of HFC2, spanning the top of HFC2 and HFC3a. The upper surface of layer 6 generally slopes toward the southeast or east in the study area (fig. 25). The layer is thin or absent in the northeastern part of the study area, and in general, about 1 to 2 ft thick over the rest of the study area (fig. 26).

Layer 7 is characterized by the lower zone of pore class II and is equivalent to the upper part of HFC2 and can include HFC2e to HFC2h. The upper surface of layer 7 generally dips toward the south and southeast (fig. 27). The layer is thinnest on the western part of the study area and thickens toward the east, especially to the northeast where the thickness exceeds 30 ft (fig. 28).

Layer 8 is characterized by the lower zone of pore class I and is equivalent to the lower part of HFC2 and can include HFC2d to HFC2a. This layer includes much of the open-hole intervals of production wells at the NWWF and West Well Field (fig. 2). Layer 8 is thickest in the northwestern part of the study area and in the vicinity of the NWWF. In general, the upper surface of layer 8 dips from west to east at about 5 ft per mile (fig. 29). The thickness of this layer ranges from about 9 ft to 45 ft (fig. 30). The lower surface of layer 8 generally dips toward the east (fig. 31).

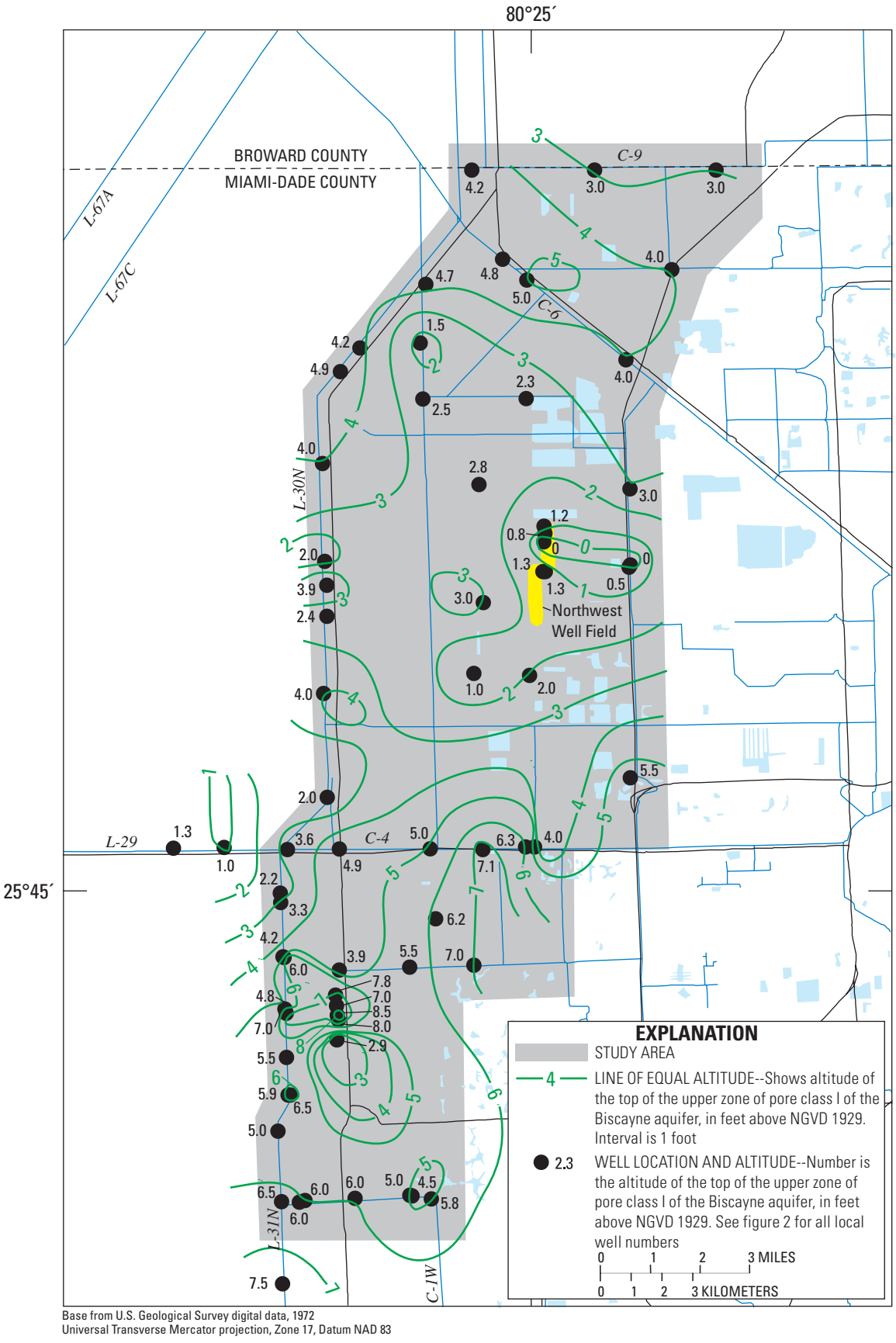

Base from U.S. Geological Survey digital data, 1972
Universal Transverse Mercator projection, Zone 17, Datum NAD 83

Figure 17. Altitude of the top of the upper zone of pore class I of the Biscayne aquifer. This zone is shown as layer 2 in figure 15.

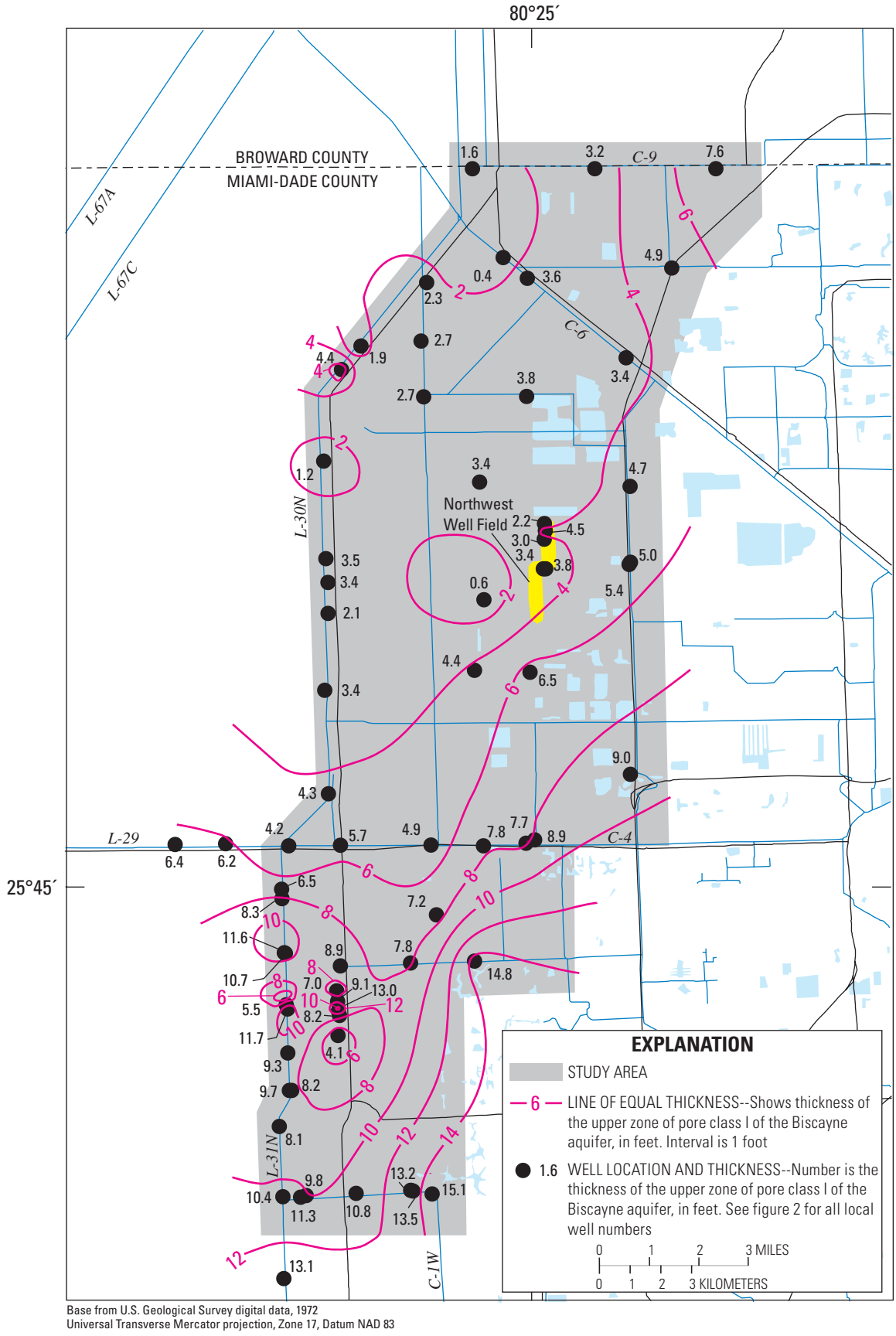

Base from U.S. Geological Survey digital data, 1972
Universal Transverse Mercator projection, Zone 17, Datum NAD 83

Figure 18. Thickness of the upper zone of pore class I of the Biscayne aquifer. This zone is shown as layer 2 in figure 15.

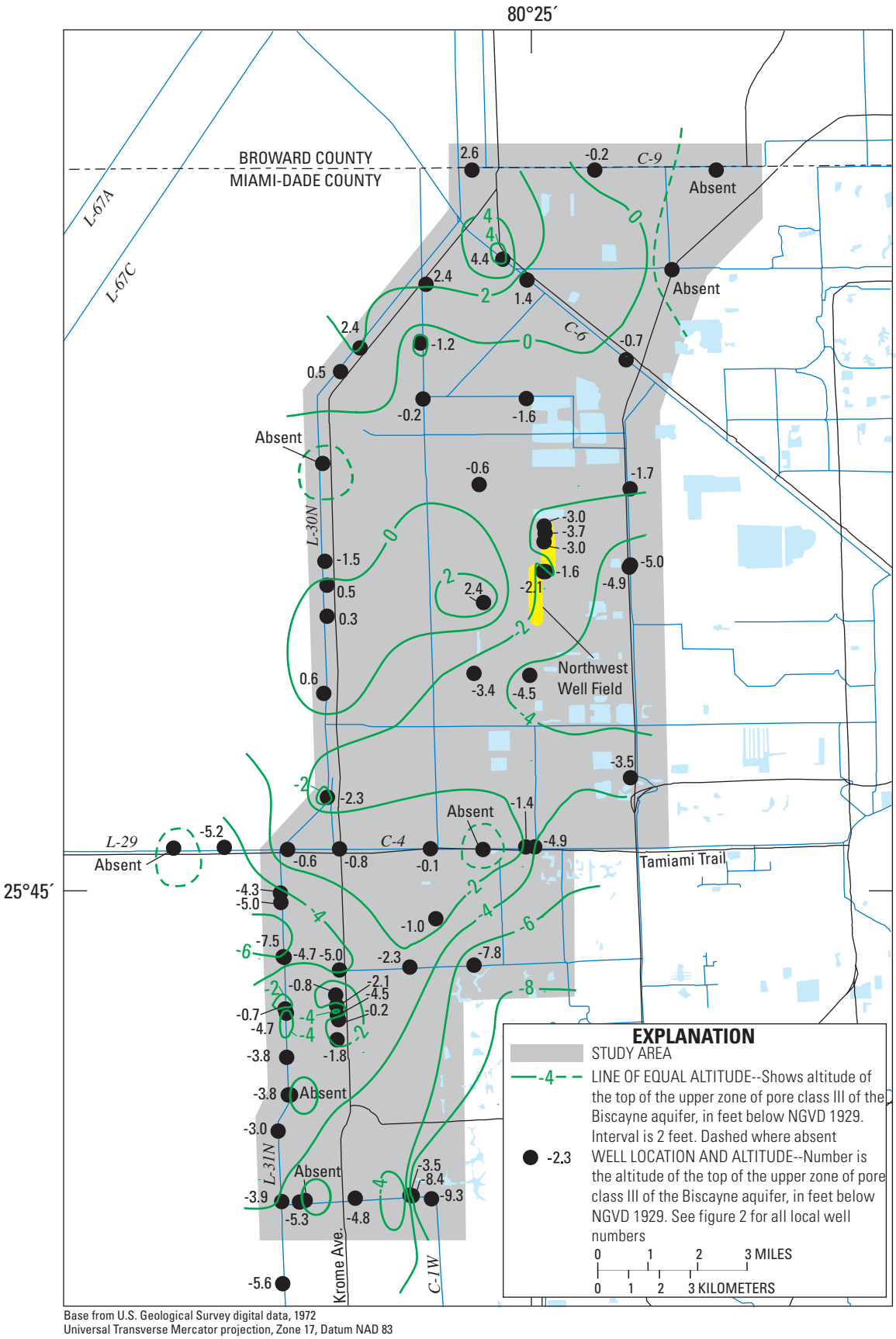

Figure 19. Altitude of the top of the upper zone of pore class III of the Biscayne aquifer. This zone is shown as layer 3 in figure 15.

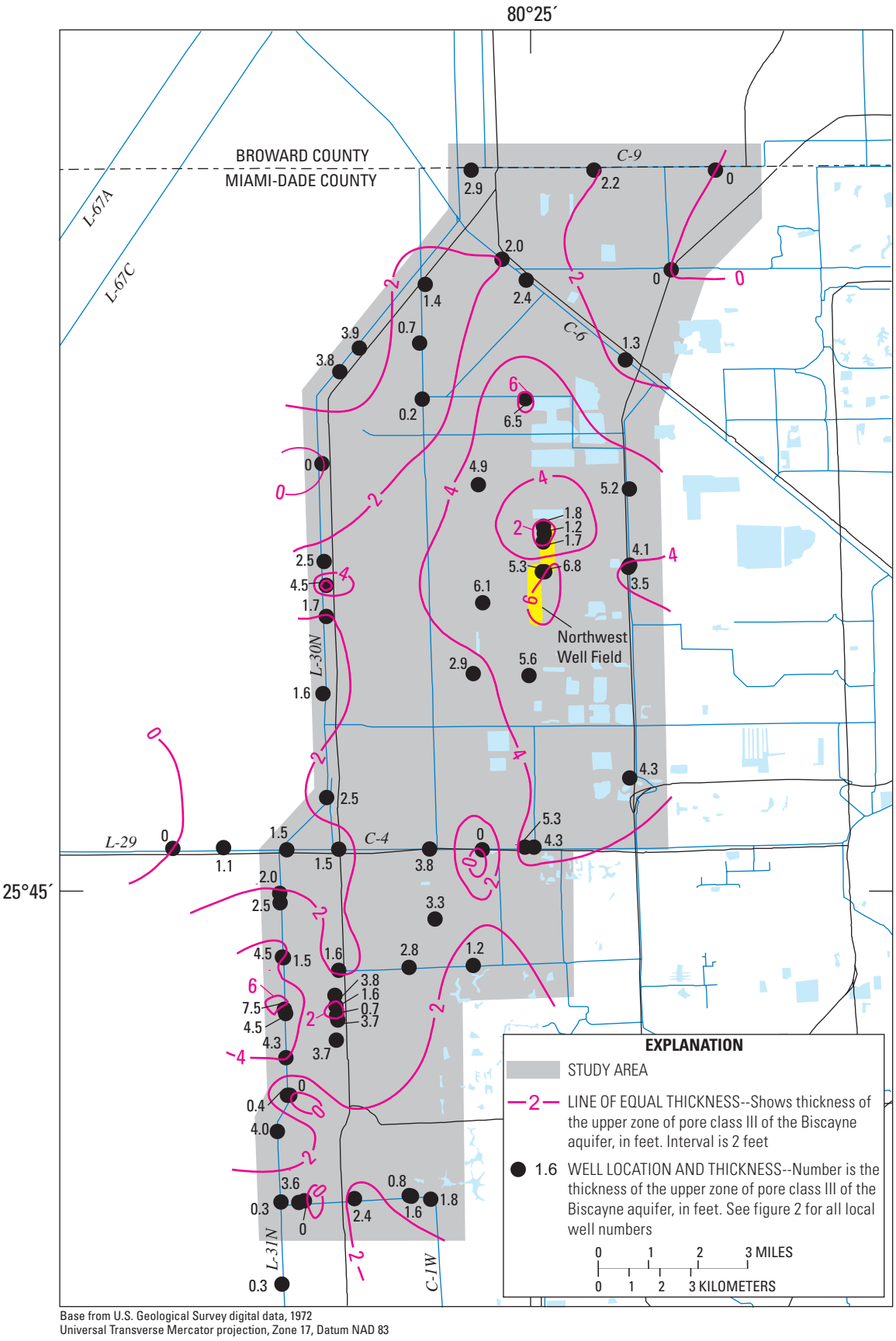

Figure 20. Thickness of the upper zone of pore class III of the Biscayne aquifer. This zone is shown as layer 3 in figure 15.

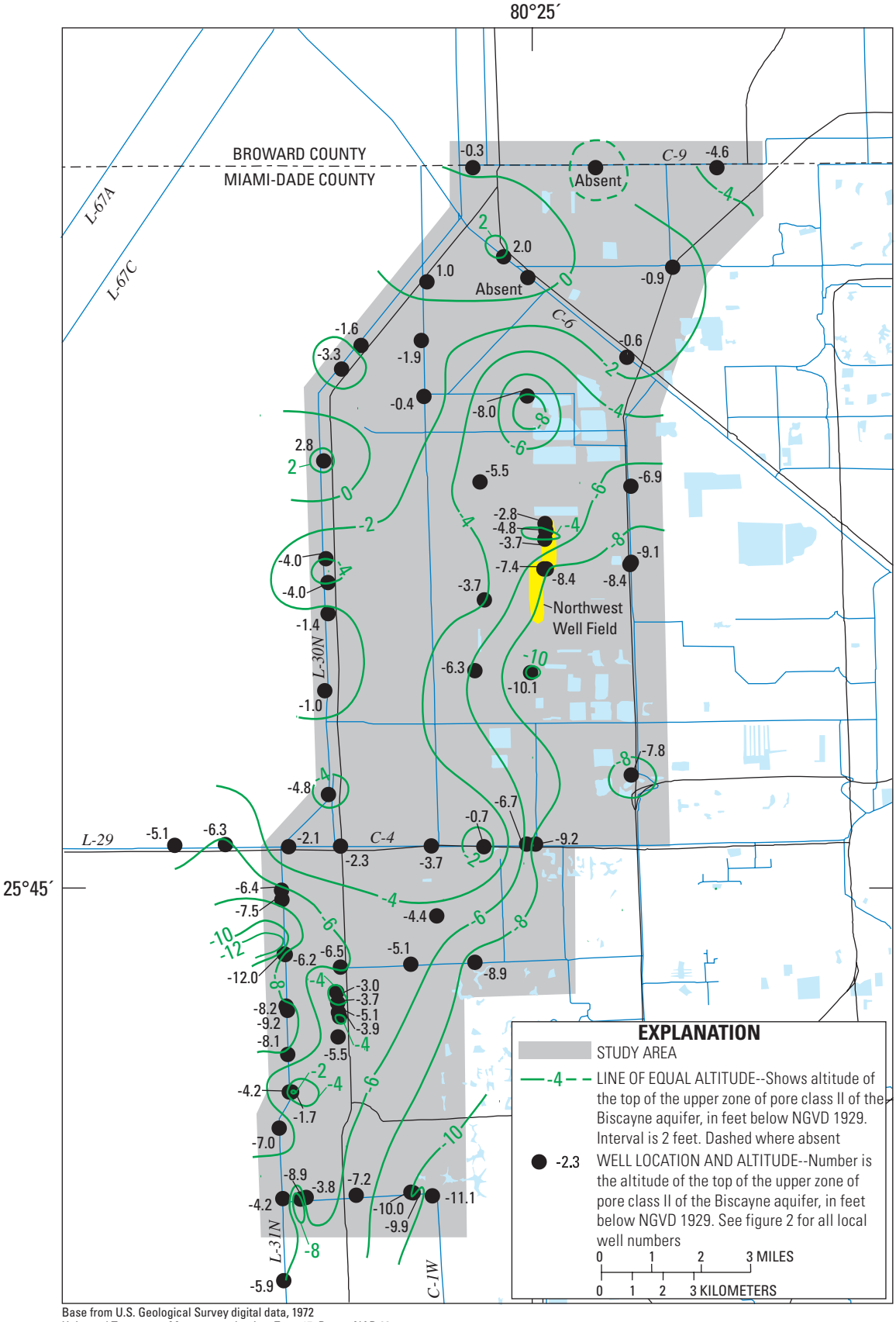

Base from U.S. Geological Survey digital data, 1972
Universal Transverse Mercator projection, Zone 17, Datum NAD 83

Figure 21. Altitude of the top of the upper zone of pore class II of the Biscayne aquifer. This zone is shown as layer 4 in figure 15.

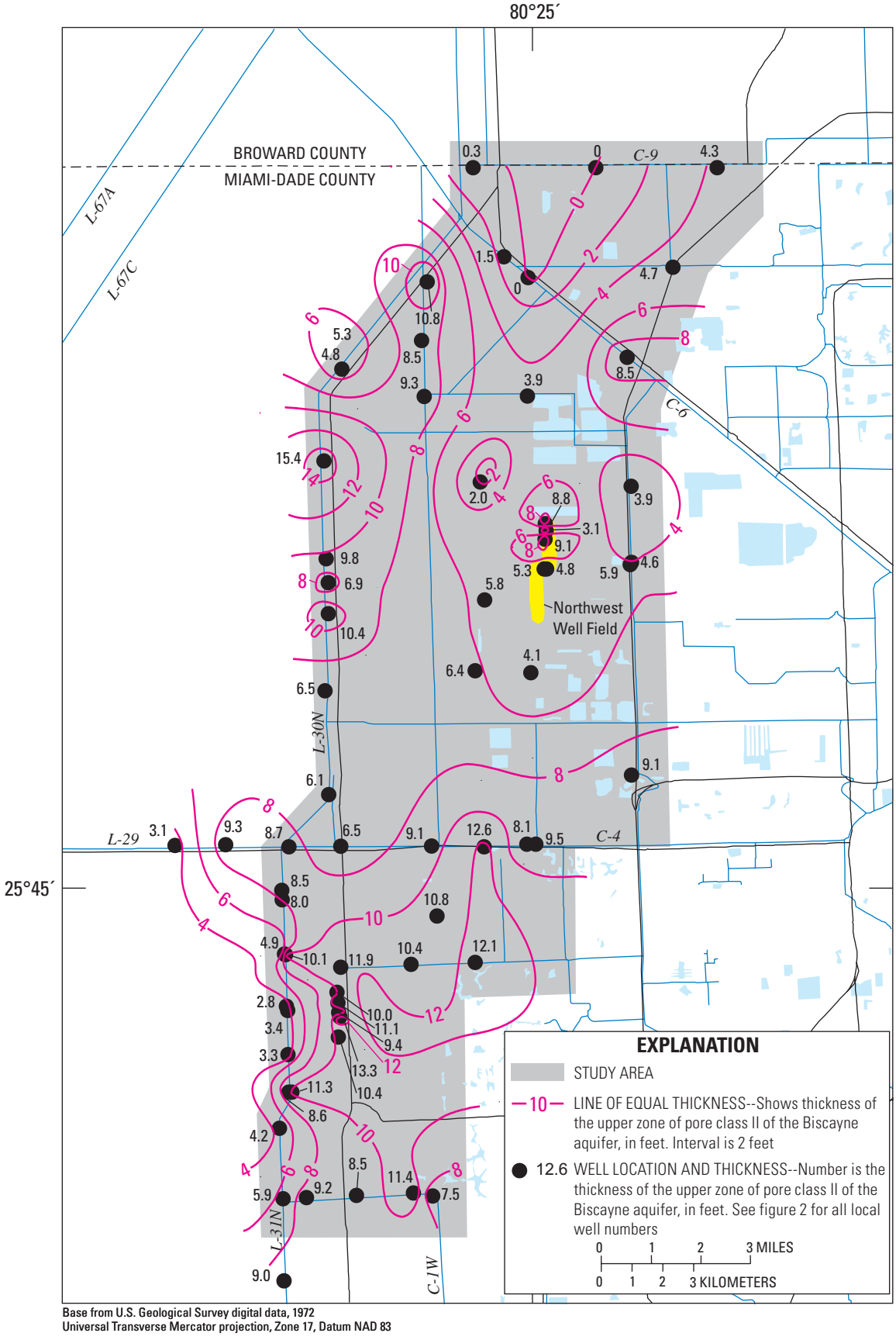

Base from U.S. Geological Survey digital data, 1972
Universal Transverse Mercator projection, Zone 17, Datum NAD 83

Figure 22. Thickness of the upper zone of pore class II of the Biscayne aquifer. This zone is shown as layer 4 in figure 15.

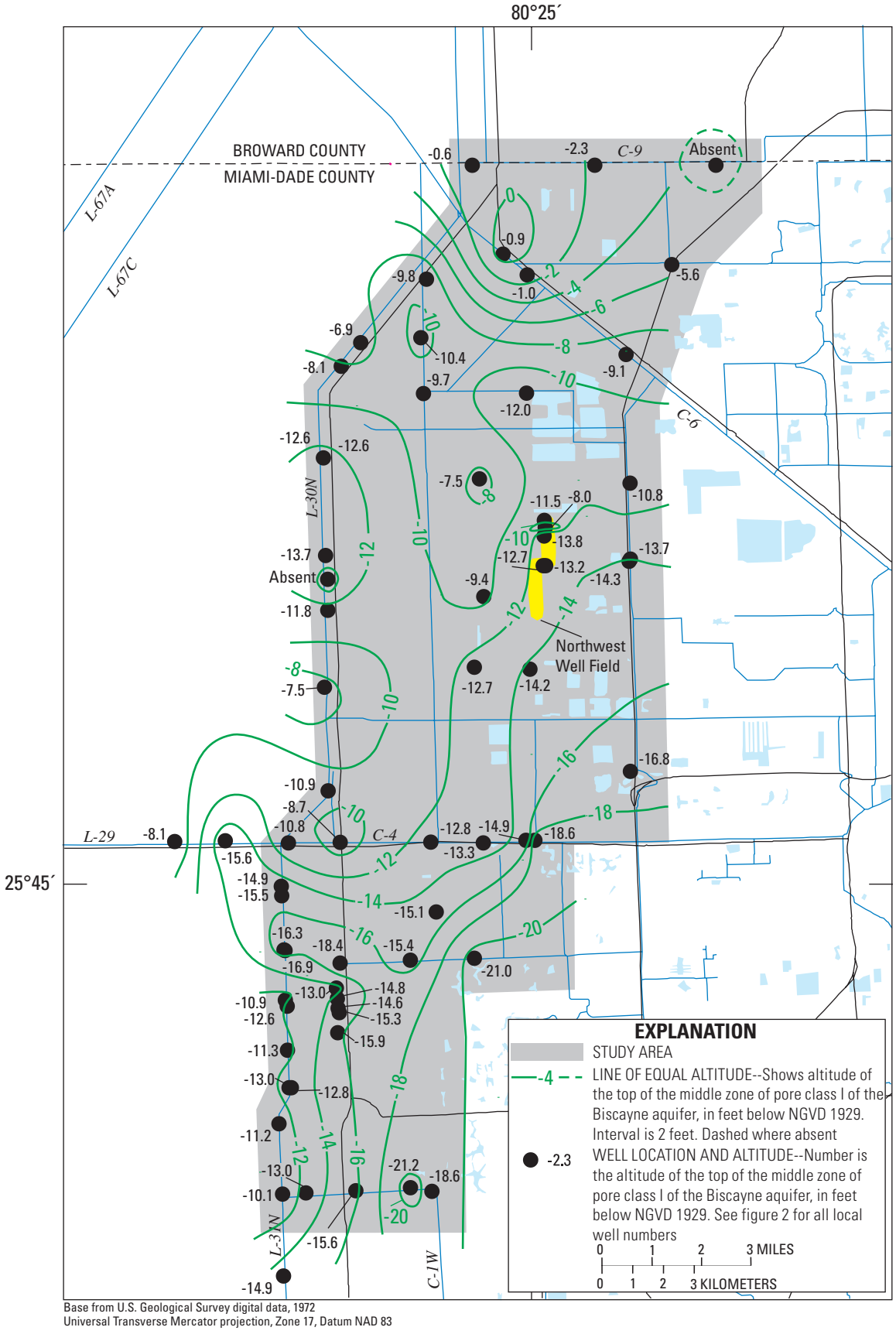

Figure 23. Altitude of the top of the middle zone of pore class I of the Biscayne aquifer. This zone is shown as layer 5 in figure 15.

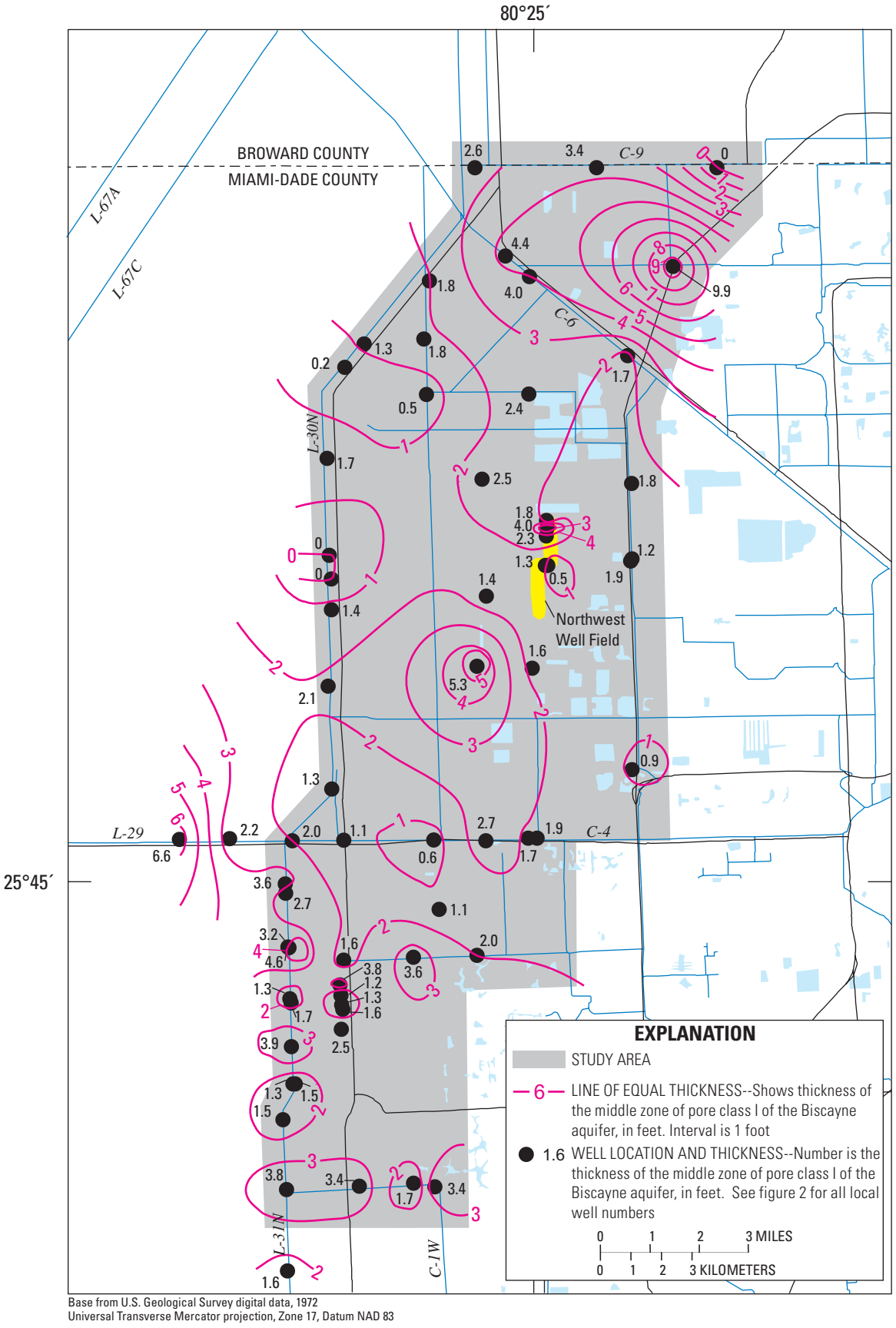

Base from U.S. Geological Survey digital data, 1972
Universal Transverse Mercator projection, Zone 17, Datum NAD 83

Figure 24. Thickness of the middle zone of pore class I of the Biscayne aquifer. This zone is shown as layer 5 in figure 15.

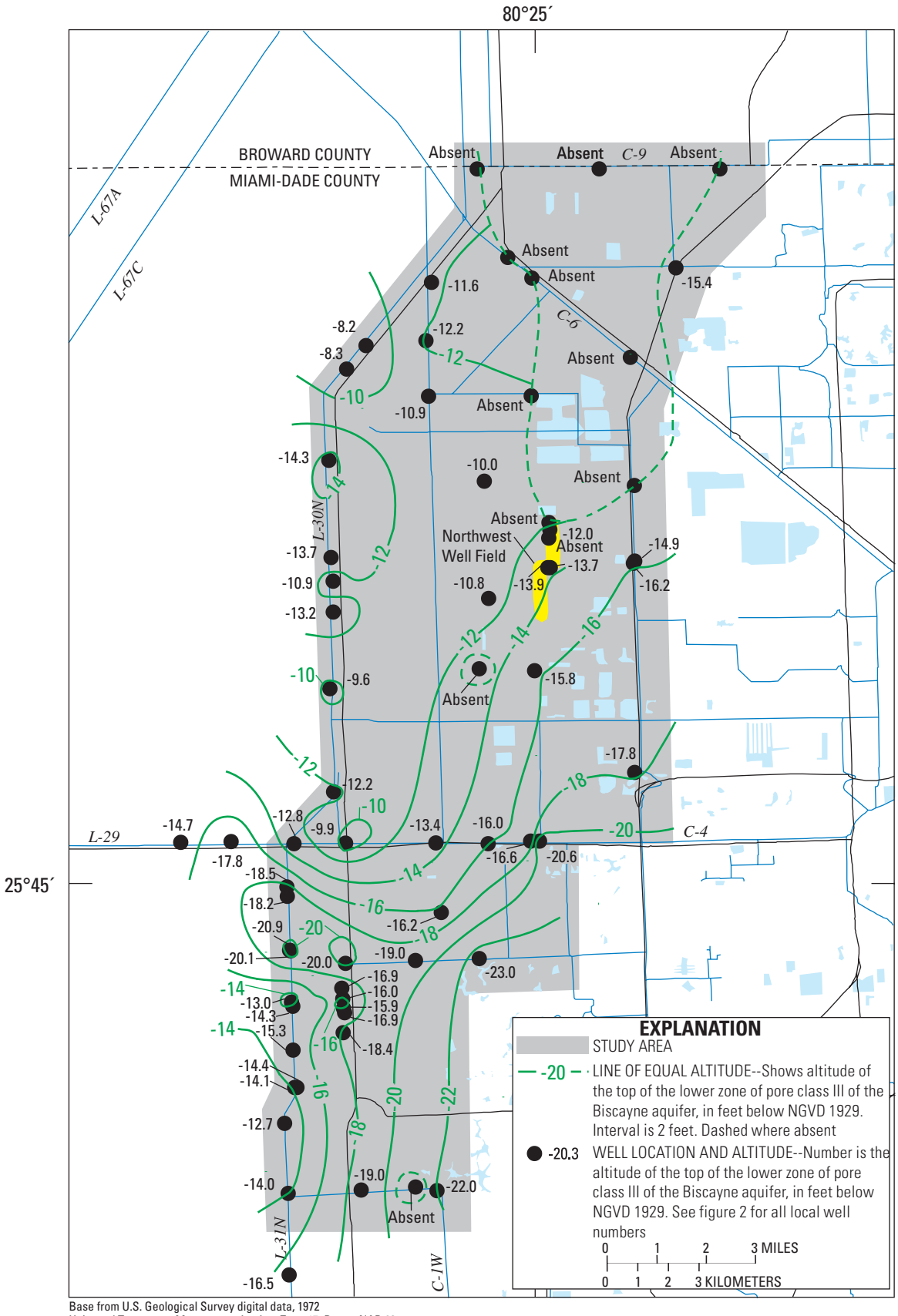

Base from U.S. Geological Survey digital data, 1972
Universal Transverse Mercator projection, Zone 17, Datum NAD 83

Figure 25. Altitude of the top of the lower zone of pore class III of the Biscayne aquifer. This zone is shown as layer 6 in figure 15.

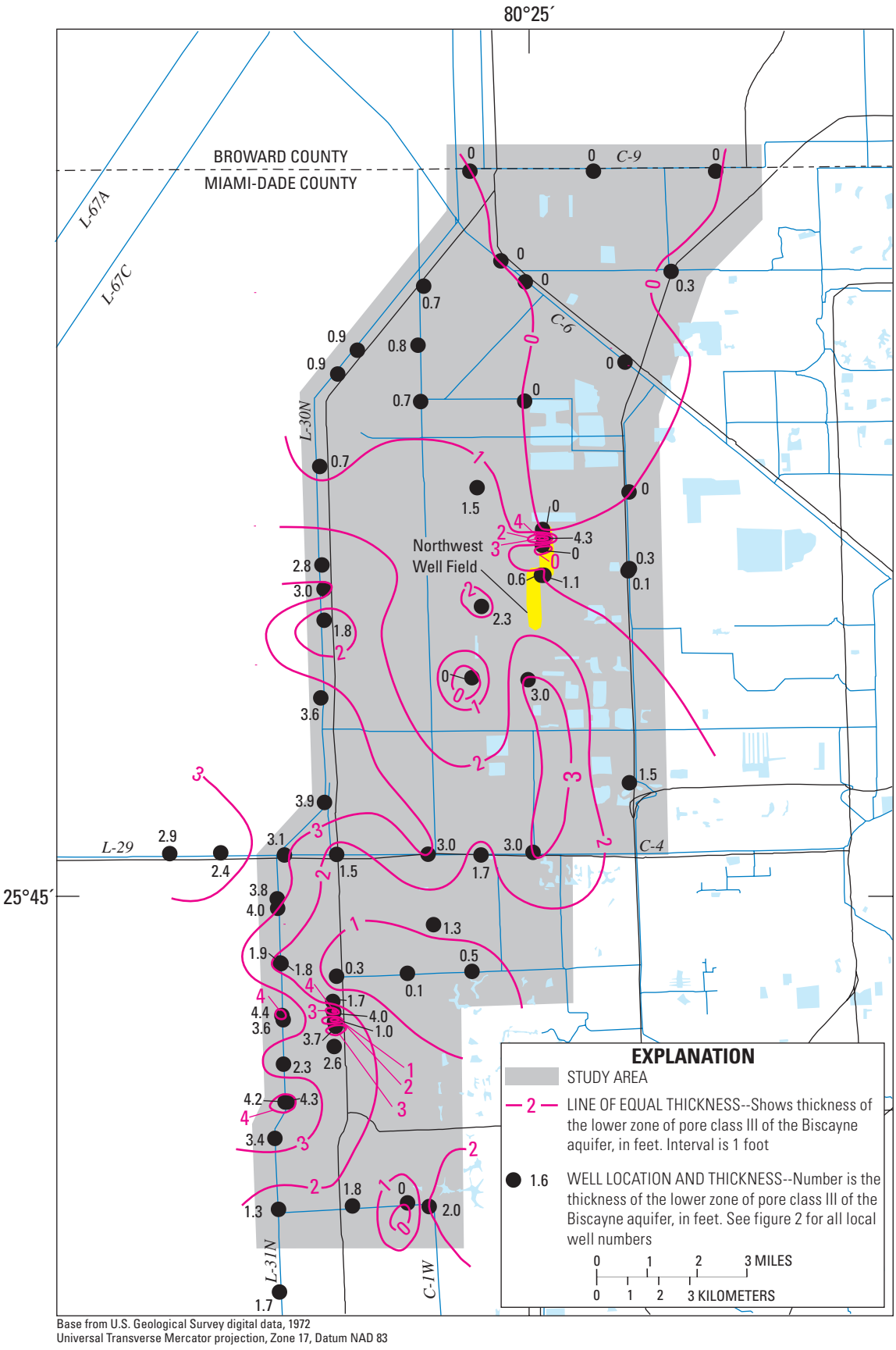

Base from U.S. Geological Survey digital data, 1972
Universal Transverse Mercator projection, Zone 17, Datum NAD 83

Figure 26. Thickness of the lower zone of pore class III of the Biscayne aquifer. This zone is shown as layer 6 in figure 15.

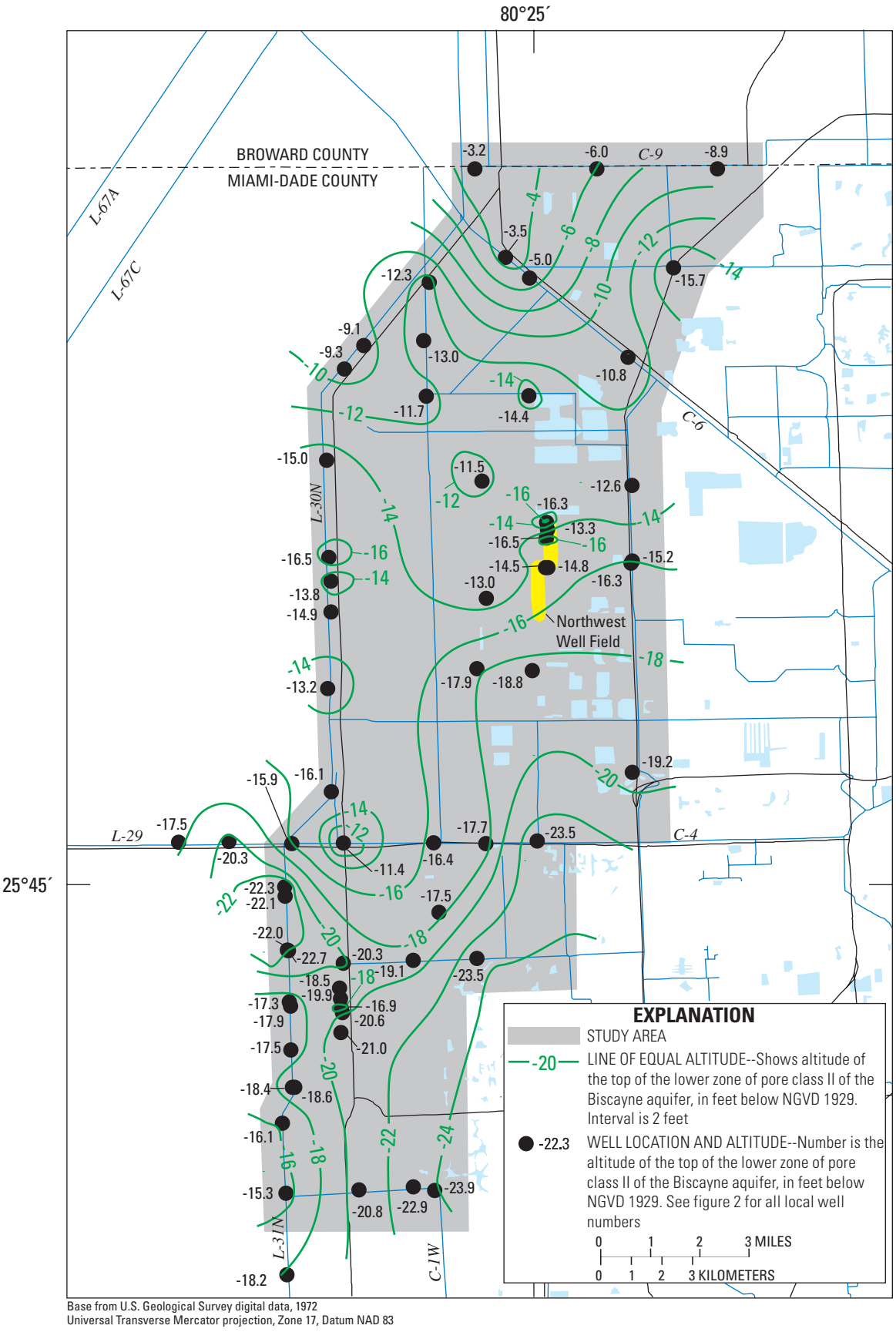

Base from U.S. Geological Survey digital data, 1972
Universal Transverse Mercator projection, Zone 17, Datum NAD 83

Figure 27. Altitude of the top of the lower zone of pore class II of the Biscayne aquifer. This zone is shown as layer 7 in figure 15.

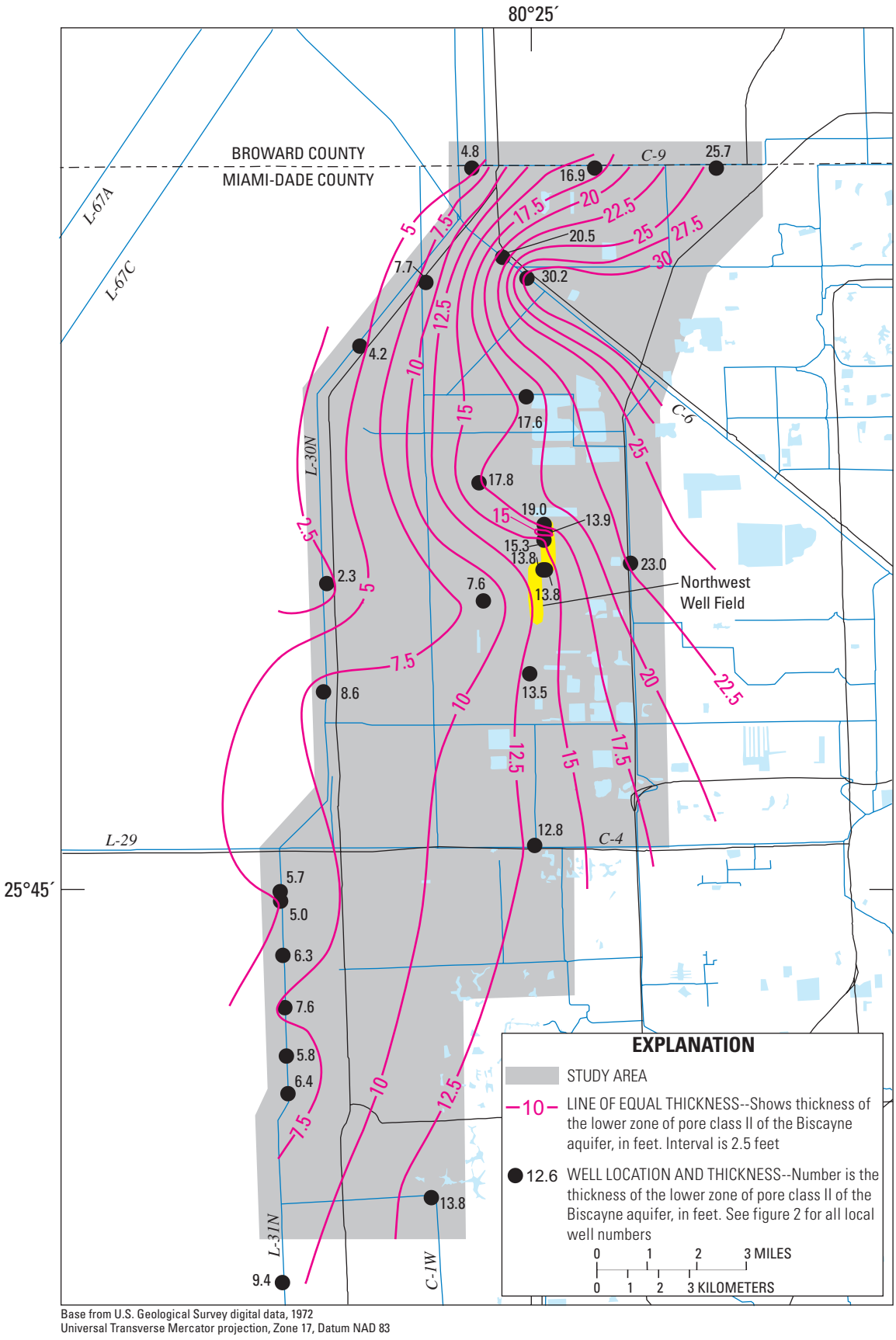

Base from U.S. Geological Survey digital data, 1972
Universal Transverse Mercator projection, Zone 17, Datum NAD 83

Figure 28. Thickness of the lower zone of pore class II of the Biscayne aquifer. This zone is shown as layer 7 in figure 15.

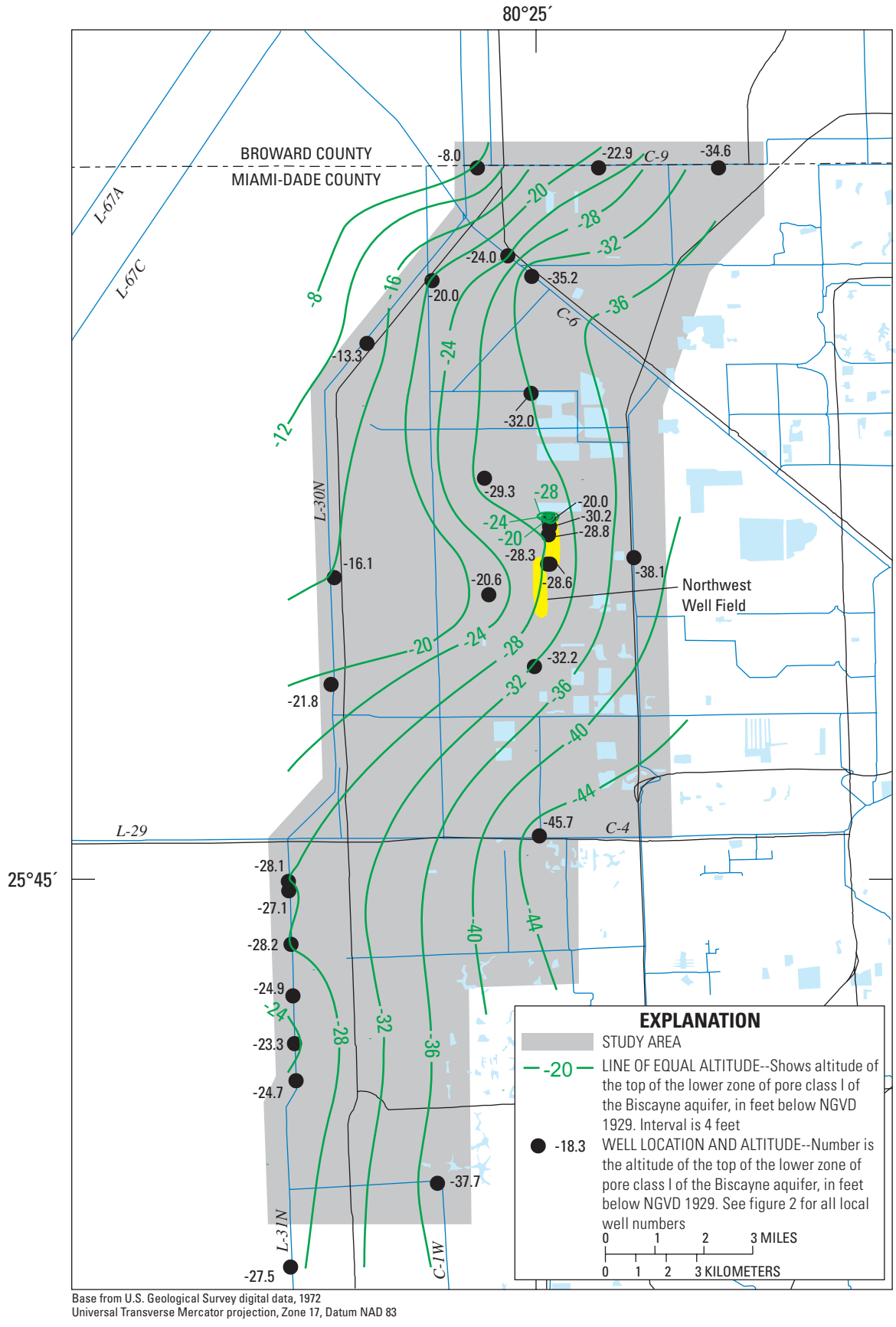

Base from U.S. Geological Survey digital data, 1972
Universal Transverse Mercator projection, Zone 17, Datum NAD 83

Figure 29. Altitude of the top of the lower zone of pore class I of the Biscayne aquifer. This zone is shown as layer 8 in figure 15.

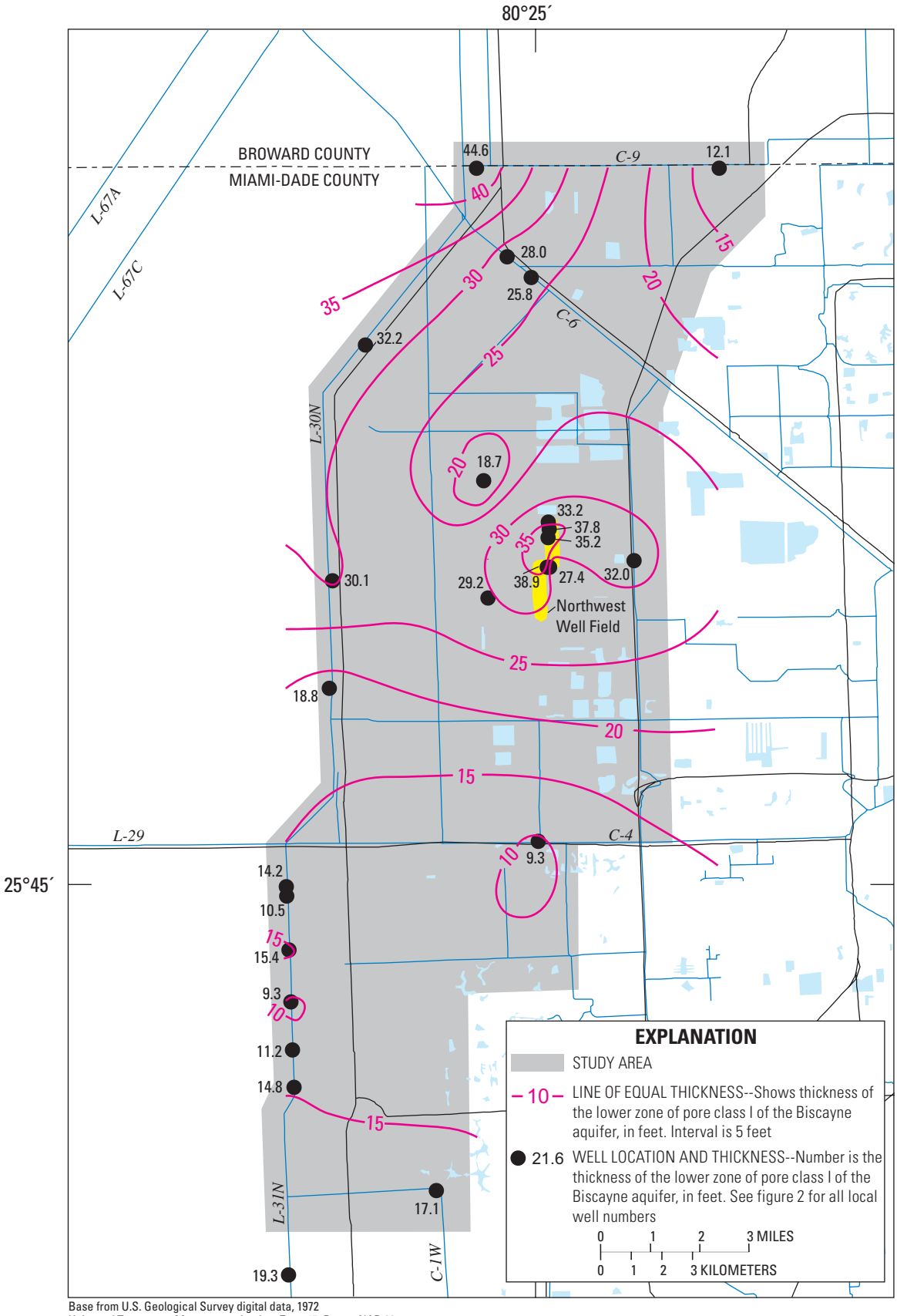

Base from U.S. Geological Survey digital data, 1972
Universal Transverse Mercator projection, Zone 17, Datum NAD 83

Figure 30. Thickness of the lower zone of pore class I of the Biscayne aquifer. This zone is shown as layer 8 in figure 15.

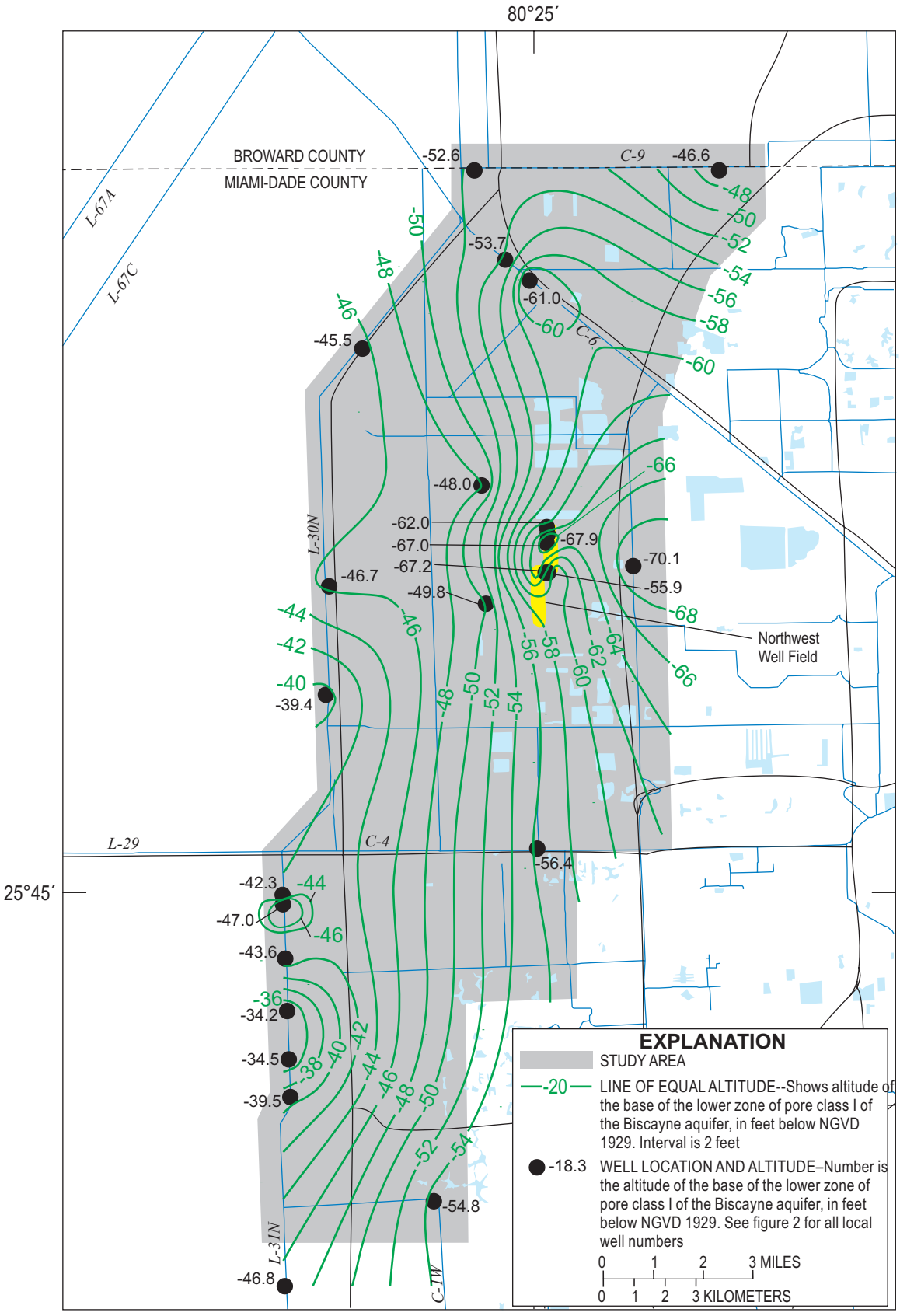

Figure 31. Altitude of the base of the lower zone of pore class I of the Biscayne aquifer. This zone is shown as layer 8 in figure 15.

Borehole-Fluid Flow

Vertical borehole flow was identified to test the hypothesis that laterally extensive units characterized by pore class I are responsible for most of the ground-water flow in the Biscayne aquifer. Borehole-fluid flow was detected in conjunction with the acquisition of borehole-flowmeter data, fluid-conductivity data, and fluid-temperature data (table 8) and also digital optical borehole images and computed vuggy porosity data. For the logs included in table 8, borehole-fluid temperature ranged from 71.6 to 88.9 °F, and borehole-fluid conductivity ranged from 336 to 807 µS/cm for measurements within the Biscayne aquifer. Intervals of boreholes where changes in borehole flow and fluid conductivity or fluid temperature or both are sharp have been identified as zones of the boreholes where there is inflow or outflow of water.

In some instances, abrupt variations in fluid conductivity, temperature, or both corresponded to sharp changes in flowmeter velocities; these flow zones mostly occurred at the base of the HFCs (table 8). Two preferential flow zones were most likely present in the upper part of the Biscayne aquifer in HFC3a and HFC5e, seven preferential flow zones were identified as important in the lower part of the Biscayne aquifer, and five zones were identified in the Biscayne aquifer where inflow and outflow from the borehole were only delineated locally (fig. 32). Examples from layers 2, 5, and 8 (figs. 15 and 16) of ground-water inflow into boreholes from preferential flow zones, represented as pore class I on the basis of digital borehole images, are shown in figures 33, 34, and 35, respectively. Both zones shown in figures 33 and 34 are part of hydrogeologic units (figs. 15 and 16, layers 2 and 5) that can be clearly correlated well beyond the limits of the study area.

In conclusion, all of HFC5e, the lower part of HFC3a, and various zones in the lower part of the Biscayne aquifer (fig. 32) likely are principal pathways for ground-water flow and solute transport in the Biscayne aquifer. Additionally, HFC5e corresponds to the regionally mapped Q5 unit of Perkins (1977), and the lower part of HFC3a occurs near the base of the Q3 unit of Perkins (1977); both are correlated, although undocumented, over a large area of Miami-Dade County. Many older preferential flow zones (fig. 32) seem to be present throughout the study area, but their extent has not been verified. Mapping shows that the preferential flow zones of local extent (fig. 32) probably are not substantial pathways for regional ground-water flow and solute transport.

Ground-Water Flow and Pore System Evolution

Movement of ground water within water-bearing strata of the Biscayne aquifer occurs within pore classes I, II, and III (table 7). Each pore class comprises a unique category of lithofacies and pore system (figs. 11 and 12, and table 7). Carbonate-rock lithofacies and pore systems can be arranged within the context of high-frequency carbonate cyclostratigraphy. The porosity of pore class I is typically characterized by touching vugs that form highly permeable stratiform passageways and less widespread bedding-plane vugs, thin solution pipes, and cavernous porosity. The size, shape, and spatial distribution of touching-vug porosity within the Biscayne aquifer can be mapped within the context of the high-frequency cyclostratigraphic framework because these attributes commonly occur in the lower part of the HFCs above flooding surfaces, which facilitates well-to-well correlation of highly porous zones. These highly porous zones commonly occur at the base of the paralic and subtidal upward-shallowing cycles of the Fort Thompson Formation and throughout the uppermost subtidal aggradational cycle of the Miami Limestone (fig. 10).

Pore class II is distinguished by interparticle and separate-vug porosity within the rock matrix and mostly contains diffuse-carbonate ground-water flow (Shuster and White, 1971; Thrailkill, 1976; Martin and Screaton, 2001). These two pore types relate to specific lithofacies at the middle of upward-shallowing cycles and the upper part of ideal subtidal upward-shallowing cycles of the Fort Thompson Formation.

The porosity of pore class III is typically distinguished by separate vugs, such as *Planorbella* molds, within a very low-permeability micrite matrix that: (1) may be perforated by thin semivertical solution pipes of limited vertical extent, or (2) may have associated bedding-plane vugs. The overall permeability of pore class III is commonly low, but vertically leaky. Pore class III is commonly associated with micrite-rich lithofacies that may cap upward-shallowing cycles of the Fort Thompson Formation.

The distribution of pore classes I, II, and III in the study area occurs within predictable vertical and horizontal spatial patterns. This can be explained by the fact that their manifestation is directly related to the vertical assemblage of lithofacies within HFCs.

It is proposed herein that karstic development of the highly permeable zones at the base of upward-shallowing cycles of the Fort Thompson Formation relates to cyclostratigraphy and Pleistocene sea-level history. This conclusion is supported by figure 8, which shows that the vertical arrangement of lithofacies and pore classes are linked within the context of ideal HFCs. Formation of secondary porosity was probably produced by meteoric water flowing through the limestone of the Fort Thompson Formation during its emergence into the vadose zone caused by periodic low stands in sea level that span Pleistocene glacial maximums inferred by Perkins (1977). The possibility exists that these episodic vadose events promoted aggressive dissolution of carbonate grains and depositional textures in the lower part of cycles as a result of perched, concentrated, down-dip flow of meteoric water above flooding surfaces. This focused, low-gradient lateral flow of meteoric water above flooding surfaces is postulated due to the presence of relatively low-permeability lithologies at cycle tops that underlie flooding surfaces and act as baffles or barriers to downward vertical drainage.

Table 8. Borehole-flowmeter, fluid-conductivity, and fluid-temperature data for wells that fully penetrate the Biscayne aquifer in the study area and collected over uncased, open-hole intervals.

[HFC, high-frequency cycle; C, conduit; TV, touching vug; —, no log was made; *Quasi-synoptic log measurements]

Local well identifier	Data collection date				Inflection depth (feet below land surface)				HFC or formation contributing flow into or out of borehole	Porosity type
	Heat-pulse flowmeter	Spinner flowmeter	Fluid conduc-tivity	Fluid temp-erature	Heat-pulse flometer	Spinner flowmeter	Fluid conduc-tivity	Fluid temp-erature		
G-3671*	9-16-03	—	9-12-03	9-12-03	29.9-29.4	—	None	None	Lower HFC3a	C
	9-16-03	—	9-12-03	9-12-03	46.8-48.0	—	None	None	Lower HFC2e2	TV
	3-16-04	—	3-16-04	3-16-04	45.9-46.9	—	None	None	Lower HFC2e2	TV
G-3733	3-8-04	—	3-8-04	3-8-04	8.5-11.5	—	None	None	Lower HFC5e	TV and C
	3-8-04	—	3-8-04	3-8-04	17.0-20.5	—	None	None	Lower HFC2h	TV
	3-8-04	—	3-8-04	3-8-04	22.4-25.0	—	None	None	Lower HFC2g3	TV
G-3770	12-20-02	—	—	—	16.1-18.4	—	—	—	Lower HFC3a	TV
	12-20-02	—	—	—	26.5-29.6	—	—	—	Lower HFC2g2	TV
	12-20-02	—	—	—	45.9-51.1	—	—	—	Middle HFC2c2	TV
	1-2-03	—	—	—	17.0-18.0	—	—	—	Lower HFC3a	TV
	1-2-03	—	—	—	49.1-51.2	—	—	—	Middle HFC2c2	TV
	1-8-03	—	—	—	16.0-18.0	—	—	—	Lower HFC3a	TV
	1-8-03	—	—	—	26.4-29.5	—	—	—	Lower HFC2g2	TV
	1-8-03	—	—	—	49.2-51.1	—	—	—	Middle HFC2c2	TV
G-3771	12-26-02	—	—	—	16.0-16.6	—	—	—	Lower HFC3a	TV
	12-26-02	—	—	—	26.1-23.5	—	—	—	Lower 2g3	TV
	12-26-02	—	—	—	34.5-41.1	—	—	—	Lower HFC2f & HFC2e2	TV and C
	12-26-02	—	—	—	41.1-45.1	—	—	—	Lower HFC2d	TV
	12-26-02	—	—	—	54.5-55.0	—	—	—	Uppermost Tamiami Formation	TV
	12-30-02	—	—	—	16.0-17.1	—	—	—	Lower HFC3a	TV
	12-30-02	—	—	—	22.0-24.0	—	—	—	Lower HFC2g3	TV
	12-30-02	—	—	—	33.1-45.3	—	—	—	Lower HFC2f, Lower HFC 2e2, Lower HFC2d	TV and C
	12-30-02	—	—	—	49.1-54.5	—	—	—	Lower HFC2c2	TV
	1-8-03	—	—	—	22.5-25.9	—	—	—	Lower HFC2g3	TV
	1-8-03	—	—	—	34.5-42.0	—	—	—	Lower HFC2f, Lower HFC2e2	TV and C
G-3778	8-7-03	—	—	—	20.5-23.5	—	—	—	Lower HFC5e	TV and C
	8-7-03	—	—	—	29.0-29.5	—	—	—	Upper HFC3a	C?
	8-7-03	—	—	—	32.0-35.5	—	—	—	Lower HFC3a	TV
	8-7-03	—	—	—	38.8-39.1	—	—	—	Upper HFC2h	Matrix
	8-7-03	—	—	—	41.0-46.5	—	—	—	Lower HFC2g3	TV
	8-7-03	—	—	—	48.0-49.5	—	—	—	Lower HFC2g2	TV?
	8-30-03	—	—	—	20.0-25.5	—	—	—	Lower HFC5e, upper HFC3b	TV and C
	8-30-03	—	—	—	25.5-29.1	—	—	—	Upper HFC3a	TV and C?
	8-30-03	—	—	—	31.8-35.5	—	—	—	Lower HFC3a	TV
G-3782	8-11-03	—	8-11-03	8-11-03	19.0-22.6	—	None	None	Upper HFC3a	C
	8-11-03	—	8-11-03	8-11-03	25.1-29.1	—	None	None	Lower HFC3a	TV
	8-11-03	—	8-11-03	8-11-03	33.0-34.0	—	None	None	Lower HFC2h	TV
	3-15-04	3-15-04	3-15-04	3-15-04	15.0-15.8	16.2-17.3	15.0-18.5	16.0-17.2	Lower HFC5e	C
	3-15-04	3-15-04	3-15-04	3-15-04	46.2-47.0	46.5-47.2	None	None	Middle HFC2d	TV
G-3783	8-19-03	—	—	—	9.9-10.5	—	—	—	Lower HFC5e	TV
	8-19-03	—	—	—	34.1-34.3	—	—	—	Lower HFC2g3	C
	8-19-03	—	—	—	34.5-35.5	—	—	—	Lower HFC2g3	C
	8-19-03	—	—	—	38.3-38.6	—	—	—	Lower HFC2f	TV
G-3783*	3-15-04	3-11-04	3-11-04	3-11-04	11.5-15.0	12.0-12.1	None	12.5-13.5	Lower HFC4	C?
	3-15-04	3-11-04	3-11-04	3-11-04	25.5-26.5	25.25-25.35	None	None	Lower HFC3a	C
	3-15-04	3-11-04	3-11-04	3-11-04	37.5-40.0	38.0-38.1	None	None	Lower HFC2f	TV
G-3784*	9-12-03	—	9-16-03	9-16-03	49.0-49.7	—	None	None	Lower HFC2e1?	C

Table 8. Borehole-flowmeter, fluid-conductivity, and fluid-temperature data for wells that fully penetrate the Biscayne aquifer in the study area and collected over uncased, open-hole intervals. (Continued)

Local well identifier	Data collection date				Inflection depth (feet below land surface)				HFC or formation contributing flow into or out of borehole	Porosity type
	Heat-pulse flowmeter	Spinner flowmeter	Fluid conduc-tivity	Fluid temp-erature	Heat-pulse flometer	Spinner flowmeter	Fluid conduc-tivity	Fluid temp-erature		
G-3788*	9-11-03	—	9-3-03	9-3-03	8.2-10.5	—	None	None	Lower HFC5e	TV
	9-11-03	—	9-3-03	9-3-03	18.3-23.2	—	None	None	Lower HFC3a	C
	9-11-03	—	9-3-03	9-3-03	32.4-35.6	—	33.4-34.1	33.8-35.5	Lower HFC2g3	TV
	9-11-03	—	9-3-03	9-3-03	38.2-40.2	—	None	None	Lower HFC2f	TV
G-3788	3-10-04	3-10-04	3-10-04	3-10-04	9.0-12.5	8.6-10.1	8.5-10.4	None	Lower HFC5e	TV
	3-10-04	3-10-04	3-10-04	3-10-04	21.4-22.0	20.0-22.3	19.8-22.6	20.5-24.5	Lower HFC3a	C
	3-10-04	3-10-04	3-10-04	3-10-04	None	37.8-38.9	None	None	Lower HFC2f	TV
	3-10-04	3-10-04	3-10-04	3-10-04	43.0-43.5	None	None	None	Upper HFC2e1?	TV
G-3789	9-12-03	—	—	—	7.5-10.5	—	—	—	Lower HFC5e	TV
	9-12-03	—	—	—	38.6-39.5	—	—	—	Lower HFC2g2	TV
	9-12-03	—	—	—	44.1-46.1	—	—	—	Middle HFC2e2	TV
	9-12-03	—	—	—	49.0-50.0	—	—	—	Lower HFC2e1?	TV
	3-9-04	3-9-04	3-9-04	3-9-04	9.0-10.0	9.8-9.9	None	None	Lower HFC5e	TV
	3-9-04	3-9-04	3-9-04	3-9-04	11.0-14.0	13.4-13.9	None	None	Lower HFC4	TV
	3-9-04	3-9-04	3-9-04	3-9-04	None	15.6-16.1	None	None	Middle HFC3b	C
	3-9-04	3-9-04	3-9-04	3-9-04	None	23.5-24.0	None	None	Lower HFC3a	TV and C?
	3-9-04	3-9-04	3-9-04	3-9-04	44.2-46.0	45.3-45.4	None	None	Middle HFC2e2	TV
	3-9-04	3-9-04	3-9-04	3-9-04	46.0-52.5	None	None	None	Lower HFC2e1?	TV
G-3790	3-17-04	3-17-04	3-17-04	3-17-04	6.0-9.0	8.5-10.5	None	None	Lower HFC5e	TV
	3-17-04	3-17-04	3-17-04	3-17-04	No data	27.8-29.7	27.8-28.3	None	Lower HFC3a	TV
	3-17-04	3-17-04	3-17-04	3-17-04	53.0-55.0	53.8-54.8	54.5-56.0	None	Lower HFC2e2	TV
	3-17-04	3-17-04	3-17-04	3-17-04	58.0-60.0	None	None	None	Lower HFC2d	TV
G-3791	4-6-04	—	4-6-04	4-6-04	9.6-14.6	—	10.0-11.0	None	Lower HFC5e	TV
	4-6-04	—	4-6-04	4-6-04	45.0-46.3	—	None	None	Lower HFC2f	TV
G-3792	2-26-04	—	—	—	10.9-14.0	—	—	—	Lower HFC5e	TV
	2-26-04	—	—	—	50.2-63.0	—	—	—	Middle HFC2c2	C
	2-27-04	—	—	—	49.5-63.9	—	—	—	Middle HFC2c2	C
	3-18-04	3-18-04	3-18-04	3-18-04	10.9-14.0	None	None	None	Lower HFC5e	TV
	3-18-04	3-18-04	3-18-04	3-18-04	46.0-49.5	47.2-47.3 49.4-49.5	None	None	Lower HFC2d	TV
	3-18-04	3-18-04	3-18-04	3-18-04	50.5-63.0	49.9-66.5	52.8-53.3	53.2-55.0	Middle HFC2c2	C and TV
G-3793*	3-3-04	3-3-04	3-2-04	3-2-04	12.5-14.5	13.45-13.65	None	None	Lower HFC3a	TV
	3-3-04	3-3-04	3-2-04	3-2-04	19.5-21.5	20.3-21.05	None	None	Lower HFC2h	TV
	3-3-04	3-3-04	3-2-04	3-2-04	None	42.2-43.0	None	None	Lower HFC2d	TV
	3-3-04	3-3-04	3-2-04	3-2-04	46.4-50.0	45.9-47.6	None	None	Lower HFC2c2	TV
	3-3-04	3-3-04	3-2-04	3-2-04	51.0-53.0	51.8-51.9	51.6-52.3	52.0-55.0	Lower HFC2c2	TV and C?
G-3794	2-27-04	—	—	—	16.5-17.5	—	—	—	Lower HFC3a	C
	2-27-04	—	—	—	51.8-54.5	—	—	—	Lower HFC2d	TV
	3-19-04	3-19-04	3-19-04	3-19-04	16.5-17.5	16.7-17.5	None	None	Lower HFC3a	C
	3-19-04	3-19-04	3-19-04	3-19-04	51.8-54.6	50.9-54.3	None	None	Lower HFC2d	TV
G-3795	3-1-04	—	—	—	21.8-23.0	—	—	—	Lower HFC3a	C
	3-1-04	—	—	—	41.0-47.0	—	—	—	Lower HFC2d	TV
	3-1-04	—	—	—	50.0-55.0	—	—	—	Lower HFC2c2	TV
	3-22-04	3-22-04	3-22-04	3-22-04	42.5-49.1	45.3-48.0	None	None	Lower HFC2d	TV
	3-22-04	3-22-04	3-22-04	3-22-04	50.0-55.0	50.3-54.9	None	None	Lower HFC2c2	TV

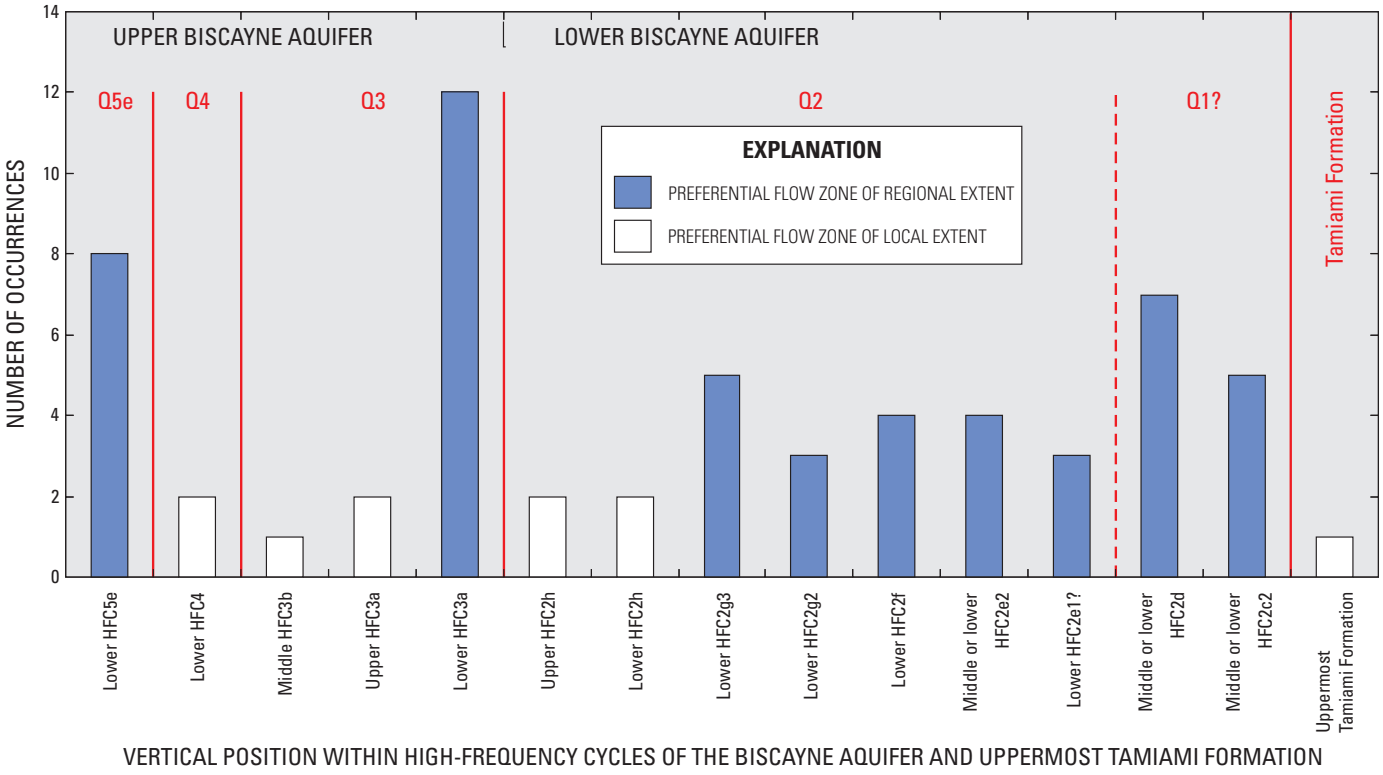

Figure 32. Number of occurrences of various preferential flow zones in 16 test coreholes fully penetrating the Biscayne aquifer in the study area, verified with heat-pulse or spinner flowmeter measurements, or both. Q units of Perkins (1977) also shown.

Summary and Conclusions

A fundamental problem in the simulation of karst ground-water flow and solute transport is how to represent aquifer heterogeneity as defined by the spatial distribution of porosity, permeability, and storage. Combined analyses of lithofacies, depositional environments, cyclostratigraphy, and borehole-geophysical logs as they relate to porosity, permeability, and storage has improved the representation of the triple-porosity karst Biscayne aquifer in an approximately 95-mi^2 study area in southeastern Florida.

Karst aquifers are traditionally characterized by three types of porosity: interparticle matrix porosity, fracture porosity, and large cavernous porosity. This has led many to view karst aquifers as two component systems, where much of the ground-water storage occurs in the matrix porosity or fractures or both, and much of the ground-water flow and transport takes place in large dissolutional conduits. In the young eogenetic karst that defines the Pleistocene limestone of the Biscayne aquifer, however, a fourth porosity type, touching-vug porosity, is especially important in terms of conveyance of ground water. The triple porosity of the Biscayne aquifer is typically: (1) matrix of interparticle and separate-vug porosity, providing much of the storage, and under dynamic conditions, diffuse-carbonate flow; (2) touching-vug porosity creating stratiform ground-water flow pathways formed by touching vugs; and (3) less common conduit porosity composed mainly of bedding-plane vugs, thin solution pipes, and cavernous vugs. These three conduit porosity types are all pathways for conduit ground-water flow.

Rock textures, faunal constituents, sedimentary structures, and relation to surfaces bounding vertical lithofacies successions were the basis for defining six principal depositional environments for the Tamiami Formation, Fort Thompson Formation, and Miami Limestone, which are major lithologic components of the Biscayne aquifer. The six depositional environments are: (1) middle ramp, (2) platform margin-to-outer platform, (3) open-marine platform interior, (4) restricted platform interior, (5) brackish platform interior, and (6) freshwater terrestrial environments. High-frequency cycles form the fundamental building blocks of the rocks of the Biscayne aquifer. Vertical lithofacies assemblages, which have stacking patterns that reoccur, fit within the high-frequency cycles. The upward-shallowing subtidal cycle, upward-shallowing paralic cycle, and aggradational subtidal cycle define three types of ideal high-frequency cycles that occur within the Fort Thompson Formation and Miami Limestone. The key to identification of the upward-shallowing paralic cycle is a capping micrite-rich carbonate lithology indicative of deposition in brackish paralic or freshwater terrestrial environments. Grouping of high-frequency cycles produced two cycle sets: one progradational (Fort Thompson Formation) and another aggradational (Miami Limestone) based on vertical cycle patterns.

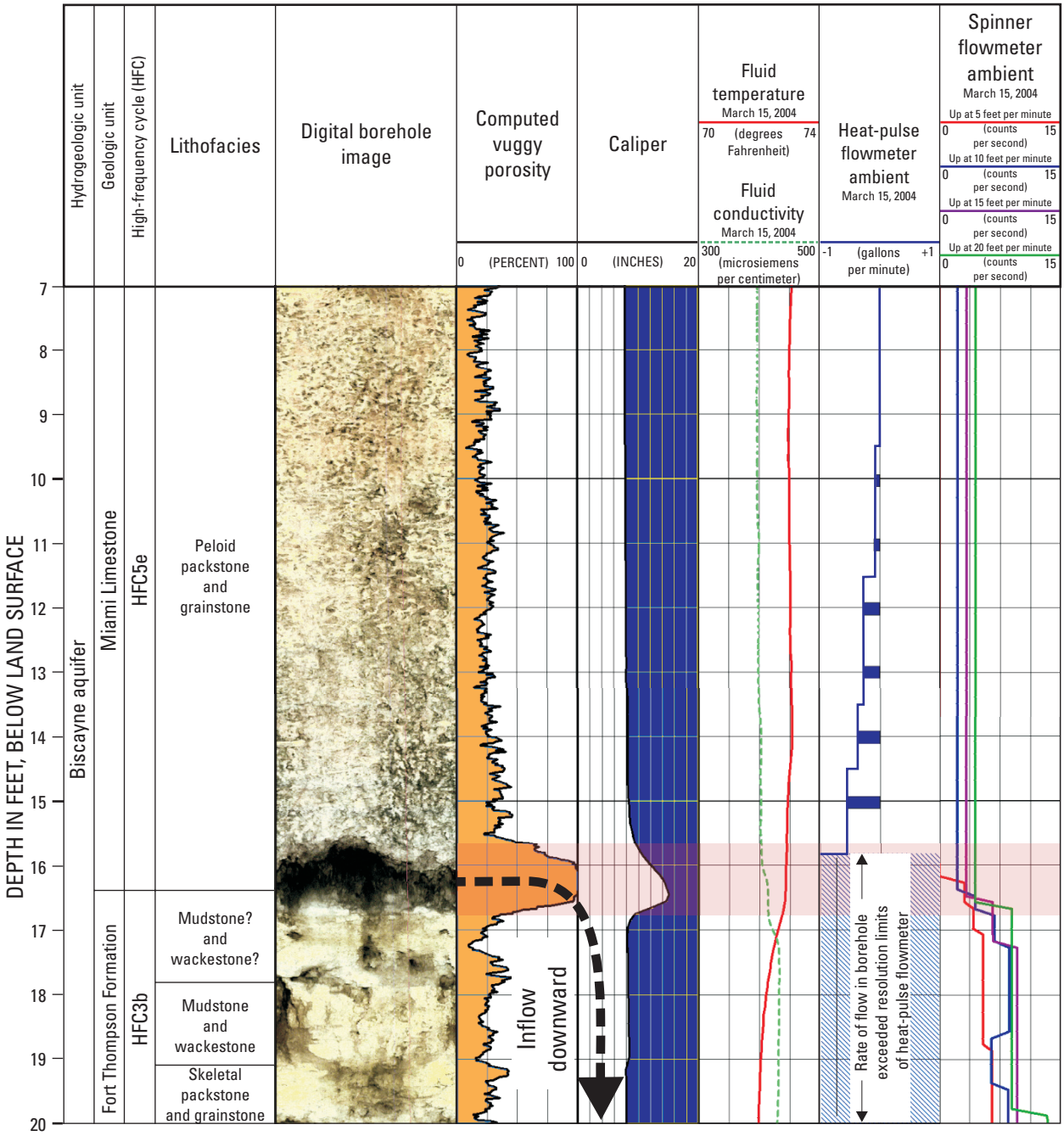

Figure 33. Comparison of borehole image, computed vuggy porosity, geophysical, and flowmeter logs showing evidence for inflow of ground water from a preferential flow zone into the borehole of the G-3782 test corehole. Most of the inflow seems to occur at a vuggy cavity at the base of HFC5e between the depths of about 15.7 and 16.8 feet below land surface (shaded in pale red).

A primary observation is that a predictable vertical pattern of porosity, permeability, and storage commonly exists within the three ideal cycles because these aquifer properties relate directly to lithofacies. Sixteen major lithofacies of the Fort Thompson Formation and Miami Limestone have been assigned to one of three pore classes (I, II, and III). Pore class I typically comprises the lower part of upward-shallowing subtidal and paralic cycles typically above flooding surfaces within the Fort Thompson Formation and an upper aggradational cycle of the Miami Limestone; touching-vug ground-water flow is typical for this pore class. Conceptualization of the touching-vug flow is movement of ground water through a stratiform passage formed by coalescence of vugs into a mostly tortuous path. Bedding-plane

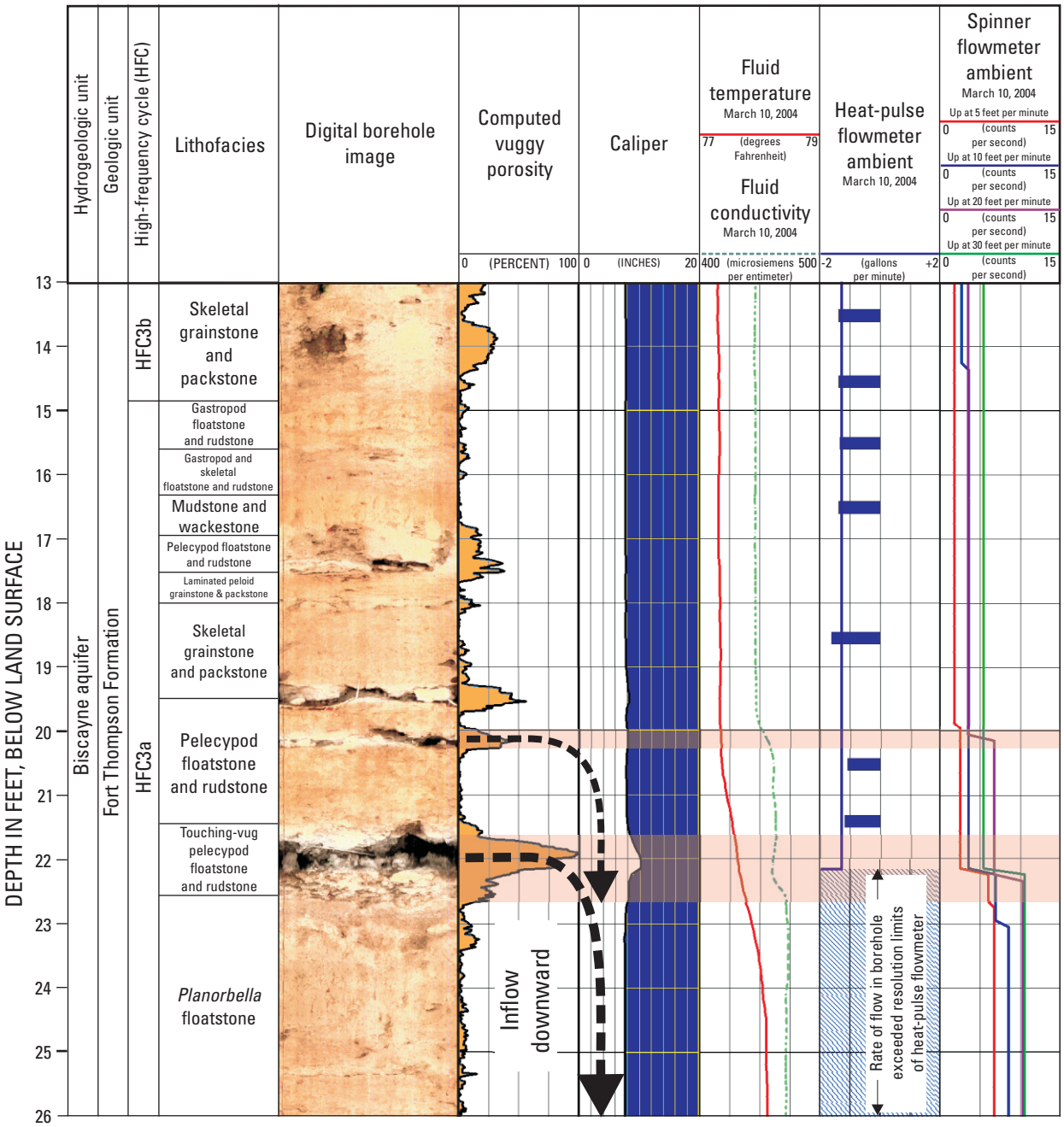

Figure 34. Comparison of borehole image, computed vuggy porosity, geophysical, and flowmeter logs showing evidence for inflow of ground water from two preferential flow zones into the borehole of the G-3788 test corehole. Most of the inflow seems to occur at a bedding-plane vug at about 20 to 20.2 feet below land surface and a cavity that is a combination of touching vugs and a bedding-plane vug at about 21.6 to 22.7 feet below land surface. Both preferential flow zones occur within HFC3a (shaded in pale red).

vugs and rare cavernous vugs form conduit porosity that occurs less commonly in pore class I. Pore class II commonly occurs in the upper part of the upward-shallowing subtidal cycle and middle part of the upward-shallowing paralic cycle. This class is principally interparticle and separate-vug porosity, and is characterized by diffuse-carbonate ground-water flow through vug-to-matrix-to-vug connections.

Micrite-dominated lithologies, which may have thin vertical solution pipes (short conduits) and separate vugs, distinguish pore class III. This class commonly caps upward-shallowing cycles and occurs throughout much of the lower aggradational cycle of the Miami Limestone. These micrite-rich lithologies leak vertically, but tend to inhibit horizontal ground-water movement.

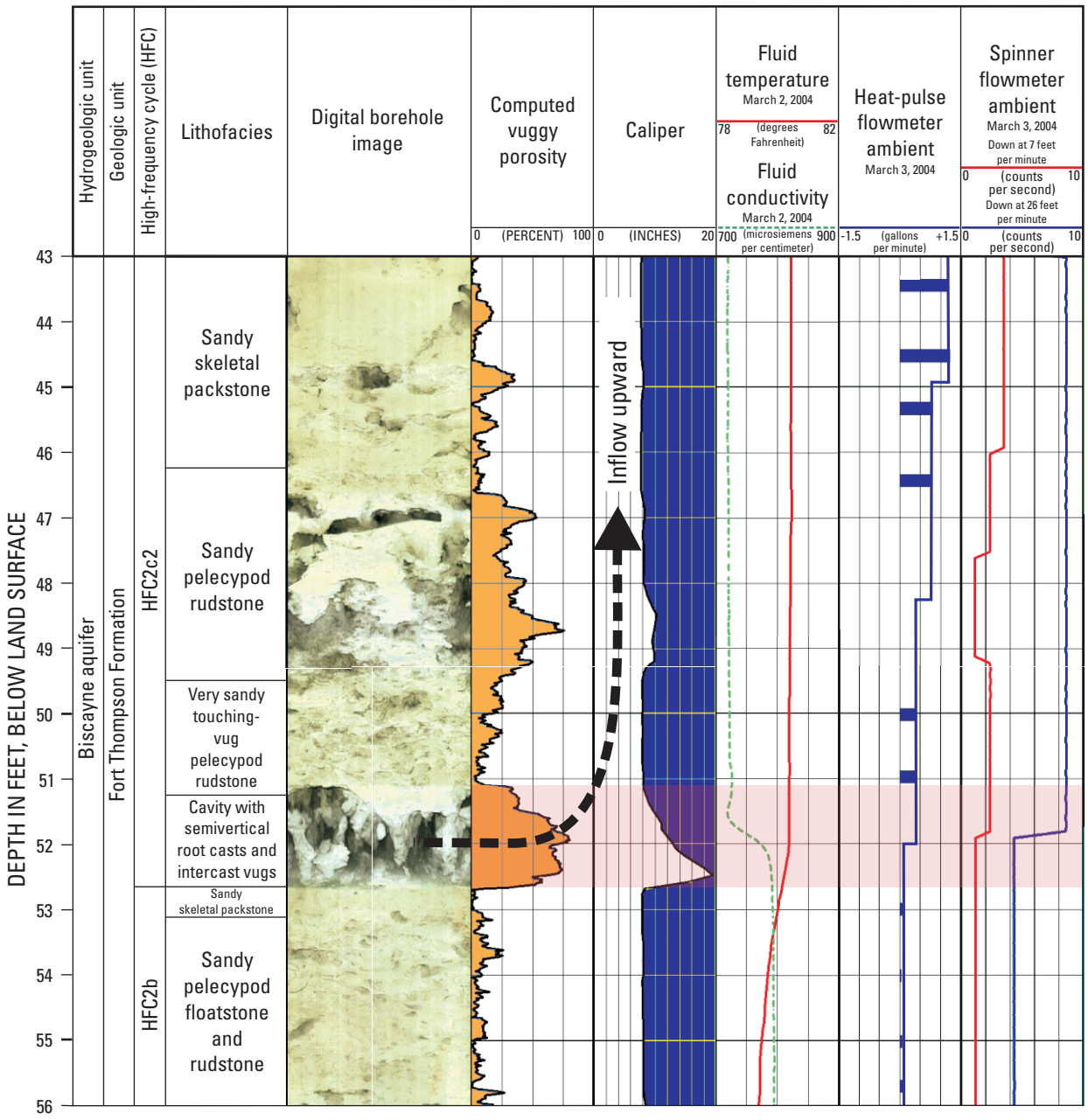

Figure 35. Comparison of borehole image, computed vuggy porosity, geophysical, and flowmeter logs showing evidence for inflow of ground water from a preferential flow zone into the borehole of the G-3793 test corehole. Most of the inflow seems to occur at a vuggy cavity at the base of HFC2c2 between the depths of about 51.1 and 52.7 feet below land surface (shaded in pale red).

It is proposed that the karstic development of the highly permeable zones at the base of upward-shallowing cycles of the Fort Thompson Formation relates to cyclostratigraphy and Pleistocene sea-level history. Formation of secondary porosity was probably produced by meteoric water flowing through the limestone of the Fort Thompson Formation during its emergence into the vadose zone, caused by periodic low stands in sea level that span Pleistocene glacial maximums. The focused, low-gradient lateral flow of meteoric water above flooding surfaces is postulated due to the presence of relatively low-permeability lithologies at cycle tops that underlie flooding surfaces and act as baffles or barriers to downward vertical drainage.

The cyclostratigraphic approach taken herein demonstrates that its combined use with borehole-geophysical logs is valuable to the development of an accurate conceptual three-dimensional hydrogeologic model. The one-dimensional cyclostratigraphic framework, or fingerprint, of each well used in the conceptual model permitted correlation of vertical lithofacies successions and high-frequency cycles and the

well-to-well connection of corresponding highly porous and permeable zones between wells. The concepts should be useful in providing a framework for numerical simulations of regional-scale dual- and triple-porosity ground-water flow and solute transport. Many karst aquifers occur in cyclic platform carbonates, so the cyclostratigraphic approach is applicable to numerous areas of the world. Applications include wellhead protection at well fields, design of tracer studies, solute-transport modeling of contaminants, saltwater intrusion modeling and monitoring in coastal areas, engineering design of underground barriers to seepage and tunnels, delineation of storage zones for aquifer storage and recovery projects, and simulation of regional-scale karst ground-water flow.

References Cited

Abbott, R.T., 1974, American seashells: New York, Van Nostrand Reinhold, 663 p.

Andrews, J.O., 1977, Shells and shores of Texas: Austin, Texas, Kingsport Press, 365 p.

Bain, R.J., and Teeter, J.W., 1975, Previously undescribed carbonate deposits on Key Largo, Florida: Geology, v. 3, no. 3, p. 137-139.

Bock, W.D., Lynts, G.W., Smith, S.L., and others, 1971, A symposium of recent south Florida foraminifera: Miami Geological Society, Memoir 1, 245 p.

Brewster-Wingard, G.L., Ishman, S.E., Edwards, L.E., and Willard, D.A., 1997, Preliminary report on the distribution of modern fauna and flora at selected sites in north-central and north-eastern Florida Bay: U.S. Geological Survey Open-File Report 96-732, 34 p.

Brewster-Wingard, G.L., Stone, J.R., and Holmes, C.W., 2001, Molluscan faunal distribution in Florida Bay, past and present: An integration of down-core and modern data: Bulletins of American Paleontology, Special Vol. 361, p. 199-231.

Brown and Caldwell Environmental Engineers and Consultants, 1998, Remedial action-plan: Old South Dade Landfill: Report prepared for Miami-Dade County Department of Solid Waste Management, variously paginated.

Budd, D.A., 2001, Permeability loss with depth in the Cenozoic carbonate platform of west-central Florida: American Association of Petroleum Geologists Bulletin, v. 85, no. 7, p. 1253-1272.

Budd, D.A., and Vacher, H.L., 2004, Matrix permeability of the confined Floridan aquifer, Florida, USA: Hydrogeology Journal, v. 12, no. 5, p. 531-549.

Burchette, T.P., and Wright, V.P., 1992, Carbonate ramp depositional systems: Sedimentary Geology, v. 79, p. 3-57.

Causaras, C.R., 1987, Geology of the surficial aquifer system, Dade County, Florida: U.S. Geological Survey Water-Resources Investigations Report 86-4126, 240 p., 3 sheets.

Cunningham, K.J., Carlson, J.I., and Hurley, N.F., 2004a, New method for quantification of vuggy porosity from digital optical borehole images as applied to the karstic Pleistocene limestone of the Biscayne aquifer, southeastern Florida: Journal of Applied Geophysics, v. 55, no. 1-2, p. 77-90.

Cunningham, K.J., Carlson, J.L., Wingard, G.L., and others, 2004b, Characterization of aquifer heterogeneity using cyclostratigraphy and geophysical methods in the upper part of the karstic Biscayne aquifer, southeastern Florida: U.S. Geological Survey Water-Resources Investigation Report 03-4208, 46 p., 5 pls.

Cunningham, K.J., Renken, R.A., Wacker, M.A., and others, 2006 (in press), Application of carbonate sequence stratigraphy to delineate porosity, preferential flow, and advective transport in the karst limestone of the Biscayne aquifer, SE Florida, USA, *in* Harmon, R.S., and Wicks, Carol, eds., Perspectives on Karst Geomorphology, Hydrology and Geochemistry—A Tribute Volume to Derek C. Ford and William B. White: Geological Society of America, Special Paper 404.

Cunningham, K.J., Wacker, M.A., Robinson, Edward, and others, 2004c, Hydrogeology and ground-water flow within the L31N Seepage Management Pilot Project area, Miami-Dade County, Florida: U.S. Geological Survey Scientific Investigations Map I-2846, 1 sheet.

Cunningham, K.J., and Wright, J.M., 1998, Sequence-stratigraphic interpretation and aquifer characterization as critical processes in aquifer management: Local aquifer remediation in the Biscayne aquifer, southeastern Florida: American Geophysical Union Fall Meeting, San Francisco, Calif., Abstracts volume, p. H242.

Dall, W.H., 1903, Contributions to the Tertiary fauna of Florida: Transactions of the Wagner Free Institute of Science of Philadelphia, v. 3, no. 6, p. 1219-1654.

Debenay, J.P., Guillou, J.J., Redois, F., and Geslin E., 2000, Distribution trends of foraminiferal assemblages in paralic environments: A base for using foraminifera as bioindicators, *in* Martin, R.E., ed., Environmental Micropaleontology: The application of microfossils to environmental geology: Topics in Geobiology, v. 15, p. 39-67.

Drummond, C.N., and Wilkinson, B.H., 1993, Carbonate cycle stacking patterns and hierarchies of orbitally forced eustatic sea level change: Journal of Sedimentary Petrology, v. 63, p. 369-377.

DuBar, J.R., 1958, Stratigraphy and paleontology of the late Neogene strata of the Caloosahatchee River area of southern Florida: Tallahassee, Florida Geological Survey Bulletin 40, 267 p.

Dunham, R.J., 1962, Classification of carbonate rocks according to depositional textures, *in* Ham, W.E., ed., Classification of carbonate rocks: American Association of Petroleum Geologists, Memoir 1, p. 108-121.

Embry, A.F., and Klovan, J.E., 1971, A late Devonian reef tract on Northeastern Banks Island, N.W.T.: Bulletin of Canadian Petroleum Geology, v. 19, no. 4, p. 730-781.

Evans, C.C., 1984, Development of an ooid sand shoal complex: The importance of antecedent and syndepositional topography, *in* Harris, P.H., ed., Carbonate sands—A core workshop: Society of Economic Petrologists and Mineralogists Core Workshop 5, p. 392-428.

Federal Register Notice, October 11, 1979, v. 44, no. 198.

Fish, J.E., 1988, Hydrogeology, aquifer characteristics, and groundwater flow of the surficial aquifer system, Broward County, Florida: U.S. Geological Survey Water-Resources Investigations Report 87-4034, 92 p.

Fish, J.E., and Stewart, Mark, 1991, Hydrogeology of the surficial aquifer system, Dade County, Florida: U.S. Geological Survey Water-Resources Investigations Report 80-4108, 50 p., 11 pls.

Galli, Gianni, 1991, Mangrove-generated structures and depositional model of the Pleistocene Fort Thompson Formation (Florida Plateau): Facies, v. 25, p. 297-314.

Genereux, David, and Guardiario, Jose, 1998, A canal drawdown experiment for determination of aquifer parameters: Journal of Hydrologic Engineering, v. 3, no. 4, p. 294-302.

Geological Society of America, 1991, Rock color chart: Baltimore, Md, Munsell color.

Guardiario, J.D.A., Jr., 1996, Determination of hydraulic conductivity and dispersivity in the Biscayne aquifer, Taylor Slough, Everglades National Park: M.S. Thesis, Florida International University, Miami, 195 p.

Halley, R.B., and Evans, C.C., 1983, The Miami Limestone: A guide to selected outcrops and their interpretation: Miami Geological Society, 67 p.

Hallock, Pamela, and Glenn, E.C., 1986, Larger foraminifera: A tool for paleoenvironmental analysis of Cenozoic carbonate depositional facies: Palaios, v. 1, no. 1, p. 55-65.

Harris, P.M., Saller, A.H., and Simo, J.A., 1999, Introduction, *in* Harris, P.M., Saller, A.H., and Simo, J.A., eds., Advances in carbonate stratigraphy: Application to reservoirs, outcrops and models: Society of Economic Mineralogists and Paleontologists (Society for Sedimentary Geology) Special Publication 63, p. 1-10.

Harrison, R.S., Cooper, L.D., and Coniglio, Mario, 1984, Late Pleistocene carbonates of the Florida Keys, *in* Carbonates in subsurface and outcrop: Canadian Society of Petroleum Geologists Core Conference, p. 291-306.

Hickey, J.J., 1993, Characterizing secondary porosity of carbonate rocks using borehole video data [abstract]: Geological Society of America, Abstracts with Programs, v. 25, Southeastern Section, p. 23.

Hickey, T.D., 2004, Geologic evolution of south Florida Pleistocene-age deposits with an interpretation of the enigmatic rock ridge development: M.S. Thesis, University of South Florida, St. Petersburg, 125 p.

Hilgen, Fredrik, Schwarzacher, Walter, and Strasser, André, 2004, Appendix: Concept and definitions in cyclostratigraphy (second report of the cyclostratigraphy working group), *in* D'Argenio, Bruno, Fischer, A.G., Premoli Silva, Isabella, and others, eds., Cyclostratigraphy: Approaches and case histories: Society of Economic Mineralogists and Paleontologists (Society for Sedimentary Geology) Special Publication 81, p. 303-305.

Hoffmeister, J.E., and Multer, H.G., 1965, Fossil mangrove reef of Key Biscayne, Florida: Geological Society of America Bulletin, v. 76, no. 8, p. 845-852.

Hoffmeister, J.E., Stockman, K.W., and Multer, H.G., 1967, Miami Limestone of Florida and its recent Bahamian counterpart: Geological Society of America Bulletin, v. 79, no. 2, p. 175-190.

Horvorka, S.D., Dutton, A.R., Ruppel, S.C., and Yeh, J.S., 1996, Edwards aquifer ground-water resources: Geologic controls on porosity development in platform carbonates, south Texas: The University of Texas at Austin, Bureau of Economic Geology, Report of Investigations 238, 75 p.

Horvorka, S.D., Mace, R.E., and Collins, E.W., 1998, Permeability structure of the Edwards aquifer, south Texas—Implications for aquifer management: The University of Texas at Austin, Bureau of Economic Geology, Report of Investigations 250, 55 p.

Hurley, N.F., Pantoja, David, and Zimmerman, R.A., 1999, Flow unit determination in a vuggy dolomite reservoir, Dagger Draw Field, New Mexico: Oslo, Norway, Transactions, June 1999.

Hurley, N.F., Zimmerman, R.A., and Pantoja, David, 1998, Quantification of vuggy porosity in a dolomite reservoir from borehole images and core, Dagger Draw Field, New Mexico: Annual Technical Conference and Exhibition, New Orleans, Society of Petroleum Engineers, Paper 49323, p. 789-802.

Ishman, S.E., Graham, Ian, and d'Ambrosio, Jill, 1997, Modern benthic foraminifer distributions in Biscayne Bay: Analogs for historical reconstructions: U.S. Geological Survey Open-File Report 97-34, 23 p.

Jackson, J.A. (ed.), 1997, Glossary of geology (4th ed.): American Geological Institute, Alexandria, Va., 769 p.

James, N.P., 1979, Shallowing-upward sequences in carbonates, *in* Walker, R.G. ed., Facies models: Geological Association of Canada, Geoscience Canada Reprint Series 1, 2d ed., p. 213-228.

Kaufman, R.S., and Switanek, M.P., 1998, Confinement of the Biscayne aquifer in northwest Dade County, Florida: Geological Society of America 47th Annual Meeting Southeastern Section Abstracts with Programs, March 30-31, Charleston, West Virginia, p. 20.

Kerans, Charles, and Tinker, S.W., 1997, Sequence stratigraphy and characterization of carbonate reservoirs: Society of Economic Paleontologists and Mineralogists, Short Course Notes 40, 130 p.

Keys, W.S., 1990, Borehole geophysics applied to ground-water investigations: U.S. Geological Survey Techniques of Water-Resources Investigations, book 2, chap. E2, 150 p.

Klein, Howard, and Sherwood, C.B., 1961, Hydrologic conditions in the vicinity of Levee 30, northern Dade County, Florida: Tallahassee, Florida Bureau of Geology Report of Investigations 24, 24 p.

Krupa, Amanda, and Mullen, V.T., 2005, Extent of a dense limestone layer in the upper portion of the Biscayne aquifer in the Pennsuco Wetlands, Miami-Dade County: West Palm Beach, South Florida Water Management District, Technical Publication HESM-1, 33 p.

Labowski, J.L., 1988, Geology, hydrology, and water monitoring program, Northwest wellfield protection area: Metropolitan Dade County, Department of Environmental Resources Management, Technical Report 88-3, 60 p.

Langevin, C.D., 2001, Simulation of ground-water discharge to Biscayne Bay, southeastern Florida: U.S. Geological Survey Water-Resources Investigations Report 00-4251, 127 p., 3 pls.

Lidz, B.H., and Rose, P.R., 1989, Diagnostic foraminiferal assemblages of Florida Bay and adjacent shallow water: A comparison: Bulletin of Marine Science, v. 44, p. 399-418.

Lucia, F.J., 1995, Rock-fabric/petrophysical classification of carbonate pore space for reservoir characterization: American Association of Petroleum Geologists Bulletin, v. 79, no. 9, p. 1275-1300.

Lucia, F.J., 1999, Carbonate reservoir characterization: Berlin, Springer-Verlag, 226 p.

Lyons, W.G., 1992, Caloosahatchee-age and younger molluscan assemblages at APAC mine, Sarasota County, Florida: Tallahassee, Florida Geological Survey Special Publication 36, p. 133-160.

Mansfield, W.C., 1932, Miocene pelecypods of the Choctawhatchee Formation of Florida: Tallahassee, Florida Geological Survey Bulletin 8, 240 p.

Mansfield, W.C., 1939, Notes on the upper Tertiary and Pleistocene mollusks of peninsular Florida: Tallahassee, Florida Geological Survey Bulletin 18, 75 p.

Martin, J.B., and Screaton, E.J., 2001, Exchange of matrix and conduit water with examples from the Floridan aquifer, *in* Kuniansky, E.L., ed., U.S. Geological Survey Karst Interest Group Proceedings, Water-Resources Investigations Report 01-4011, p. 38-44.

Miall, A.D., 1997, The geology of stratigraphic sequences: New York, Springer-Verlag, 433 p.

Miami-Dade County Lake Belt Plan Implementation Committee, 1998, Progress report: West Palm Beach, South Florida Water Management District Visual Communications Division, 17 p.

Multer, H.G., Gischler, Eberhard, Lundberg, Joyce, and others, 2002, Key Largo Limestone revisited: Pleistocene shelf-edge facies, Florida Keys, USA: Facies, v. 46, p. 229-272.

Nemeth, M.S., Wilcox, W.M., and Solo-Gabriele, H.M., 2000, Evaluation of the use of reach transmissivity to quantify leakage beneath Levee 31N, Miami-Dade County, Florida: U.S. Geological Survey Water-Resources Investigations Report 00-4066, 80 p.

Newberry, B.M., Grace, L.M., and Stief, D.D., 1996, Analysis of carbonate dual porosity systems from borehole electrical images: Permian Basin Oil and Gas Recovery Conference: Midland, Texas, Society of Petroleum Engineers Paper 35158, p. 123-125.

Olsson, A.A., 1967, Some Tertiary mollusks from south Florida and the Caribbean: Ithaca, N.Y., Paleontological Research Institution, 61 p.

Olsson, A.A., and Harbison, Anne, 1953, Pliocene mollusca of southern Florida: Academy of Natural Sciences of Philadelphia Monograph 8, p. 1-361.

Olsson, A.A., and Petit, R.E., 1964, Some Neogene mollusca from Florida and the Carolinas: Bulletins of American Paleontology, v. 47, no. 217, p. 509-575.

Paillet, Fredrick, 2004, Borehole flowmeter applications in irregular and large-diameter boreholes: Journal of Applied Geophysics, v. 55, no. 1-2, p. 39-59.

Parker, G.G., 1951, Geologic and hydrologic factors in the perennial yield of the Biscayne aquifer: American Water Works Association Journal, v. 43, no. 10, p. 817-835.

Parker, G.G., and Cooke, C.W., 1944, Late Cenozoic geology of southern Florida with a discussion of the ground water: Tallahassee, Florida Geological Survey Bulletin 27, 119 p.

Parker, G.G., Ferguson, G.E., Love, S.K, and others, 1955, Water resources of southeastern Florida: U.S. Geological Survey Water-Supply Paper 1255, 965 p.

Perkins, R.D., 1977, Depositional framework of Pleistocene rocks in south Florida, *in* Enos, Paul, and Perkins, R.D., eds., Quaternary sedimentation in south Florida: Geological Society of America Memoir 147, p. 131-198.

Perry, L.M., and Schwengel, J.S., 1955, Marine shells of the west coast of Florida: Ithaca, N.Y., Paleontological Research Institution, 318 p.

Poag, C.W., 1981, Ecologic atlas of benthic foraminifera of the Gulf of Mexico: New York, Academic Press, 174 p.

Portell, R.W., Schindler, K.S., and Morgan, G.S., 1992, The Pleistocene molluscan fauna from Leisey shell pit 1, Hillsborough County, Florida: Tallahassee, Florida Geological Survey Special Publication 36, p. 181-194.

Reese, R.S., and Cunningham, K.J., 2000, Hydrogeology of the gray limestone aquifer in southern Florida: U.S. Geological Survey Water-Resources Investigations Report 99-4213, 244 p.

Renken, R.A., Shapiro, A.M., Cunningham, K.J., and others, 2005, Assessing the vulnerability of a municipal well field to contamination in a karst aquifer: Environmental & Engineering Geology, v. XI, no. 4, p. 319-331.

Rose, P.R., and Lidz, Barbara, 1977, Diagnostic foraminiferal assemblages of shallow-water modern environments: South Florida and the Bahamas: Sedimenta VI: Comparative Sedimentology Laboratory, University of Miami, Division of Marine Geology and Geophysics, 55 p.

Scott, T.M., 2001, Text to accompany the geologic map of Florida: Tallahassee, Florida Geological Survey Open-File Report 80, 30 p.

Shackleton, N.J., Sánchez-Goñi, M.F., Pailler, Delphine, and Lancelot, Yves, 2003, Marine isotope substage 5e and the Eemin Interglacieal: Global and Planetary Change: v. 36, p. 151-155.

Shinn, E.A., 1968, Burrowing in recent lime sediments of Florida and the Bahamas: Journal of Paleontology, v. 42, no. 4, p. 879-894.

Shinn, E.A., and Corcoran, Eugene, 1988, Contamination by landfill leachate, south Biscayne Bay, Florida: Gainesville, University of Florida, Final Report to Sea Grant, 11 p.

Shuster, E.T., and White, W.B., 1971, Seasonal fluctuations in the chemistry of limestone springs: A possible means for characterizing carbonate aquifers: Journal of Hydrology, v. 14, p. 93-128.

Shuter, Eugene, and Teasdale, W.E., 1989, Application of drilling, coring, and sampling techniques to test holes and wells: U.S. Geological Survey Techniques of Water-Resources Investigations Report, book 2, chap. F1, 97 p.

Solo-Gabriele, Helena, and Sternberg, Leonel, 1998, Tracers of Everglades waters: Water Environment Federation Technical Exhibition and Conference 1998, Proceedings of the Water Environment Federation 71st Annual Conference and Exposition, Orlando, Fla., v. 4, p. 323-333.

Sonenshein, R.S., 2001, Methods to quantify seepage beneath Levee 30, Miami-Dade County, Florida: U.S. Geological Survey Water-Resources Investigations Report 01-4074, 36 p.

Thrailkill, J.V., 1976, Carbonate equilibria in karst waters, *in* Karst hydrology and water resources, Proceedings of the U.S.-Yugoslavian Symposium, Dubrovnik, June 2-7, 1975: Fort Collins, Colo., Water Resources Publications, p. 745-771.

Vacher, H.L., and Mylroie, J.E., 2002, Eogenetic karst from the perspective of an equivalent porous medium: Carbonates and Evaporites, v. 17, no. 2, p. 182-196.

Van Wagoner, J.C., Posamentier, H.W., Mitchum, R.M., and others, 1988, An overview of the fundamentals of sequence stratigraphy and key definitions, *in* Wilgus, C.K., Hastings, B.J., Posamentier, H.W., and others, eds., Sea-level change: An integrated approach: Society of Economic Paleonotologists and Mineralogists Special Publication 42, p. 39-46.

Ward, L.W., and Blackwelder, B.W., 1987, Late Pliocene and early Pleistocene mollusca from the James City and Chowan River Formations at the Lee Creek Mine: Smithsonian Contributions to Paleontology, no. 61, p. 113-282.

Ward, W.C., Cunningham, K.J., Renken, R.A., and others, 2003, Sequence-stratigraphic analysis of the Regional Observation Monitoring Program (ROMP) 29A test corehole and its relation to carbonate porosity and regional transmissivity in the Floridan aquifer system, Highlands County, Florida: U.S. Geological Survey Open-File Report 03-201, 34 p., accessed on August 11, 2005 at *http://fl.water.usgs.gov/Abstracts/ofr03_201_ward.html*

Warmke, G.L., and Abbott, R.T., 1962, Caribbean seashells: Narberth, Pa., Livingston Publishing Co., 348 p.

White, W.B., 1999, Conceptual models for karstic aquifers, *in* Palmer, A.N., Palmer, M.V., and Sasowsky, I.D., eds., Karst modeling: Karst Waters Institute Special Publication, v. 5, p. 11-16.

White, W.B., 2002, Karst hydrology: Recent developments and open questions: Engineering Geology, v. 65, no. 2-3, p. 85-105.

White, W.B., and White, E.L., 2001, Conduit fragmentation, cave patterns, and localization of karst ground water basins: The Appalachians as a test case: Theoretical and Applied Karstology, v. 13-14, p. 9-23.

Wilcox, W.M., Solo-Gabriele, H.M., and Sternberg, L.O., 2004, Use of stable isotopes to quantify flows between the Everglades and urban areas in Miami-Dade County Florida: Journal of Hydrology, v. 293, nos. 1-4, p. 1-19.

Williams, J.H., and Johnson, C.D., 2000, Borehole-wall imaging with acoustic and optical televiewers for fractured-bedrock aquifer investigations: Proceedings 7th Minerals and Geotechnology Logging Symposium, Golden, Colo., October 24-26, 2000, p. 43-53.

Wilsnak, M.M., Welter, D.E., Nair, S.K., and others, 2000, North Miami-Dade County ground water flow model: West Palm Beach, South Florida Water Management District, Hydrologic Systems Modeling Department, 40 p.

Zühlke, Rainer, 2004, Integrated cyclostratigraphy of a model Mesozoic carbonate platform—The Latemar (middle Triassic, Italy), *in* D'Argenio, Bruno, Fischer, A.G., Premoli Silva, Isabella, and others, eds., Cyclostratigraphy: Approaches and case histories: Society of Economic Paleontologists and Mineralogists Special Publication 81, p. 103-122.